Ictogenesis— Insights into the contribution of GABAergic mechanisms

Rochelle Herrington

Degree of Doctor of Philosophy

Integrated Program in Neuroscience
McGill University
Montreal, QC, Canada

October, 2015

A thesis submitted to the faculty of Graduate Studies and Research in partial fulfillment of the requirements of the degree of Doctor of Philosophy

I dedicate these words to my family, one by one and all together.

Thank you.

多
謝

ACKNOWLEDGMENTS

First and foremost, I would like to express the most sincere gratitude and thanks for my supervisor Dr. Massimo Avoli. His expertise, patience, and creativity made my graduate studies at McGill a highly enriching and positive experience. Through his guidance, not only did I learn how to formulate scientific questions and design experiments, but I also learned how to find the pertinent answers.

The environment of Dr. Avoli's lab is one of support and encouragement, and this was due in no small part to my lab mates. To Dr. Maxime Lévesque and Dr. Gabriella Panuccio, thank you for teaching me the experimental techniques. To Shabnam Hamidi, thank you for sharing your slices and never being too busy to troubleshoot a recording problem. To Dr. Pariya Salami, thank you for giving me my first introduction to Matlab. Dr. Charles Behr, thank you for teaching me how to perform *in vivo* surgeries. And thank you to Zahra Shiri, it was a pleasure to collaborate on the pilo experiments. Without these people, my time would have been *significantly* less interesting.

No thesis is complete without becoming at least a little lost along the way, so to my committee members (Dr. Anne McKinney and Dr. Derek Bowie) and to my IPN mentor (Dr. Edith Hamel), I would like to express my gratitude and appreciation for the advice and guidance they offered.

Thank you to Ms. Toula Papadopoulos for help with administrative duties, to NeuroMedia (Susan Kaupp and Jean-Paul Acco) for putting the final touches on posters and figures, and to Animal Care Facility at the Montreal Neurological Institute for their readiness to help with anything, even on short notice.

To LJB, proof reading is no small task, and I am so grateful for your help going over the little details.

Finally, I would like to thank my family in Canada and Hong Kong for their never-ending support and encouragement.

TABLE OF CONTENTS

LIST OF FIGURES

ABSTRACT

Epileptic disorders are caused by a wide array of underlying mechanisms. The presentation of epileptic seizures, brain areas affected, and pathological substrates can vary from patient to patient, research model to research model. In order to develop effective antiepileptic therapeutic approaches, it is imperative to identify the specific mechanisms underlying these events. In a series of four studies, we analyzed the patterns of ictal and interictal activity induced *in vitro* by 4-aminopyridine (4AP) in horizontal rat brain slices and then further explored the effects induced by neurosteroids on ictogenesis. We concentrated specifically on structures that are relevant to temporal lobe epilepsy such as the entorhinal cortex, subiculum, CA3 region of the hippocampus, and piriform cortex.

In the first study, we addressed quantitatively the characteristics of epileptiform synchronization in the entorhinal cortex in rat brain slices. We identified two types of interictal discharges, isolated slow interictal discharges and polyspike interictal discharges that were associated with low-voltage fast onset and sudden onset ictal discharges, respectively. We also found that networks generating isolated slow interictal discharges continued to produce this interictal pattern during blockade of glutamatergic transmission. In the second study, we established the contribution of neural networks located in the entorhinal cortex and subiculum to these two types of interictal/ictal activity. Low-voltage fast onset ictal events appeared to more likely arise from the subiculum and sudden onset ictal events from the entorhinal cortex. After severing connections between the two regions, however, the propensity for the entorhinal cortex to sustain ictal discharges was much greater than for subiculum.

Neurosteroids were employed in the third study to gain insight into how the potentiation of $GABA_A$ receptor signaling modulates the two types of interictal spikes recorded in CA3 during 4AP application. Overall, neurosteroids differentially modulated slow and fast interictal discharges and their associated high frequency oscillations, which are important biomarkers for the localization of the seizure onset zone. Finally, in the fourth study, we assessed how neurosteroids modulate ictal discharges in the piriform cortex of brain slices in which isolated slow interictal discharges were recorded. As observed in the CA3 subfield, neurosteroids increased slow interictal discharge duration but reduced the duration of, and even abolished, ictal discharges. Collectively, these studies demonstrate the existence of different mechanisms contributing to distinct patterns of *in vitro* synchronous epileptiform activity and they highlight potential targets for antiepileptic intervention.

RÉSUMÉ

Plusieurs causes sont sous-jacentes à l'épilepsie. Les crises, les régions cérébrales affectées et les substrats pathologiques peuvent varier d'un patient à l'autre et d'un modèle de recherche à un autre. Afin de développer des thérapies anti-épileptiques efficaces, il est impératif d'identifier les mécanismes sous-jacents à ces événements. Dans une série de quatre études, nous avons analysé les activités ictale et interictale induites par la 4-aminopyridine (4A) dans des tranches cérébrales de rat, et exploré les effets induits par les neurosteroïdes sur l'ictogénèse. Nous nous sommes concentrés sur les structures impliquées dans l'épilepsie du lobe temporal, soit le cortex entorhinal, le subiculum, la région CA3 de l'hippocampe et le cortex piriforme.

Dans la première étude, nous avons étudié, dans des tranches cérébrales de rats, la synchronisation épileptiforme dans le cortex entorhinal. Nous avons identifié deux types de pointes interictales, á savoir, les pointes lentes isolées associées aux décharges ictales à activité rapide de basse fréquence et les décharges poly-pointes, associées aux décharges ictales à début soudain. Nous avons aussi découvert que les réseaux neuronaux qui génèrent les pointes lentes isolées continuent de produire ce patron de décharge interictale lors d'un blocage de la transmssion glutamatergique. Dans la seconde étude, nous avons définit la contribution des réseaux neuronaux du cortex entorhinal et du subiculum à ces deux types d'activité interictale/ictale. Nous avons découvert que l'origine des décharges ictales à activité rapide de basse fréquence est plus fréquemment retrouvée dans le subiculum tandis que les décharges ictales à début soudain débutent plus fréquemment dans le cortex entorhinal. Par contre, lorsque les connections entre le subiculum et le cortex entorhinal sont sectionnées, les décharges ictales sont seulement visibles dans le cortex entorhinal et non dans le subiculum. Les neurostéroïdes ont été employé dans la troisième étude afin d'étudier comment la potentialisation de l'activité associé aux récepteur $GABA_A$ affecte les deux types d'activité interictale enregistrés dans CA3.

Nous avons découvert que les neurostéroïdes modulent de manière différente les pointes lentes et rapides et les oscillations à hautes fréquences qui leur sont associées, qui sont d'importants marqueurs de la zone épileptogène. Finalement, dans la quatrième étude, nous avons étudié l'effet des neurostéroïdes sur les décharges ictales dans le cortex piriforme de tranches cérébrales dans lesquelles des pointes interictales lentes ont été enregistrées. Tel qu'observé dans la CA3, les neurostéroïdes induisent une augmentation de la durée des pointes interictales mais réduisent la durée des décharges ictales ou les abolissent complètement. Ces études démontrent l'existence de

mécanismes distincts comme causes de différents patrons d'activité épileptiforme synchrone *in vitro*, et identifient des cibles potentielles pour des traitements anti-épileptiques.

CONTRIBUTION OF AUTHORS

The research presented in this thesis is grouped into four main chapters (sections 2-5), representing original work that has been published. The manuscripts for chapters 3, 4, and 5 were written by me, and that of chapter 2 was written by Dr. Avoli.

Chapter 2:

Avoli M, Panuccio G, Herrington R, D'Antuono M, de Guzman P, Lèvesque M (2013) *Two different interictal spike patterns anticipate ictal activity in vitro.* Neurobiol Dis. 52: 168-76

This study represents a collaborative effort between current and past members of Dr. Avoli's laboratory. Dr. Panuccio, Dr. D'Antuono, and Dr. de Guzman conducted the experiments. Dr. Avoli, Dr. Lévesque, and I contributed to analyzing the field potential recordings and the high frequency oscillations. Dr. Lévesque and I jointly contributed to performing the statistical analysis. Dr. Avoli wrote the original draft of the manuscript that was edited by Dr. Lévesque, Dr. D'Antuono and me.

Chapter 3:

Herrington R, Lèvesque M, Avoli M (2015) *Subiculum-entorhinal cortex interactions during in vitro ictogenesis.* Seizure. doi:10.1016/j.seizure.2015.07.002

This study was initiated based on Dr. Avoli's observation that low voltage fast activity in the subiculum often preceded that in the entorhinal cortex. I contributed to the study by performing a subset of the experiments, analyzing the data, and writing the manuscript. Dr. Avoli provided invaluable support to the editing and fine tuning of the final manuscript along. Dr. Lévesque provided support for the analysis and interpretation of the data.

Chapter 4:

Herrington R, Lèvesque M, Avoli M (2014) *Neurosteroids modulate epileptiform activity and associated high-frequency oscillations in the piriform cortex.* Neuroscience. 256:467-77

We decided to segue into the study of neurosteroids following some early experiments demonstrating the these compounds have potential anti-epileptogenic effects (Biagini et al., 2006,

2009). Here, I performed experiments testing the anti-ictogenic properties of THDOC, analyzed the data, and contributed significantly to writing the manuscript. Dr. Lévesque helped with the interpretation of the high frequency oscillation data and statistical analysis. Dr. Avoli contributed greatly to the interpretation of the results and to streamlining the manuscript.

Chapter 5:

Herrington R, Lèvesque M, Avoli M (2014) *Neurosteroids differentially modulate fast and slow interictal discharges in the hippocampal CA3 area*. Eur J Neurosci. 41(3):379-89

This study was conceived due to the need for a greater understanding of how THDOC could modulate glutamatergic versus GABAergic events. In this study, I performed the experiments, data analysis, and I wrote the manuscript draft Dr. Lévesque contributed to the interpretation of the HFO results and to the statistical analysis. Dr. Avoli's comments and advice was crucial for the interpretation of the results as a whole, and for editing the final manuscript.

CHAPTER 1: INTRODUCTION

1.1. Epilepsy

Affecting between 0.5-1% of any given population worldwide, epilepsy is one of the most common neurological disorders and can be characterized by many different underlying mechanisms (Leach and Abassi, 2013). The International League Against Epilepsy (ILAE) formally defines an epileptic seizure as "a transient occurrence of signs and/or symptoms due to abnormal excessive or synchronous neuronal activity in the brain" (Fisher et al., 2005). However, a single seizure does not necessarily constitute epilepsy as this neurological disorder is defined by the ILAE as "a chronic condition of the brain characterized by an enduring propensity to generate epileptic seizures, and by the neurobiological, cognitive, psychological, and social consequences of this condition. The definition of epilepsy requires the occurrence of at least one epileptic seizure" (Fisher et al., 2005).

The aetiology of epilepsy can be classified into three main categories: genetic, structural-metabolic, and unknown (Teskey and Farrell, 2015). Genetic epilepsies are associated with genetic mutations that promote a hypersynchronous state in the brain. Structural-metabolic epilepsy, as the name suggests, arises from changes in either the structure of the brain or its metabolism. These changes can be associated to febrile seizures, brain tumors, vascular malformations, strokes, brain ischemia, Alzheimer's disease and brain infection (Patil, 2007). Specific metabolic disorders that can lead to epilepsy include diabetes, uremia, phenylketouremia, and electrolyte imbalance (Patil, 2007). The differentiation between genetic and metabolic-structural epilepsies is not always definitive. Indeed, genetics along with changes in brain structure and metabolism can interact to cause an epileptic condition. Epilepsies that are not associated with a known genetic or structural-metabolic abnormality are classified as unknown. Counter intuitively, unknown epilepsies are distinct from those of idiopathic origin wherein a genetic cause is implied (Bray, 1972; Shorvon, 2011). This final category continues to decrease in size with the development of new diagnostic technologies used to identify structural, metabolic and genetic causes (Teskey and Farrell, 2015).

Seizures themselves can be further conceptualized into two groups: generalized and focal. Generalized seizures can either originate locally and then rapidly spread bilaterally to engage distributed neural networks in both hemispheres or, as in the case of primary generalized epilepsy, begin in widespread neural networks (Berg et al., 2010). On the other hand, focal seizures originate within networks limited to a single hemisphere and the symptoms depend on the networks that are recruited (Berg et al., 2010).

In most cases seizures self-terminate within a few minutes. If a seizure fails to terminate, it can continue into a state called *status epilepticus*, which is defined as continuous seizure activity lasting for 5 minutes or longer, or multiple (2 or more) discrete seizures occurring over a period of 5 minutes or longer between which there is an incomplete recovery of consciousness (Lowenstein et al., 1999). Definitions of what constitutes a seizure and what constitutes *status epilepticus* have shifted over the years based on average seizure duration, research on patient outcomes, and when acute treatment should be administered in the clinic (Lowenstein et al., 1999). *Status epilepticus* is associated with significant levels of morbidity and mortality (DeLorenzo et al., 1996), and in some cases it can even lead to the development of epilepsy (Pitkänen, 2010). Seizures themselves can also be associated with a degree of morbidity and mortality.

Patients experiencing seizures are exposed to the risk of sudden unexpected death in epilepsy (so-called SUDEP), the leading cause of death in refractory epilepsy, wherein the occurrence of seizures is presumably related to respiratory or cardiac failure (Massey et al., 2014). Epilepsy is also linked to cognitive and behavioural disturbances that arise as consequences from a number of overlapping influences such as underlying neuropathologies, neuronal discharges (ictal and interictal), sustained use of antiepileptic drugs, and psychosocial issues arising from social stigma (Kwan and Brodie, 2001).

Antiepileptic drugs (AEDs) provide the first line of treatment for patients with epileptic disorders. These compounds inhibit the development and propagation of seizures by increasing the seizure threshold, but they fail to treat the underlying mechanisms of the disorder and provide a cure (Schmidt and Schachter, 2014). Most AEDs exert their effects through, the stabilization of the inactive state of voltage-gated Na^+ channels, the inactivation of T-type Ca^{2+} channels, and/or the potentiation of GABA receptor mediated signalling (Mantegazza et al., 2010; Schmidt and Schachter, 2014; Teskey and Farrell, 2015). In most cases AEDs are effective, with 65-70% of patients attaining long-term seizure freedom after the first or second antiepileptic drug tried (Leach and Abassi, 2013). However, the remainder is cause for concern. TLE, for example, is often refractory to AEDs and can be associated with hippocampal sclerosis (Engel, 1996). Patients with this disorder are often considered candidates for surgical removal of the seizure onset zone if AEDs are ineffective.

1.2. Seizures Beget Seizures

It is important to control seizures because their occurrence over time can contribute to the development of epilepsy. The mechanism through which seizures can contribute to the progression

of epilepsy disorders is multifaceted. First, seizures can lead to the excessive activation of glutamate receptors, and in turn this can lead to neuronal excitotoxicity and ultimately cell necrosis. The full extent of the molecular cascades involved in excitotoxicity is not yet fully understood, but factors at play include impaired intracellular Ca^{2+} homeostasis, osmotic stress, compromised cellular organelle function, increased nitric oxide and free radical production, persistent activation of proteases and kinases, and increased expression of pro-death transcription factors (Wang and Qin, 2010). It is worth mentioning that excitotoxic effects are greatest when Ca^{2+} influx is mediated through NMDA receptor channels (Liot et al., 2009), which has potential application to the pharmacological treatment of recurrent seizures. Second, there is experimental evidence suggesting that seizures are also capable of activating intrinsic and extrinsic apoptosis pathways (Henshall, 2007). Samples of hippocampus obtained from TLE patients present with raised levels of pro-apoptotic factors; however, few cells exhibit end-stage DNA fragmentation, suggesting that anti-apoptotic processes may also be engaged (Henshall et al., 2000).

Seizures can also cause long-lasting alteration in neuromodulator and neurotransmitter systems. Neuronal activity can lead to changes in gene expression and this process is particularly robust following the occurrence of seizures. Granule cells, classically glutamatergic neurons, can express heightened levels of glutamic acid decarboxylase and GABA following the occurrence of spontaneous epileptiform discharges in the limbic system (Sloviter et al., 1996). Selective changes in $GABA_A$ receptor subunit expression are also associated with TLE. For instance, pilocarpine induced *status epilepticus* can lead to an increased expression of α1, β4, δ and ε subunits in the hippocampus as well as increased $GABA_A$ receptor density (Brooks-Kayal et al., 1998). Understanding whether these changes contribute to or protect against the development of TLE and the occurrence of seizures is fundamental in contributing to effective therapies and could even contribute to understanding how neurosteroids can modulate epileptiform activity.

1.3. Temporal Lobe Epilepsy

Temporal lobe epilepsy (TLE) is a form of focal epilepsy in which seizure discharges originate from (or primarily involve) the hippocampus proper and para-hippocampal structures, including the amygdala, entorhinal cortex and temporal neocortex (Engel, 1996). TLE affects between 50-60% of patients suffering from focal epilepsy, and up to 75% of these patients are non-responsive to AEDs (Spencer, 2002; Wiebe, 2000). There are two major types of TLE identified as mesial and lateral. In mesial TLE, seizures arise from the hippocampus, amygdala or other medial structures of the limbic

system, whereas in lateral TLE seizures arise from the temporal neocortex; lateral TLE, however, makes up only a minority of TLE cases (<10%) (Kuzniecky and Jackson, 2005).

TLE, and in particular mesial TLE, is often associated with a brain insult that presumably triggers a series of neurobiological events during the latent period, which coincides with the process of epileptogenesis, ultimately leading to the generation of spontaneous seizures and the diagnosis of epilepsy (Pitkänen and Sutula, 2002). Examples of the initial insult include early childhood events such as birth trauma and complicated febrile seizures, or events occurring later in life such as head trauma, brain tumor, bacterial or viral infections affecting the central nervous system, and *status epilepticus* (Engel, 1996; French et al., 1993; Ono and Galanopoulou, 2012). The cascade of molecular, cellular and network changes that are associated with epileptogenesis do not stop at the onset of the chronic period since recurring seizures are thought to contribute to the progression of this disorder (Pitkänen and Sutula, 2002).

Histopathologically, patients with mesial TLE, especially those who remain unresponsive to AEDs, present with sclerosis of hippocampal and parahippocampal structures, which can be characterized by the loss of pyramidal cells, dispersion of granule cells and reactive gliosis (Blümcke et al., 2002). The degree of sclerosis is divided into three classes: Ammon's horn sclerosis (changes in CA1 to CA4 areas), hippocampal sclerosis (changes in CA1 to CA4 areas, dentate gyrus, and subiculum), and mesial temporal sclerosis (changes in amygdala, hippocampus and entorhinal cortex) (Kuzniecky and Jackson, 2005). As a result, patients with refractory TLE may experience a degree of memory loss or cognitive impairment, and present with behavioural abnormalities that can limit their daily functioning. In these cases, epilepsy may resemble a neurodegenerative disease (Ono and Galanopoulou, 2012).

1.4. The Structure of the Hippocampal Formation and Piriform Cortex

The hippocampal formation is a temporal lobe structure that is comprised of the dentate gyrus, the hippocampus proper or Ammon's horn, and the subiculum (Hayashi et al., 2015; Lopes da Silva et al., 1990). Together, these structures play an important role in the consolidation of working and spatial memory (Olton and Paras, 1979; Scoville and Milner, 1957). Classically, information is considered to flow from the entorhinal cortex to the dentate gyrus, from the dentate gyrus to the CA3 subfield of the hippocampus, and then from the CA3 to CA1 subfield through a series of pathways that form the trisynaptic circuit, which consists of the perforant pathway, mossy fiber pathway, and Schaffer collaterals, respectively (Andersen et al., 1971). The reverberation of activity

through the trisynaptic circuit has been shown to sustain and amplify epileptiform activity (D'Antuono et al., 2002; Pare et al., 1992).

At the head (or at the end) of the trisynaptic circuit, the entorhinal cortex serves as the major interface between the hippocampus and sensory cortices (Insausti et al., 1987). The entorhinal cortex contributes to the processing of spatial information (Killian et al., 2012) and must remain intact for the process of memory consolidation (Lu et al., 2013). Structurally, the entorhinal cortex consists of six layers. Beginning at the outermost layer, layer I contains a dense band of transversely oriented fibres and is relatively free of neurons; layer II is a narrow cellular layer containing modified pyramidal or stellate cells; layer III is composed of medium sized pyramidal cells that are organized in a columnar fashion; layer IV or the *lamina dissecans* is cell free; layer V contains large pyramidal cells; and layer VI is multilayered zone (Amaral et al., 1987; Insausti, 1993). Approximately one third of the inputs to the entorhinal cortex are derived from the piriform cortex, while other major inputs come from the temporal and frontal cortices (Vismer et al., 2015).

As mentioned, the entorhinal cortex sends important afferents to the hippocampal formation via the perforant pathway, which mainly terminates in the dentate gyrus (Hjorth-Simonsen, 1972; Steward, 1976; Witter and Groenewegen, 1984). Functionally, the dentate gyrus is considered to play a role in the differential storage of similar experiences and contexts (Vivar and Van Praag, 2013). Anatomically, the dentate gyrus is a three layered structure containing the molecular, granule cell, and polymorphic cell layers. The molecular cell layer, which contains the dendrites of the principal cells from the granule cell layer and interneurons, receives input from layer II of the entorhinal cortex through the perforant path (Witter, 2007). In turn, the dentate gyrus sends afferents to the hippocampus proper. The hippocampus proper is associated with spatial learning, short-term, and long-term memory (Hayashi et al., 2015). It is a seven layer structure consisting of the *stratum moleculare* (fibres and dendritic terminals), *stratum lacunosum* (bundles of parallel fibers), *stratum radiatum* (apical dendritic arborisation of pyramidal cells, sparse cell bodies and Schaffer collaterals), stratum pyramidale (densely packed pyramidal cell bodies), stratum oriens (basal dendritic arborisations of pyramidal cells and interneurons), alveus (pyramidal cell axons and incoming fibres), and epithelial zone (lining of ventricular surface of hippocampus) (Lopes da Silva et al., 1990). The hippocampus proper mainly receives input from the dentate gyrus through the mossy fibre projections of granule cells, which terminate on pyramidal cells in the CA3 subfield (Lopes da Silva et al., 1990). Schaffer collaterals of CA3 pyramidal cell axons then project to pyramidal cells of the CA1 subfield, ultimately facilitating the cortical storage of information (Amaral

and Witter, 1989). In addition to these local connections, the CA3 and CA1 areas also receive direct inputs from the entorhinal cortex. Projections from more lateral regions of the entorhinal cortex terminate at the dendritic shaft of parvalbumin positive interneurons located in the stratum lacunosum/moleculare, and in turn these interneurons innervate the perisomatic area and axon initial segment of pyramidal cells (Kiss et al., 1996). Physiologically, the monosynaptic-multisynaptic components of the perforant path could provide a functional advantage to information coding in the hippocampus proper as CA1 pyramidal cell firing would depend on the convergent excitation of the direct and indirect perforant path input (Buzsáki et al., 1995). Returning to the classical pathway, information then passes from the CA1 to the subiculum, a structure strategically placed to act as an interface between the hippocampus proper and parahippocampal regions.

Functionally, the subiculum seems to play a role in spatial encoding, but it also serves as the major output of the hippocampus and projects to structures that play various roles in learning and memory (Sharp and Green, 1994). It receives extensive projections from the CA1 hippocampal region (Finch and Babb, 1981; Witter and Groenewegen, 1990) and projects towards limbic and extralimbic areas including the amygdala (Canteras and Swanson, 1992), perirhinal cortex (Witter and Groenewegen, 1990), entorhinal cortex (Witter et al., 1989) and the thalamus (Canteras and Swanson, 1992; Witter et al., 1990). Although less extensive, a direct projection originating from layer III of the entorhinal cortex and terminating in the subiculum has also been reported (Van Groen and Lopes da Silva, 1986). This short entorhinal-subicular subicular-entorhinal circuit is functionally active, thus suggesting that hippocampal inputs and outputs can be modulated locally between these two regions (Van Groen and Lopes da Silva, 1986). Anatomically, the subiculum is a three-layered structure composed of a molecular layer, an enlarged pyramidal cell layer, and a polymorphous layer. The molecular layer is continuous with the *stratum lacunosum/moleculare* of the CA1 subfield; the pyramidal cell layer is less densely packed than in the CA1 and sends apical dendrites into the molecular layer, basal dendrites deeper into the pyramidal cell layer, and axons into the polymorphic (O'Mara et al., 2001; Stafstrom, 2005).

The piriform cortex is a three layer structure that receives input from the olfactory bulb and has strong connections to regions located within the limbic system, particularly the entorhinal cortex, amygdala, and subiculum (Vaughan and Jackson, 2014). The perception of odours involves the recruitment of distributed cortical and subcortical networks. Interaction with the orbitofrontal cortex either directly or indirectly through the thalamus contributes to identifying odours, assigning valance to a given odour, and predicting anticipated odour stimuli (Kringelbach and Rolls, 2004).

Limbic processing of olfactory stimuli mediated through entorhinal cortex and hippocampal formation plays an important role in memory, emotion and social behaviour (Royet et al., 2003). Furthermore, the activation of the amygdala in response to odour exposure may reflect the pleasantness and overall emotional value of the odour (Winston et al., 2005). The piriform cortex can also engage the fronto-temporal cortical stream in order to process information related to the naming of odours (Nigri et al., 2013). Like the hippocampus proper, the piriform cortex contains microcircuitry that provides excitation, feed-forward inhibition, and feedback inhibition (Vaughan and Jackson, 2014). Because of these extensive intrinsic projections and the high degree of connectivity to the entorhinal cortex, the piriform cortex is a common target of epileptiform discharge spread in temporal lobe epilepsy. This is supported by EEG-fMRI studies conducted in epileptic patients, which have shown that olfactory auras preceding seizures are associated with both lesions in the temporal lobe and the activation of the piriform cortex (Acharya et al., 1998; Laufs et al., 2011).

1.5. Epileptiform Synchronization

Coordinated neural activity, including interactions between neurons and between neuronal populations, is a hallmark of a healthy brain. The precise integration of neural activity occurs at specific spatiotemporal scales that range from milliseconds to hours and span short to long intra-cerebral distances (Jiruska et al., 2013; Varela et al., 2001). In epilepsy, neuronal activity displays abnormally enhanced excitability and synchronization, referred to as hypersynchronous activity (Jiruska et al., 2013). Hypersynchronous activity occurring spontaneously in a recurrent manner characterizes epilepsy, and this activity can be induced in the normal brain of species ranging from the fruit fly to the human, it can affect almost all neuronal networks, and its electrographic morphology is conserved despite the underlying pathology (TLE, Alzheimer's, stroke, autism, brain trauma, etc.) (Jirsa et al., 2014).

Neuronal synchronization in epilepsy, like in the healthy brain, can occur at different spatiotemporal scales and can be mediated by both synaptic and non-synaptic mechanisms (Jefferys et al., 2012a). Pharmacological manipulations that block GABAergic inhibition (penicillin, bicuculline, picrotoxin), boost glutamatergic excitation (medium containing low-Mg^{2+}), increase intrinsic excitability (low Ca^{2+}), or enhance both excitatory and inhibitory transmission by blocking K^{+} channels (4-aminopyridine or tetraethylammonium) have the ability to produce interictal and ictal events (Avoli et al., 1996a; Stanton et al., 1987; Swartzwelder et al., 1988). This wide array of

convulsants potentially demonstrates the diverse nature of mechanisms that can underlie epileptiform synchronization.

The extensive axon collateral network of pyramidal cells that, for example, project within the CA3 to the CA1, septum, and contralateral CA3 can play a role in synaptic synchronization (Prince, 1978; Queiroz and Mello, 2007; Traub and Wong, 1982). Under specific conditions, CA3 pyramidal cells can fire bursts of action potentials, and recruit a critical number of neurons to produce interictal and ictal events (Traub and Wong, 1982; Traub et al., 1993). Overtime, these synchronous pathways can be strengthened through sprouting of new connections in the chronic epileptic brain (Chen et al., 2013).

Inhibitory networks, can also contribute to the generation of ictal and interictal events. These networks entrain populations of excitatory neurons to generate hypersynchronous activity (Mann and Mody, 2008). $GABA_A$ receptor currents are mediated by the flux of Cl^- and HCO_3^- anions. In the adult brain in physiological conditions, the usually dominant Cl^- component is considered to be hyperpolarizing whereas HCO_3^- the component is generally depolarizing (Kulik et al., 2000). HCO_3^- is replenished in the cell by the activity of carbonic anhydrase and Cl^- is normally maintained at low intracellular concentrations by the KCC2 cotransporter (Miles et al., 2012; Payne et al., 2003). Excessive firing of inhibitory neurons can lead to an accumulation of intracellular Cl^-, and the increased extrusion of Cl^- and K^+ into the extracellular space (Viitanen et al., 2010). This can lead to a positive shift in the K^+ reversal potential or the generation of extracellular K^+ transients, which are a hallmark of epileptiform activity (McNamara, 1994). Furthermore, Cl^- accumulation can allow HCO_3^- to dominate the $GABA_A$ receptor-mediated current, leading to depolarization or even excitation. These findings suggest that $GABA_A$ receptor activation can lead to a depolarizing shift in E_{GABA}, producing a positive feedback loop that contributes to the initiation of seizure activity (Lillis et al., 2012). This view is supported by optogenetic studies conducted during bath application of 4AP to an *in vitro* hippocampal preparation; these experiments have shown that light-driven activation of parvalbumin positive interneurons induces ictal discharges resembling those that occur spontaneously (Shiri et al., 2015).

With the application of 4-aminopyridine (4AP; a K_{V1} channel blocker) *in vitro*, slow interictal events persist following the blockade of glutamatergic ionotropic transmission. These events, termed synchronous GABAergic events, can be abolished with either picrotoxin or bicuculline as well as by inhibiting GABA release from interneurons with mu opioid receptor agonists, and they are associated with marked increases in extracellular K^+ (Avoli et al., 1996a). Depolarizing $GABA_A$

receptor mediated events can lead to the generation of seizure-like events (Avoli, 1990) and in some cases may even be the sole synaptic mechanism leading to occurrence of ictal discharges (Uusisaari et al., 2002). Hyperpolarizing currents can also lead to a hyperexcitable state due to rebound excitation activated through the I_h current or the T-type current. Since a single interneuron innervates a large population of principal cells, rebound excitation driven by an interneuronal network can lead to epileptiform activity in pathological situations (Cobb et al., 1995; Surges et al., 2006).

During synchronous epileptiform events, extracellular Ca^{2+} levels have been found to decrease, presumably due to sustained membrane depolarization and action potential firing (Avoli et al., 1996b). It is worthwhile to note, however, that seizure-like events can also persist following blockade of synaptic transmission with low (or zero) extracellular Ca^{2+}, suggesting that synaptic transmission is not necessary for the generation of epileptiform activity (Jefferys and Haas, 1982; Yaari et al., 1983). Gap junctions can synchronize interneurons of the same subtype to promote synchronous firing of interneuronal populations (Beierlein et al., 2000). Neuronal activity can also generate electric fields, which can modulate the excitability of neighbouring neurons. These ephaptic effects may be at play during seizures, where fields of up to 20 mV can be generated, contributing to hypersynchronous activity (Jefferys, 1995). Increases in extracellular K^+ can also increase excitation synchronously for all neurons exposed to the ionic change (Heinemann et al., 1986). Whether synaptic or non-synaptic, the specific mechanisms underlying the generation of seizure-like events may represent potential targets to prevent epileptiform activity.

1.6. Interictal Discharges

Interictal discharges are hypersynchronous events recorded between seizures in epileptic patients, and in *in vivo* and *in vitro* animal models mimicking this neurological disorder. Although physiologically these events tend to be absent from the brain, interictal discharges have been detected in a small population of healthy subjects (Gregory et al., 1993; Jabbari et al., 2000). Furthermore, while it has been demonstrated that interictal discharges can herald the onset of an ictal discharge (Ayala et al., 1973), it has also been found that interictal discharges can also interfere with the occurrence of ictal events (Engel and Ackermann, 1980). Despite this, interictal events remain an important biomarker of epilepsy and they are one of the components used for diagnostic and localization purposes (Wirrell, 2010).

Early studies using penicillin to establish an epileptic focus found that neurons participating in the generation of interictal events generate a paroxysmal depolarizing shift coupled with sustained action potential firing, which is often followed by a long-lasting hyperpolarization (Matsumoto and Marsan, 1964; Sherwin, 1984). Building on these early studies, using the 4AP model, at least two types of interictal discharges have been identified. The first is between 50-300 ms in duration, occurs at a frequency of 0.25-2 Hz, and is consistently initiated by CA3 networks (Benini et al., 2003; De Guzman et al., 2004; Perreault and Avoli, 1991; Voskuyl and Albus, 1985). The second type of interictal discharge has a duration lasting up to 2.5 s, an interval of occurrence between 2 s and 50 s, and can be initiated by any limbic area, including the hippocampus proper (Perreault and Avoli, 1991; Voskuyl and Albus, 1985). These two types of interictal discharges have also been identified in the presence of pilocarpine (Nagao et al., 1996).

CA3-driven interictal events, or fast interictal events, can be recorded from the hippocampus proper and parahippocampal areas (Benini et al., 2003; De Guzman et al., 2004). Recurrent excitatory connections existing within populations of CA3 pyramidal cells contribute to the synchronization of local circuits (Miles and Wong, 1987, 1983). Fast interictal discharges can also be induced with $GABA_A$ receptor antagonists and they can be abolished by NMDA receptor antagonists, but persist when non-NMDA glutamatergic signaling is blocked (Perreault and Avoli, 1991). These fast interictal events are presumably mediated by a loss of inhibitory control over the spread of activity between CA3 pyramidal cells coupled with an intrinsic propensity for burst firing (Wong and Prince, 1981). Following their initiation in the CA3, these fast discharges can spread to the entorhinal cortex and other para-hippocampal structures through the Schaffer collaterals (Barbarosie and Avoli, 1997).

Long-lasting or slow interictal discharges were first identified in isolated hippocampal slices and they were found to co-exist with fast discharges (Voskuyl and Albus, 1985). These slow events do not have a fixed site of initiation, and they have been identified in the entorhinal an perirhinal cortices (De Guzman et al., 2004), the insular cortex (Sudbury and Avoli, 2007), the cingulate cortex (Panuccio et al., 2009), piriform cortex (Panuccio et al., 2012), and amygdala (Benini et al., 2003). Pharmacologically, these slow events are abolished by the application of $GABA_A$ receptor antagonists but persist in the presence of glutamatergic blockade (Panuccio et al., 2009; Perreault and Avoli, 1992). It is proposed that underlying slow events are long-lasting depolarizing potentials associated with action potential discharge in interneuronal networks (Avoli et al., 1996a; Michelson and Wong, 1994). Here, depolarizing $GABA_A$ receptor mediated signaling is capable of mediating a

form of excitatory communication among interneurons (Michelson and Wong, 1991). To date, the prognostic value of interictal discharge occurrence still needs to be clearly established. It is clear that interictal events play an important role in epilepsy, but a greater understanding of the mechanisms underlying interictal event generation, clear cut classification of interictal event types, and use of additional biomarkers will ultimately contribute to better diagnostic and localization methods in epilepsy patients.

1.7. Ictal Onset Patterns

A seizure is a dynamic event, and electrographically they can take on a number of morphologies (Schindler et al., 2007). One straightforward way to illustrate this phenomenon is the simple fact that an ictal event must begin and end, and while doing so is preceded by a pre-ictal period, possibly passes through a tonic and clonic period, and is then followed by the post-ictal period. Understanding why a seizure starts and stops is fundamental to the current paradigm used to treat epilepsy, i.e., seizure control. Despite the availability of pharmacological and surgical interventions, how the brain moves between physiological and hypersynchronous states, and *vice versa*, remains one of the most important but unanswered questions in epileptology. Second, ictal events themselves can be characterized by different onset patterns (Perucca et al., 2013). These ictal onset patterns may potentially provide insight into the underlying pathological substrate that leads to seizure activity in a given patient.

Studies addressing the spatial progression of a single seizure using EEG demonstrate that neuronal synchrony changes as the ictal event approaches and progresses. During the pre-ictal period, when analyzing the minutes leading up to a seizure, human studies demonstrate a decrease in synchronization between brain structures (Mormann et al., 2003). When assessing the seconds leading up to the seizure, the synchrony between brain regions was found to increase (Bartolomei et al., 2004). Thus the initiation of the seizure is presumably heralded by a period of desynchronous activity and a shorter period of synchronous activity occurring seconds before seizure onset. Once brain structures are initially synchronized, there is a period of rapid discharge (tonic component) which is characterised by the uncoupling of the brain regions involved (Bartolomei et al., 2004). As the seizure continues to evolve towards the late stage, the synchronicity between structures increases until the point of termination (Schindler et al., 2007). This hypersynchronous neuronal activity at the termination point, as reflected by EEG regional correlation studies, may also contribute to

explaining why seizures have a tendency to stop simultaneously in many regions (Schindler et al., 2007).

To probe further, the specific mechanisms that underlay the evolution of neuronal synchrony during the ictal event are presumably more nuanced. Since seizures are caused by different pathologies, the substrate mediating synchrony and desychrony between neural networks can vary. By understanding the networks and neurons involved in generating different ictal onset patterns, it is also possible to gain insight into the specific mechanisms underlying the state of synchronicity characterizing the epileptic network.

Clinically, temporal lobe seizures have been identified to display two main types of ictal onset patterns: hypersynchronous onset and low-voltage fast (LVF) onset (Ogren et al., 2009; Perucca et al., 2013; Velasco et al., 2000). Similar patterns of ictal onset have been identified in animal models of TLE *in vivo* (Bragin et al., 2005; Lévesque et al., 2012). It has also been proposed that LVF and hypersynchronous ictal onset patterns depend on the activity of distinct neural networks (Lévesque et al., 2012). LVF ictal onset patterns are characterized by low amplitude oscillations occurring at around 5-30 Hz (Bragin et al., 1999a; Velasco et al., 2000) and in most cases are preceded by an initial slow wave (Bragin et al., 2005). While it still remains unclear, it is suggested that the initial slow wave contributes to synchronizing the neuronal network, and in turn precipitating the seizure (Bragin et al., 2005). A computational modelling study suggests that LVF onset ictal events are linked to the abnormal and continuous generation of IPSPs mediated through a fast inhibitory feedback loop constituted by somatic projections from interneurons to pyramidal cells and the impairment of dendritic projections from interneurons to pyramidal cells (Wendling et al., 2002). Furthermore, a recent optogenetic study confirmed that under the application of 4AP, activation of parvalbumin positive interneurons can lead to the generation of LVF onset ictal events (Shiri et al., 2015). In animal models of TLE, LVF onset ictal discharges are found to correlate more with active wakefulness and paradoxical sleep (Bragin et al., 1999a). In most cases, LVF ictal patterns seem to be necessary for the propagation of the seizure to neocortical areas, which results in motor signs and an impairment of consciousness (Engel, 2001).

Hypersynchronous onset ictal events are characterized by low frequency high amplitude spikes occurring below 2 Hz and they have a tendency to be associated with greater neuronal loss and sclerosis in the hippocampus proper (Velasco et al., 2000). These ictal events were most likely to occur during sleep and immobility (Bragin et al., 1999a). It is postulated that hypersynchronous seizures are mediated dually by an increase in excitation and in inhibition. This hypothesis is

supported by indirect evidence demonstrating that inhibition is either preserved or enhanced in regions of sclerotic hippocampus (Bragin et al., 1999b; Wilson et al., 1998). Presumably, enhanced inhibition plays a role in suppressing seizures during the ictal event, while pathological recurrent excitatory circuits coupled with the presence of enhanced inhibition could contribute to driving the hypersynchronization of principal neurons for seizure genesis (Wilson et al., 1998). Unlike LVF ictal discharges, hypersynchronous seizures tend to be restricted to the hippocampus proper and adjacent structures, they take more time to spread to contralateral structures, and they either have no clinical correlate or correspond to auras (Engel, 2001).

1.8. High Frequency Oscillations

High frequency oscillations (HFOs, 80-500 Hz) were initially identified in the hippocampus and found to occur during slow-wave sleep, consummatory behaviours, and behavioural immobility (Buzsáki et al., 1992; Ylinen et al., 1995). They contribute to coordinating neuronal activity, consolidating synaptic plasticity, and are thought to be important in episodic memory (Axmacher et al., 2006; Buzsaki, 2009). Subsequently, HFOs have been recorded in the EEG of epileptic patients and in animal models of epilepsy, including models of TLE (Engel and Lopez da Silva, 2012; Jefferys et al., 2012). Studies analyzing patients' EEGs have demonstrated that HFOs are localized specifically to regions of seizure generation, and may be a better marker of the seizure onset zone than interictal spikes, which are considered to be the clinical standard (Jacobs et al., 2008, 2010). These pathological HFOs are commonly characterized as ripples (80-200 Hz) and fast ripples (250-500 Hz), and are thought to reflect the activity of dysfunctional neural networks.

Presumably, ripples represent principal neurons that are entrained by networks of synchronously active interneurons (Buzsáki et al., 1992; Ylinen et al., 1995). The synchronous firing of interneurons leading to ripples may arise through their phasic activation and subsequent generation of rhythmic inhibitory postsynaptic potentials in principal neurons (Ylinen et al., 1995). It is also possible that synchrony mediated through gap junctions between pyramidal cells or even interneurons in local networks can lead to ripples (Draguhn et al., 1998; Traub et al., 2001). In the pathological context, ripples can occur in brain regions that do not normally generate HFOs. For example, physiological ripples have yet to be detected in the dentate gyrus, but can be found under pathological situations (Bragin et al., 2004). Ripples can also be used as markers for ictogenesis since they were found to increase before the start of a seizure in rats and patient EEGs (Lévesque et al., 2012; Zijlmans et al., 2011).

Unlike ripples, fast ripples may not require the contribution of interneuronal activity since they can be recorded in the presence of $GABA_A$ receptor blockade (Dzhala and Staley, 2004). Instead, fast ripples are thought to be mediated either through principal cell synchronization or the loss of synchrony in a population of cells bursting at lower frequencies (100-200 Hz) (Bragin et al., 2011; Engel Jr et al., 2009; Ibarz et al., 2010). Initially identified in patients with mesial TLE and in pilocarpine-treated rats, fast ripples were found to be associated with interictal discharges and seizure onset (Bragin et al., 1999b, 1999c). Since fast ripples seem to be uniquely associated with regions that are capable of generating spontaneous seizures, they have emerged as a potential biomarker of epileptogenic regions in patients (Staba et al., 2002).

HFOs also occur differentially with respect to ictal onset patterns. LVF onset events, which generally occur during wakefulness of paradoxical sleep when fast ripple occurrence is low, were found to be associated with lower levels of fast ripples (Bragin et al., 1999a). Hypersynchronous onset events, which most likely occur during sleep or quiet mobility, when fast ripple occurrence is high, were found to be associated with higher levels of fast ripples (Bragin et al., 1999a). Another study found that LVF onset events are associated with a greater increase in the ripple rate compared to the fast ripple rate, whereas the inverse was observed in hypersynchronous onset ictal events (Lévesque et al., 2012). It has therefore been suggested that hypersynchronous events could involve the same neural mechanisms that mediate fast ripples and LVF events could involve mechanisms underlying ripple generation; however, caution should be exercised when interpreting these results (Lévesque et al., 2012).

1.9. Cellular Components of the Ictogenic Network

The neuronal networks implicated in epileptiform synchronization are extensive and involve both excitatory and inhibitory components. Classically, the generation of epileptiform activity was attributed to excessive glutamatergic activity coupled with a reduction of inhibition (Ayala et al., 1973). Conceptualizing a hyperexcitable network in terms of a dichotomous inhibitory-excitatory relationship, however, fails to capture the full extent of mechanisms that underlie epileptic disorders. To date, studies suggest that inhibition is often maintained in the epileptic brain and they can contribute to the generation of both interictal spikes and seizures (Avoli and de Curtis, 2011).

While TLE can be associated with the selective loss of specific interneuronal subtypes, compensatory mechanisms can contribute to preserving inhibitory mechanisms. In the CA1 of pilocarpine or kainate treated rats, both parvalbumin positive axo-axonic cells and somatostatin

containing interneurons with axons projecting to the stratum lacunosum-moleculare (O-LM cells) degenerate following status epilepticus (Dinocourt et al., 2003; Ratté and Lacaille, 2006). In patients with refractory TLE, the loss of axo-axonic cells has also been described in the neocortex (Marco et al., 1996), whereas axo-axonic cells terminating on dentate granule cells are found to be preserved (Wittner et al., 2001). Despite the degeneration of some interneuronal subtypes in specific brain regions, functional studies have found that inhibition in patients with and animal models of TLE remain intact. In one study, the loss of GABAergic inhibition in pyramidal cell dendrites was accompanied by an increase in inhibition at the cell soma (Cossart et al., 2001). On one hand, the deficit in dendritic inhibition could lower the seizure threshold but conversely, the enhanced somatic inhibition could increase the seizure threshold. Overall, it has been suggested that the sprouting and synaptogenesis of existing interneurons can mediate a compensatory restoration of inhibitory mechanisms (Cossart et al., 2001; Maglóczky et al., 2000; Wyeth et al., 2010). However, despite the preservation of GABAergic mechanisms, epileptic activity persists in animal models of TLE and in patients with TLE.

Interestingly, evidence obtained from acute models of ictogenesis *in vitro* suggests that the reorganization of the interneuronal network may contribute to sustaining ictogenesis. The application of 4AP to hippocampal slices obtained from young rodents has revealed that prolonged epileptiform discharges are preceded by interneuron firing and the activation of $GABA_A$ receptors (Avoli and de Curtis, 2011; Jefferys et al., 2012a). 4AP is a convulsant that enhances the release of both excitatory and inhibitory neurotransmitters without influencing the postsynaptic response of hippocampal pyramidal cells to GABA (Perreault and Avoli, 1991). One of the possible mechanisms contributing to the initiation and maintenance of ictal events by $GABA_A$ receptor mediated currents is the concurrent increase of local extracellular $[K^+]$, which in turn should excite neighbouring neurons (Avoli et al., 1996a, 1996b).

The involvement of interneuron activity (and thus of GABA release) in seizure initiation is corroborated by *in vivo* studies that examined the relationship between the recorded local field potential and the single unity activity of hippocampal neurons in pilocarpine treated epileptic rats. The authors found that as the epileptic network transitioned from the interictal period to the ictal event, interneurons were increasingly coherent with oscillations in the gamma frequency range and displayed higher firing rates (Grasse et al., 2013). Principal neurons were recruited following the onset of the ictal event, and as the rate of pyramidal cell firing increased, interneuronal firing rates dropped (Grasse et al., 2013). These findings are supported by evidence, again obtained from

pilocarpine treated epileptic rats, that show interneurons in the subiculum, dentate gyrus, and CA1 are activated during the preictal period and decrease their activity only after the onset of the ictal event (Fujita et al., 2014; Toyoda et al., 2015). In the neocortex of patients with refractory epilepsy, studies implementing microelectrode arrays to identify putative interneurons and principal cells also demonstrate that the increase of interneuronal activity during the preictal period was significantly greater than the corresponding increase observed in principal neurons (Truccolo et al., 2011). Together, these findings contribute to the growing body of evidence that GABAergic synchronization can play an important role at seizure onset in TLE.

In addition to GABAergic mechanisms, the involvement of the glutamatergic system should not be discounted. The first line of evidence suggesting that glutamate also plays an important role in TLE is the clinical use of Perampanel, an AMPA receptor antagonist, for controlling focal onset seizures (Schmidt and Schachter, 2014). Studies conducted in laboratory animals show that glutamate and glutamate analogues such as kainate can reproduce neuronal excitotoxicity, ultimately resulting in the occurrence of spontaneous limbic seizures that coincide with neuronal loss (Olney et al., 1986). Animal studies also demonstrate that the persistent electrical stimulation of the perforant path, which is composed of excitatory afferents, is also capable of generating spontaneous seizures (Sloviter, 1983). In *in vitro* studies, the application of a NMDA receptor antagonist to 4AP treated slices effectively abolishes the occurrence of ictal events and the further use of a non-NMDA receptor antagonist is capable of abolishing all epileptiform activity with the exception of isolated slow events (Avoli et al., 1996a).

1.10. Glial Cells in Hyperexcitable Networks

Glial cells are considered to be important components of the neural network. In the central nervous system, three main types of glial cells have been identified—astrocytes, oligodendrocytes and microglia. Astrocytes have a star-like appearance and function to maintain the surrounding environment to optimize neuronal signalling; oligodendrocytes lay the myelin sheath around axons to facilitate signal propagation; and microglia act as scavenger cells to remove cellular debris in regions of cell damage or cell turnover (Seifert and Steinhäuser, 2013). Glial cells outnumber neurons by a ratio of 3-to-1, and astrocytes (~17% of glial cells) and microglia (~6.5% of glial cells) are thought to contribute significantly to the pathophysiology of epilepsy (Devinsky et al., 2013). For instance, the sclerotic tissue often found in the hippocampus of TLE patients and in animal models

of epilepsy is characterized by the activation and proliferation of astrocytes and microglia coupled with the increased arborisation of and complexity of astrocytic processes (Devinsky et al., 2013).

Astrocytes are involved in guiding neuronal migration, modulating synaptic function and plasticity, buffering neurotransmitter, ion and water concentrations, regulating local blood flow and delivering energy substrates, and maintaining the blood brain barrier. In addition, they can also actively participate to processing neural information (Devinsky et al., 2013). Like neurons, astrocytes also express a similar array of ion channels and transmitter receptors, and thus are able to detect and respond to neuronal activity (Verkhratsky and Steinhäuser, 2000). A seminal study characterizing the cross-talk between neurons and astrocytes found that astrocytes were capable of regulating neuronal calcium levels through the Ca^{2+} dependent release of glutamate (Parpura et al., 1994). Since this study, it has been established that astrocytes can integrate synaptic activity, and release gliotransmitters such as glutamate, D-serine, and ATP depending on intracellular Ca^{2+} levels (Halassa et al., 2007). The interconnection between astrocytes and neurons have given rise to the concept of the tripartite synapse which includes, pre-synaptic elements, post-synaptic elements, and astrocytic processes (Halassa et al., 2007).

During seizure, patients show an additional increase in extracellular glutamate to levels 6-fold higher than those recorded during the interictal period, and levels remain elevated for a period of up to twenty minutes following seizure (During and Spencer, 1993). It appears that astrocytic dysfunction could be one of the main culprits. Physiologically, glutamate released into the brain is cleared from the synaptic space predominantly through astrocyte-mediated reuptake, followed by conversion to glutamine (Lanerolle et al., 2010). Glutamine is then released by astrocytes into the extracellular space allowing for neuronal uptake and conversion to glutamate (Lanerolle et al., 2010). This glutamine-glutamate cycle is slowed and glutamate reuptake is impaired in the sclerotic hippocampus (Seifert and Steinhäuser, 2013). It is also suggested that astrocytes of the sclerotic hippocampus may be capable of Ca^{2+} dependent exocytotic release of glutamate through either astrocyte swelling or through the activation of specific transcription factors (Lanerolle et al., 2010).

Astrocytes can also contribute to the maintenance of extracellular K^+ levels through spatial buffering. This process is dually driven by the glial syncytium membrane potential and the local K^+ membrane potential (Seifert and Steinhäuser, 2013). Spatial buffering depends on the proper distribution of gap junctions between astrocytes, K^+ channels, and water pores (Seifert and Steinhäuser, 2013). It is suggested that impaired spatial buffering in the sclerotic hippocampus is due to the down-regulation of astrocytic K_{ir} channels (Kivi et al., 2000). Interestingly, the down-

regulation of K_{ir} channels is also associated to the impairment of glutamate reuptake from the extracellular space (Djukic et al., 2007) and it can contribute to the induction of NMDA-receptor mediated hyperexcitability (Friedman et al., 2009).

In addition to astrocytes, seizures can also activate microglia (Devinsky et al., 2013). Currently, research suggests that the functional outcome of microglial activation is context dependant. For instance, the prolonged activation of microglia can lead to cellular dysfunction and death, while a discrete activation can have anti-inflammatory effects (Devinsky et al., 2013). Findings obtained in the epileptic tissue suggest that the extent of microglia activation correlates with both the disease duration and seizure frequency, but activated microglia can reduce seizure thresholds (Vezzani et al., 2011). Therefore, glial cells play an important role in the establishment of hyperexcitable networks.

1.11. Steroid Hormones, a Background in Epilepsy

Steroid hormones have long been established to be important modulators of neuronal activity. Early studies showed that progesterone can produce deep anaesthesia while testosterone is capable of inducing slowly developing but prolonged anaesthesia that in some cases is preceded by convulsions; in contrast, estrogens did not produce anaesthetic effects (Selye, 1941). Generally, progesterone and its metabolites are found to have anti-convulsant properties, whereas estrogens are pro-convulsant. The effects of androgens have a tendency to be more varied but overall they have anti-convulsant effects; however, estrogen is among one of their metabolites (Taubøll et al., 2015). Today, the effects of steroid hormones are recognized to have important implications in the progression and treatment of epilepsy.

Both men and women with TLE can experience sexual and reproductive dysfunction. In patients with pharmacoresistant focal epilepsy, levels of sex steroids in the serum normalize following the surgical removal of the epileptic foci (Bauer et al., 2000). It has been proposed that these effects may be attributed to the suppression of the hypothalamic-pituitary-gonadal axis by limbic seizures (Bauer et al., 2002; Herzog et al., 1986). Additionally, catamenial seizure exacerbations can affect up to 70% of women with epilepsy who are in their reproductive years (Reddy, 2004a). In these patients seizures occur in cyclical patterns associated with specific phases of the menstrual cycle suggesting that this phenomenon reflects of the fluctuation of neurosteroids (Scharfman, 2003). Evidence suggests that steroid hormones are capable of affecting neural excitability through molecular interactions with both intracellular signalling pathways and receptors

proteins located at the level of the membrane (McEwen, 1991); however, neurosteroids are regarded to have a more potent effect on neural excitability (Taubøll et al., 2015).

1.12. Neurosteroids in Epilepsy

Neurosteroids are a class of compounds that exert no known genomic effects but instead have the ability to modulate neuronal excitability at the level of ion channels and membrane receptors (Akk et al., 2009; Mellon and Griffin, 2002). These compounds are endogenously synthesized from circulating steroidal precursors in both glial cells and principal neurons (Baulieu, 1998; Compagnone and Mellon, 2000). The enzymes involved in the production of neurosteroids are differentially localized between glial cells and neurons, as well as within different regions of the brain; these findings suggest that different cell types must cooperate to produce appropriate levels of active neurosteorids, and that neurosteroids may have regionally specific roles (Mellon and Griffin, 2002; Mellon et al., 2001). Neurosteroids fall into three main classes; the pregnane, androstane and sulfated neurosteroids (Reddy, 2010). The former two exert mainly inhibitory effects and the latter, excitatory (Majewska, 1992; Reddy, 2010).

The direction in which neurosteroids modulate excitability depends on the type of receptor and the receptor binding site that is targeted. For example, sulphated neurosteroids such as dehydroepiandrosterone generate an increase in neuronal excitability by interacting with the picrotoxin site of the $GABA_A$ receptor (Park-Chung et al., 1999; Sousa and Ticku, 1997). Pregnenolone sulfate, another example of sulphated neurosteroid, acts as a positive allosteric modulator of the NMDA receptor (Wu et al., 1991). In addition, some sulphated neurosteroids, such as 3α-Hydroxy-5β-pregnan-20-one sulfate, have been identified to inhibit NMDA receptor Ca^{2+} responses but not those induced by kainate or high levels of extracellular K^+ (Irwin et al., 1994). Thus, sulfated neurosteroids exert their effect through a number of different mechanisms; however, overall they generally lead to an enhancement of brain excitability. On the other hand, non-sulphated neurosteroids such as allotetrahydrodeoxycorticosterone (THDOC), pregnanolone, and allopregnanolone, positively modulate $GABA_A$ receptors by binding to two sites within the transmembrane domain of the α and β subunits (Hosie et al., 2006). Endogenous neurosteroids play an important role in the regulation of neuronal excitability and they can even influence seizure susceptibility (Członkowska et al., 2000).

Pregnane neurosteroids such as THDOC and allopregnanolone are found endogenously at nanomolar concentrations (Reddy, 2011). These compounds increase the channel open probability

of $GABA_A$ receptor channels by facilitating late channel openings, which ultimately result in the prolongation of the slow deactivation phase (Zhu and Vicini, 1997). Furthermore, by increasing the mean open time of $GABA_A$ receptors channels, these compounds can potentiate both phasic and tonic currents (Reddy, 2011; Wohlfarth et al., 2002); however, it is worth noting that the δ subunit of the $GABA_A$ receptor confers a greater transduction of the neurosteroid signal upon binding of THDOC (Mihalek et al., 1999; Wohlfarth et al., 2002). $GABA_A$ receptors containing the δ subunit are mainly found extrasynaptically and are more resistant to desensitization but have a low affinity to GABA, even at saturating concentrations (Glykys and Mody, 2007; Wohlfarth et al., 2002). THDOC can enhance the tonic current generated by these receptors in a way that increasing GABA alone cannot (Wohlfarth et al., 2002).

In patients with TLE and in animal models of the disease, $GABA_A$ receptor expression is extensively altered in a region and neuronal-subtype specific manner, which ultimately affects both phasic and tonic forms of inhibition (Fritschy et al., 1999; Loup et al., 2000). For instance, following the induction of TLE in rats with continual hippocampal stimulation, δ subunit containing receptor expression is reduced in dentate gyrus granule cells while there is an increase in the expression of $\alpha_4\gamma_2$ containing subunits (Rajasekaran et al., 2010). The increase in $\alpha_4\gamma_2$ containing subunits presumably acts as a compensatory mechanism for the initial reduction in tonic inhibition. Similar findings were also observed in pilocarpine treated mice, but the authors also found that δ subunit containing receptor expression increased in hippocampal interneurons (Peng et al., 2004). Furthermore, dentate gyrus granule cells exhibit an increase in the expression of synaptic $GABA_A$ receptors, which is coupled with a reduced sensitivity to benzodiazepines (Leroy et al., 2004). The down regulation of δ subunit containing receptors combined with the reduced benzodiazepine sensitivity of existing receptors suggest that TLE may be associated with reduced levels of neurosteroid sensitivity (Leroy et al., 2004). Additional changes in epileptic animals which can also alter neurosteroid sensitivity include a loss of GABAergic neurons in the subiculum (Knopp et al., 2008) and a shift in inhibition such that principal cell GABAergic input is reduced while interneuronal GABAergic input is enhanced in the piriform cortex (Gavrilovici et al., 2006). These changes have important implications for understanding how neurosteroids modulate neurotransmission in the epileptic brain, especially because anti-convulsant effects of neurosteroids have been reported in the literature (*cf.* Reddy, 2011).

THDOC and allopregnanolone act as a broad spectrum anticonvulsants that act by modulating the efficacy of $GABA_A$ receptor function to enhance the inhibitory tone of the brain

(Reddy, 2004b; Rupprecht et al., 1996). Both these compounds protect against seizures induced by pilocarpine, kindling and $GABA_A$ receptor antagonists in animal models of epilepsy *in vivo* (Belelli et al., 2002; Gangisetty and Reddy, 2010; Kaminski et al., 2005). *In vitro* studies performed in rat hippocampal slices have shown that inhibitory neurosteroids can produce a concentration dependent suppression of epileptiform activity in 4AP and picrotoxin treated slices (Salazar et al., 2003). Furthermore, i*n vitro* studies conducted in the pilocarpine model of TLE have shown that the acute application of THDOC confers a greater degree of anti-ictogenic effect following the application of 4AP compared to non-epileptic controls (Shiri et al., 2015). Following pilocarpine treatment in rats, *in vivo* studies show that the induction of neurosteroid synthesis can potentially delay the development of spontaneously occurring seizures following *status epilepticus* (Biagini et al., 2006, 2009). Together this evidence suggests that despite changes in $GABA_A$ receptor subunit expression, neurosteroids have important anti-ictogenic and anti-epileptogenic properties.

1.13. Research Rationale & Specific Objectives

Acute *in vitro* convulsant models of ictogenesis have contributed greatly to our understanding of the fundamental mechanisms underlying hyperexcitability of neuronal networks in epilepsy. While such acute convulsant models are not capable of simulating epilepsy as a disorder, they can act as a powerful tool that reveals the involvement of different structures, pathways, and cell types in the generation of specific patterns of epileptiform activity. 4AP is one such convulsant that is capable of generating a dynamic range of epileptiform activity containing periods of ictal and interictal discharges. Taking advantage of these aspects, I set out to address the following questions:

a. What patterns of ictal onset can be identified *in vitro* in the 4AP model of ictogenesis? (*Chapter 2*)
b. Can distinct patterns of interictal activity predict ictal onset patterns? (*Chapter 2*)
c. How do reciprocal connections between the subiculum and entorhinal cortex contribute to the generation of epileptiform activity? (*Chapter 3*)
d. Do neurosteroids differentially modulate the anterior and posterior piriform cortices? (*Chapter 4*)
e. Do neurosteroids differentially modulate patterns of high frequency oscillations in a regionally specific manner? (*Chapter 4*)

f. How do neurosteroids modulate interictal discharges predominantly mediated by glutamatergic mechanisms (*fast* events) vs those mediated by predominantly GABAergic mechanisms (*slow* events)? (*Chapter 5*)

The existence of two types if interictal discharges has been well established in the 4AP model (reviewed in *Chapter 1.6*); however the patterns of ictal onset have yet to be systematically described. In the first study of my thesis, the aim was to quantitatively describe the patterns of ictal onset observed in the entorhinal cortex during the application of 4AP with respect to preceding patterns of interictal activity and high frequency oscillations. As different patterns of ictal onset can be identified in *in vivo* models of epileptiform synchronization and in patients with temporal lobe epilepsy (Lévesque et al., 2012; Perucca et al., 2013), it is important to identify whether isolated networks *in vitro* are capable of generating different ictal onset patterns. Findings have the potential to provide further insight into the mechanisms underlying the generation of these patterns. Furthermore, because different ictal onset patterns are presumably associated with distinct underlying mechanisms (Lévesque et al., 2012), AEDs could differentially modulate these patterns of epileptiform activity.

In *Chapter 3* of my thesis, I addressed how the connectivity between the hippocampus proper and the entorhinal cortex contributes to the generation of the previously described ictal onset patterns and their associated interictal discharge patterns. To this end, I turned by attention to the subiculum and the entorhinal cortex. The subiculum is strategically located to control the spread of epileptiform activity between the hippocampus proper to the parahippocampal areas of the limbic system. As long as $GABA_A$ receptor mediated signalling was maintained, the subiculum was capable of blocking the propagation of CA3 driven interictal events to the entorhinal cortex (Benini and Avoli, 2005). Because GABAergic contributions were identified to be an important component of LVF onset ictal activity (Avoli et al., 2013; Lévesque et al., 2012; Shiri et al., 2015), the aim of this study was to understand how local subiculum-entorhinal cortex connections contribute to the generation of LVF and sudden onset ictal events.

After systematically characterizing the patterns of ictal onset activity and establishing how they can be modulated between the hippocampus proper and entorhinal cortex, in *Chapter 4* & *5* I addressed how the neurosteroid THDOC can modulate ictal and interictal events in the piriform cortex and the CA3 subfield of the hippocampus, respectively. In *Chapter 4*, I specifically addressed how THDOC could modulate ictogenesis between the anterior and posterior piriform cortices.

These regions are of interest because they receive differential degrees of GABAergic input (Vismer et al., 2015). Understanding how differences in GABAergic tone can affect the efficacy of neurosteroids is important to understanding their potential as an AED in TLE because, as previously reviewed in *Chapter 1.13*, $GABA_A$ receptor expression is altered. In *Chapter 5*, I then assessed how neurosteroids modulated *fast* and *slow* interictal discharges—two types of epileptiform events with different GABAergic and glutamatergic components.

2. TWO DIFFERENT INTERICTAL SPIKE PATTERNS ANTICIPATE ICTAL ACTIVITY IN VITRO

By Avoli M, Panuccio G, Herrington R, D'Antuono M, de Guzman P, Lèvesque M

Published in Neurobiology of Disease, 2013

2.1. Rationale and Objective

4AP is widely employed in *in vitro* studies to generate hyperexcitable activity, allowing for greater understanding of the mechanisms underlying ictogenesis. To date, there is no detailed information characterizing the patterns of epileptiform synchronization generated in this *in vitro* model. Furthermore, studies conducted on seizure onset patterns in *in vivo* animal models and in patients reveal that specific ictal onset patterns can be identified in TLE (reviewed in section 1.6). In order to establish specific patterns associated with ictal discharges recorded *in vitro*, we performed a quantitative analysis of the electrophysiological characteristics of interictal and ictal events generated during 4AP application in the entorhinal cortex. Furthermore, we analyzed the association of ripples and fast ripples to ictal onset patterns because of their importance in localizing the seizure onset zone and their different underlying mechanisms. It has been suggested that distinct ictal onset patterns could be associated with different underlying mechanisms and identifying these differences could have important implications in the interpretation of results obtained *in vitro* under 4AP, in the understanding of the mechanisms underlying any given epileptiform event, and can even contribute to treatment paradigms to be employed in the future.

2.2. Abstract

4-Aminopyridine (4AP, 50 μM) induces interictal- and ictal-like discharges in brain slices including parahippocampal areas such as the entorhinal cortex (EC) but the relation between these two types of epileptiform activity remains undefined. Here, by employing field potential recordings in rat EC slices during 4AP application, we found that: (i) interictal events have a wide range of duration (0.4-3.3 s) and interval of occurrence (1.4-84 s); (ii) ictal discharges are either preceded by an isolated "slow" interictal discharge (ISID; duration=1.5 ± 0.1s, interval of occurrence=33.8 ± 1.8 s) or suddenly initiate from a pattern of frequent polispike interictal discharge (FPID; duration=0.8 ± 0.1 s; interval of occurrence=2.7 ± 0.2 s); and (iii) ISID-triggered ictal events have longer duration (116 ± 7.3s) and interval of occurrence (425.8 ± 42.3 s) than those

initiating suddenly during FPID (58.3 ± 7.8 s and 202.1 ± 21.8 s, respectively). Glutamatergic receptor antagonists abolished ictal discharges in all experiments, markedly reduced FPIDs but did not influence ISIDs. We also discovered that high-frequency oscillations (HFOs, 80-500 Hz) occur more frequently during ISIDs as compared to FPIDs, and mainly coincide with the onset of ISID-triggered ictal discharges. These findings indicate that interictal events may define ictal onset features resembling those seen in vivo in low-voltage fast activity onset seizures. We propose a similar condition to occur in vivo in temporal lobe epileptic patients and animal models.

2.3. Introduction

Brain slices maintained in vitro generate electrographic seizure-like events – which may represent the equivalent of ictal phenomena seen in patients and in animal models in vivo – when $GABA_A$ receptor mediated inhibition is not fully blocked or even enhanced (see for review Avoli and de Curtis, 2011). Procedures capable of eliciting these long lasting (ictal-like) epileptiform discharges include decreased Mg^{2+} (Köhling et al., 2000; Zhang et al., 2012) or increased K^+ (Jensen and Yaari, 1997; Traynelis and Dingledine, 1988) in the superfusing medium, bath application of the K^+ channel blocker 4-aminopyridine (4AP) (Avoli et al., 1993, 1996; Benini et al., 2003; Dzhala and Staley, 2003; Lillis et al., 2012) or combinations of them (Ziburkus et al., 2006).

Studies performed in adult rodent parahippocampal structures have shown that during 4AP application, ictal-like (hereafter referred as ictal) discharges recorded from the entorhinal cortex (EC), amygdala or insular cortex are shortly preceded (and thus heralded) by an isolated "slow" interictal-like spike (ISIS) similar to those recurring at long intervals between successive ictal discharges (see for review Avoli and de Curtis, 2011). This type of interictal activity is largely contributed by $GABA_A$ receptor signaling, and it is associated with transient increases in $[K^+]_o$ (Avoli et al., 1996; Lopantsev and Avoli, 1998b). However, in some experiments, 4AP induces a different type of epileptiform synchronization in the EC; this pattern is characterized by frequent polispike interictal discharges (FPIDs) that are suddenly interrupted by an ictal event (Lopantsev and Avoli, 1998a).

Although the in vitro 4AP model has been widely employed to understand the cellular and pharmacological mechanisms underlying ictogenesis (see for review Avoli and de Curtis, 2011), no detailed information on these different patterns of epileptiform synchronization is available. Therefore, we performed here a quantitative analysis of the electrophysiological characteristics of interictal- and ictal-like discharges generated during 4AP application by the EC in brain slices that

also included the hippocampus proper. However, since ictogenesis in parahippocampal areas can be controlled by hippocampal output activity (Avoli and de Curtis, 2011; Barbarosie and Avoli, 1997; Benini et al., 2003), the EC was either functionally or surgically disconnected from the hippocampus to allow ictal discharge generation. In addition, we established the occurrence of high frequency oscillations (HFOs, 80–500 Hz) during these different patterns of interictal and ictal epileptiform activity. HFOs occur in limbic structures such as the EC and hippocampus, and are thought to reflect the activity of dysfunctional neural networks (Bragin et al., 2004; see for review Jefferys et al., 2012; Engel and Lopes da Silva, 2012).

2.4. Methods

Slice preparation and maintenance **-** Male, Sprague-Dawley rats (150–300 g) were decapitated under isoflurane anesthesia according to procedures established by the Canadian Council on Animal Care. All efforts were made to minimize suffering and the number of animals used. The brain was quickly removed and placed in cold, oxygenated artificial cerebrospinal fluid (ACSF). The brain's dorsal side was cut along a horizontal plane that was tilted by a 10^{o} angle along a posterosuperior-anteroinferior plane passing between the lateral olfactory tract and the base of the brainstem (Avoli et al. 1996). Horizontal slices (450 μm thick) containing the EC and the hippocampus were cut from this brain block using a vibratome. Slices were then transferred into an interface tissue chamber where they layed between ACSF (pH 7.4) and humidified gas (95% O2, 5% CO2) at a temperature of 32-34 °C. ACSF composition was (in mM): NaCl 124, KCl 2, KH_2PO_4 1.25, $MgSO_4$ 2, $CaCl_2$ 2, $NaHCO_3$ 26, and D-glucose 10. 4AP (50 μM), 6-cyano-7-nitroquinoxaline-2,3-dione (CNQX, 10 μM), 3,3-(2-carboxypiperazin-4-yl)-propyl-1-phosphonate (CPP, 10 μM), and picrotoxin (50 μM) were bath-applied. Chemicals were acquired from Sigma (St Louis, MO, USA). Surgical separation of the EC from the hippocampus proper was performed in some experiments with a knife mounted on a micromanipulator at the beginning of the experiment to further minimize the influence exerted by CA3-driven activity on EC epileptiform synchronization (Barbarosie & Avoli, 1997; Benini et al., 2003)

Electrophysiological recordings **-** Field potential recordings were made with ACSF-filled, glass pipettes (resistance= 2-10 MΩ) that were connected to high-impedance amplifiers. The recording electrodes were positioned in the EC deep layers. Field potential signals were fed to a computer interface (Digidata 1322A, Molecular Devices, Palo Alto, CA, USA) and acquired and stored using

the pCLAMP 9 software (Molecular Devices). Subsequent analysis of these data was made with the Clampfit 9 software (Molecular Devices).

Detection of high-frequency oscillatory events - A multi-parametric algorithm was employed to identify oscillations in each frequency range, using routines based on standardized functions (Matlab Signal Processing Toolbox). Raw field potential recordings were band-pass filtered in the 80-200 Hz and in the 250-500 Hz frequency range using a Finite Impulse Response (FIR) filter. Zero-phase digital filtering was used to avoid phase distortion. A 10 s artifact-free period (40-50 s before the onset of an ictal event for the analysis of HFOs during ictal activity and a 10 s artifact-free time-period for the analysis of HFOs during interictal activity) was selected as a reference for signal normalization. In this way, field potential recordings were normalized using their own reference period.

To be considered as HFO candidates, oscillatory events in each frequency band had to show at least four consecutive cycles having amplitude of 3 SD above the mean of the reference period. The time lag between two consecutive cycles had to be between 5 and 12.5 ms for ripples (HFOs at 80-200 Hz) and between 2 and 4 ms for fast ripples (HFOs at 250-500 Hz). Ripples were kept for analysis only if they were visible in the 80-200 Hz range, whereas fast ripples were kept only if they were visible in the 250-500 Hz range. Oscillatory events containing overlapping ripples and fast ripples were excluded from the analysis.

During ictal discharges, field recordings were analysed for the occurrence of HFOs during the pre-ictal period (from 40 s to the time of ictal event onset) and during the ictal period. To account for differences between the duration of ictal events, the ictal event was normalised from 0 (start of the event) to 100 (end of the event). The pre-ictal and ictal periods were then divided in three equal parts and rates of ripples and fast ripples in each part were compared using non-parametric Wilcoxon signed rank tests followed by Bonferroni-Holm corrections for multiple comparisons. This allowed us to evaluate whether ripples or fast ripples predominated during specific moments of the pre-ictal and ictal periods.

Database and analysis - Throughout this study we arbitrarily termed as 'interictal' and 'ictal' the synchronous epileptiform events with durations shorter or longer than 3 s, respectively (*cf.* Traub et al., 1996). Epileptiform activity was recorded during continuous 4AP application from over 100 brain slices of which 82 were quantitatively analyzed. HFOs analysis was performed in 34 of these

experiments. Measurements in the text are expressed as mean ± SEM and *n* indicates the number of slices included in any specific measurement. Data were compared with non-parametric Mann-Whitney tests and Kruskall-Wallis tests followed by Bonferroni post-hoc tests for multiple comparisons. Wilcoxon signed rank tests were applied to compare rates of HFOs between ictal discharges that were ISIS-triggered or occurred suddenly during FPID. The level of significance was set to $P < 0.05$.

2.5. Results

Epileptiform activity induced by 4AP in the EC - We recorded both ictal (dotted lines in Figs. 1A and B) and interictal (arrows in Figs. 1A and B) discharges from the EC of "intact" brain slices (n=84) during 4AP application. Ictal events lasted 100.7 ± 6.1 s (mean ± SEM) and occurred every 316.4 ± 27.1 s while interictal activity had duration of 1.2 ± 0.1 s and interval of occurrence of 21.7 ± 2 s. Simultaneous recordings obtained from EC and CA3 showed that the frequent (0.5–1 Hz) interictal activity generated by CA3 networks (Perreault and Avoli, 1992) did not occur in the EC in these experiments (not illustrated). Hence, we presumed that the EC and the hippocampus were functionally disconnected (cf., Avoli et al., 1996; Benini and Avoli, 2005).

To further ensure that CA3-driven output activity did not influence the epileptiform activity generated by EC neuronal networks, we also performed experiments in slices (n=19) in which the connections between the hippocampus and this limbic area had been surgically cut. The duration and interval of occurrence of interictal (1.5±0.1 s and 26.2±4.4 s, respectively) and ictal (103.9±11.2 s and 302.9±54.3 s, respectively) discharges recorded in the EC in these surgically cut slices were similar to those seen in the "intact" experiments. Hence, the epileptiform activity induced by 4AP was further analyzed in this study by pooling the data obtained from these two sets of experiments.

As shown in Fig. 1, a striking feature of the interictal activity recorded from the EC was its frequency of occurrence that could be categorized in different experiments as either slowly or frequently occurring (panels A and B, respectively). Interictal events occurring at a slow pace consisted of an initial fast transient followed by a biphasic (Fig. 1Ca) or monophasic (Fig. 1Cb) slow wave of negative polarity, and they will be hereafter termed isolated "slow" interictal spikes (ISISs). In contrast, interictal activity that occurred frequently was usually typified by a negative slow transient associated to multiple population spikes; these interictal events will be hereafter called frequent polispike interictal discharges (FPIDs) (Fig. 1Cc). Interestingly, the mean duration and the mean interval of occurrence of the interictal discharges analyzed in these experiments did not appear

to be segregated in two distinct groups but rather they represented a continuum (Figs. 1D and E). However, by plotting the duration versus the respective interval of occurrence of interictal activity recorded from the EC in these slices, we could identify two distinct groups of interictal events that were confirmed by a K-mean cluster analysis (Fig. 1F).

Interictal discharges and ictal discharge onset - Next, we established whether the presence of specific patterns of interictal activity (i.e., ISISs and FPID) correlated with identifiable types of ictal discharge onset as qualitatively suggested by our previous studies (Avoli et al., 1996; Lopantsev and Avoli, 1998a). As illustrated in Fig. 2A, ictal discharges recorded from brain slices that generated ISISs (n=66), were characterized in 62 experiments by the occurrence of an ISIS that consistently occurred during the 10 s preceding their onset and could lead to an initial ictal phase that was associated to low-voltage oscillations at 10 Hz. In contrast, ictal activity in slices (n=18) that generated FPIDs rose suddenly from an interictal background. The rate of occurrence of interictal spikes that preceded FPIDs did not show any change before ictal onset (Fig. 2B). In the remaining 4 slices generating ISISs during the interictal phase, ictal discharge onset was preceded by an acceleration of the rate of occurrence of interictal events (Fig. 3A).

As illustrated in Fig. 3B, ISIS-triggered ictal discharges had longer duration (116.0 ± 7.3 s; n=62) and interval of occurrence (425.8 ± 42.3 s; n= 62) as compared to those arising suddenly from a FPID background (58.3 ± 7.8 s, $P<0.0001$ and 202.1 ± 21.8 s, $P<0.005$, respectively; n= 18). As expected, we also found in these experiments that ISISs had duration (1.5±0.1 s) and interval of occurrence (34.5 ± 2.4 s) that were significantly longer than in FPIDs (duration= 0.8 ± 0.1 s, $P<0.0001$; interval of occurrence= 4.5 ± 2.4 s, $P<0.0001$) (Fig. 3C). The duration of the ictal discharges that were characterized in 4 experiments by an accelerating ISIS onset pattern was 75.9 ± 8 s while their interval of occurrence was 319.4 ± 81.9 s. In addition, the interictal activity measured before the appearance of ISIS acceleration lasted 1.3 ± 0.2 s and recurred at an interval of 22.3 ± 4.1 s. However, due to the small number of experiments showing this accelerating ISIS onset pattern we could not perform any statistical comparison with the values obtained from the experiments characterized by ictal discharges that were ISIS-triggered or occurred suddenly.

Synchronous interictal activity recorded during ionotropic glutamatergic receptor antagonism - Previous studies have shown that the typical interictal events recorded in the presence of 4AP (i.e., the ISISs) continue to occur following application of ionotropic glutamatergic

antagonists while ictal discharges are readily abolished (cf., Avoli and de Curtis, 2011). Hence, we compared the effects induced by concomitant application of CNQX and CPP on the epileptiform activity recorded from slices that generated either ISIDs or FPIDs. As illustrated in Figs. 4A and B, block of glutamatergic transmission abolished ictal discharges in both experimental groups. In contrast, interictal activity was influenced in a type specific manner by this pharmacological procedure: (i) ISISs continued to occur at similar frequency and with similar duration and amplitude in all experiments (n=6); while (ii) FPIDs were abolished in 3 of 7 slices and were reduced in duration ($P<0.05$), rate of occurrence ($P<0.001$) and amplitude ($P<0.01$) in the remaining experiments (Figs. 4C–E). As previously reported (cf. Avoli and de Curtis, 2011), these synchronous, glutamatergic-independent events were abolished in both types of experiments by applying the $GABA_A$ receptor antagonist picrotoxin thus ruling out that the different effects seen during CNQX+CPP application were not a consequence of ineffective pharmacological blockade of glutamatergic transmission.

High-frequency oscillations in EC during interictal and ictal discharges - Finally, we analyzed the occurrence of HFOs in both ripple (80–200 Hz) and fast ripple (250–500 Hz) frequency ranges during the different types of interictal and ictal activity induced by 4AP in the EC. As illustrated in Figs. 5A and C, HFOs could be observed during both types of interictal activity, and they coincided with the initial component of each discharge. However, the majority of ISISs (69.9%; n=93 events recorded from 7 slices) and FPIDs (95.7% n=869 from 7 slices) did not show HFOs. In addition, HFOs occurred more often during ISISs (10.8% for ripples and 18.3% for fast ripples) (Fig. 5B) than during FPIDs (3.6% for ripples and 0.6% for fast ripples) (Fig. 5D).

HFOs also occurred during ictal discharges both when they were characterized by an ISIS-triggered onset (n=21) and when they emerged suddenly from a FPID background (n=9) (Fig. 6A). Rates of both ripples ($P<0.005$) and fast ripples ($P<0.001$) were, however, higher during ISIS-triggered as compared to suddenly arising ictal events (Figs. 6A, B). In addition, we found that ISIS-triggered ictal discharges were characterized by a higher proportion of ripples when compared to ictal discharges suddenly arising from a FPID background both during the onset ($P<0.001$) and the middle part ($P<0.05$) of the discharge (Fig. 6C, Ripples). In contrast, there was no significant difference between the two types of ictal discharge, when comparing rates of fast ripples over time (Fig. 6C, Fast Ripples). Ripples and fast ripples did also occur when ictal discharges were heralded by an accelerating ISIS onset pattern. However, due to the small number of experiments we could

not statistically compare them with those seen when ictal discharges were ISIS-triggered or occurred suddenly.

2.6. Discussion

To the best of our knowledge, this is the first study to address quantitatively the characteristics of the epileptiform activity generated in vitro by the rat EC during application of 4AP; the EC plays a prominent role in the generation of seizures induced in vivo by electrical stimulation (Stringer and Lothman, 1992) and in vitro in several models of ictogenesis (cf., Avoli et al., 2002). In addition, EC dysfunction has been documented in temporal lobe epilepsy patients (Rutecki et al., 1989; Spencer and Spencer, 1994) where its surgical removal may be required for achieving seizure control (Goldring et al., 1992). The main findings of our study can be summarized as follows. First, interictal activity generated by EC neuronal networks presents with a wide range of duration and rate of occurrence that can be epitomized at the two extremes as ISISs and FPIDs. Second, ictal discharges can either be shortly preceded by an ISIS or arise suddenly from a pattern of FPIDs. Third, ISIS-triggered ictal-like events have longer duration and interval of occurrence than those emerging suddenly during FPIDs. Fourth, HFOs are recorded more frequently during ISISs than FPIDs, and their rates are higher during ISIS-triggered as compared to suddenly arising ictal discharges. Finally, we found that EC networks in brain slices that responded to 4AP by generating ISISs continued to do so during application of glutamatergic receptor antagonists; in contrast, this pharmacological procedure greatly reduced and even abolished FPIDs.

Interictal activity induced by 4AP in the EC - We have found that the interictal activity recorded in the majority of experiments (i.e., 78.5%) occurred at a slow pace and was characterized by a succession of events predominated by a slow wave. Intracellular recordings obtained from principal neurons in the EC have shown that these interictal spikes – which were termed here as ISISs – correspond to a long-lasting depolarization that triggers few action potentials and is abolished by pharmacological procedures that interfere with $GABA_A$ receptor signaling (Lopantsev and Avoli, 1998b). Moreover, similar slow interictal events have been reported to occur during 4AP treatment in several hippocampal areas (Perreault and Avoli, 1992) and in other cortical (see for review Avoli et al., 2002; Avoli and de Curtis, 2011) and subcortical structures (Lévesque et al., in press). In the remaining experiments (22.5%), we could identify interictal discharges that occurred more frequently and were associated to multiple population spikes, thereby being defined as FPIDs; we have

reported that the intracellular events associated to FPIDs consist of robust discharges of action potentials riding over a depolarization (Lopantsev and Avoli, 1998a).

It is well established that 4AP blocks type A outward potassium currents and slows action potential repolarization (Storm, 1987). This action should change neuronal firing but even more so enhance transmitter release at both glutamatergic and GABAergic terminals (see for review Avoli et al., 2002). It is, however, unknown why 4AP can induce these two types of interictal activity in EC slices that were obtained from animals of similar age and strain. We are inclined to propose that these two patterns mirror a different involvement of GABAergic networks that may result from their different preservation following brain slicing. This view is supported by experiments in which we tested the effects of glutamatergic receptor antagonists on the epileptiform activity induced by 4AP; this pharmacological procedure greatly reduced the duration, the amplitude and the rate of occurrence of FPIDs suggesting that this type of interictal pattern is largely contributed by ionotropic glutamatergic receptor mechanisms. At variance, ISISs continued to occur with amplitudes and rates that were similar to those seen under control conditions (i.e., 4AP treatment). Slow interictal events with electrographic features similar to the ISISs are recorded during 4AP treatment in the hippocampus, EC and several other cortical structures as well as that they continue to occur during blockade of glutamatergic transmission (see for review Avoli et al., 2002; Avoli and de Curtis, 2011). In addition, the only study available on 4AP-induced interictal activity with characteristics reminiscent of FPIDs reported that these events were abolished by concomitant application of NMDA and nonNMDA glutamate receptor antagonists (Lopantsev and Avoli, 1998a).

We are inclined to exclude that the two different patterns of interictal activity resulted from the influence exerted by hippocampal output activity, and more specifically by CA3-driven interictal discharges (Barbarosie and Avoli, 1997). In line with this view, both ISISs and FPIDs could be recorded in the presence of 4AP from slices in which the connections between the hippocampus and the EC had been surgically cut.

Ictal discharge onsets - The onset of ictal discharges recorded from slices characterized by ISISs was heralded in the majority of experiments by the occurrence of an ISIS that was followed by field oscillations at 10–20 Hz then leading to overt ictal activity; these characteristics were reminiscent of the low-voltage, fast activity onset reported to occur in vivo both in epileptic patients (Ogren et al., 2009; Velasco et al., 2000) and in animal models (Bragin et al., 1999, 2005; Lévesque et al., 2012).

These results are also similar to those occurring in vivo following systemic administration of 4AP in rodents (Lévesque et al., in press). In these experiments we have observed a high proportion of low-voltage fast-onset seizures while in a few cases the ictal discharge onset was characterized by acceleration of ISISs; this second type of onset was indeed similar to the hypersynchronous onset type reported to occur in epileptic patients (Ogren et al., 2009; Velasco et al., 2000), in animal models of temporal lobe epilepsy (Bragin et al., 1999; Lévesque et al., 2012), and in rodent brain slices superfused with low Mg2+ medium (Zhang et al., 2012).

In contrast, ictal discharges recorded in brain slices generating FPIDs occurred suddenly and thus their initiation was not preceded by any detectable change in interictal activity. Remarkably, both the duration and the interval of occurrence of ISIS-triggered ictal events were longer than what was observed in those suddenly rising. These features have also been recently reported in an in vivo model of temporal lobe epilepsy where low-voltage fast-onset seizures occurring spontaneously in pilocarpine-treated epileptic rats have longer duration compared to hypersynchronous onset seizures (Lévesque et al., 2012).

Differences in the duration of ISIS-triggered and suddenly arising ictal discharges may be related to, at least, two mechanisms. The first may result from activity-dependent modulation of epileptiform synchronization, i.e., from the higher frequency of occurrence of interictal events in brain slices generating suddenly arising ictal discharges. We have in fact reported that simulating interictal activity by repetitive stimuli delivered at different fixed frequencies influences the duration of 4AP-induced ictal discharges in the EC and specifically that their duration decreases when stimulation is more frequent (D'Arcangelo et al., 2005). The second mechanism, as already discussed above, may relate to a different participation of GABAergic conductances to the two patterns of ictal activity. By using sharp intracellular recordings from EC deep layers, we have found that $GABA_A$-receptor mediated conductances play an active role in the maintenance of 4AP-induced ictal discharges that are initiated by ISISs (Lopantsev and Avoli, 1998b). More recently, Lillis et al. (2012) have reported that pre-ictal $GABA_A$ receptor mediated Cl^- influx produces a positive feedback loop that contributes to the initiation of seizure-like activity in the 4AP in vitro model.

HFOs and epileptiform discharges induced by 4AP - HFOs were more frequently observed during ISISs compared to FPIDs. This finding supports the view that ISISs and FPIDs should mirror different neuronal mechanisms as reported in two early intracellular studies performed in the rat EC during 4AP application; it was shown there that ISISs were essentially associated to

synchronous $GABA_A$ receptor-mediated IPSPs (Lopantsev and Avoli, 1998b) while FPIDs mostly mirror glutamatergic depolarizations (Lopantsev and Avoli, 1998a). Accordingly, it has been proposed that ripples reflect IPSPs generated by principal neurons entrained by a network of synchronously active interneurons (Buzsaki et al., 1992; Ylinen et al., 1995) while fast ripples would not strictly depend on GABA receptor signalling (Bragin et al., 2011; Dzhala and Staley, 2003; Engel et al., 2009). Thus, the preferential occurrence of HFOs during ISISs could be caused by the concomitant occurrence of synchronous IPSPs that, interestingly, are also generated in the presence of 4AP even when glutamatergic excitatory transmission is blocked (Avoli and de Curtis, 2011).

HFOs were also observed during ictal discharges, mostly at their onset. However, ISIS-triggered ictal discharges were characterized by a higher rate of ripples compared to ictal discharges suddenly arising from a FPID background, while no difference was seen for fast ripples. This is similar to what has been previously reported in the piriform cortex, since ripples predominated over fast ripples during 4AP-induced ictal discharges, which shared similar morphological features with the ISIS-triggered ictal discharges recorded here from the EC (Panuccio et al., 2012). Our in vitro findings are also in agreement with what has been found in vivo, since low-voltage fast onset seizures were shown to be related to activity in the ripple frequency range, with a low proportion of fast ripples (Bragin et al., 1999; Lévesque et al., 2012). Thus, the relation between ripples and ISIS-triggered ictal discharges supports further the hypothetical link between GABAergic synchronization and a specific type of seizure onset. More specifically, ISIS-triggered ictal discharges, as low-voltage fast-onset seizures observed in vivo, could depend on increased interneuron activation, which would therefore explain the high proportion of ripples recorded here compared to fast ripples.

Concluding remarks **-** Our findings show that interictal spike patterns can define ictal onset features resembling those seen in vivo in epileptic patients and in animal models of temporal lobe epilepsy. Specifically, we have found that ISIS occurrence is associated with a type of ictal onset that is reminiscent of low-voltage fast onset seizures. Moreover, this interictal pattern, which is associated to synchronous $GABA_A$ receptor-mediated IPSPs, leads to ictal discharges that are more robust than those arising suddenly during FPIDs. We propose that a similar condition may occur in vivo both in animal models and in humans.

2.7. Figures

Figure 2-1

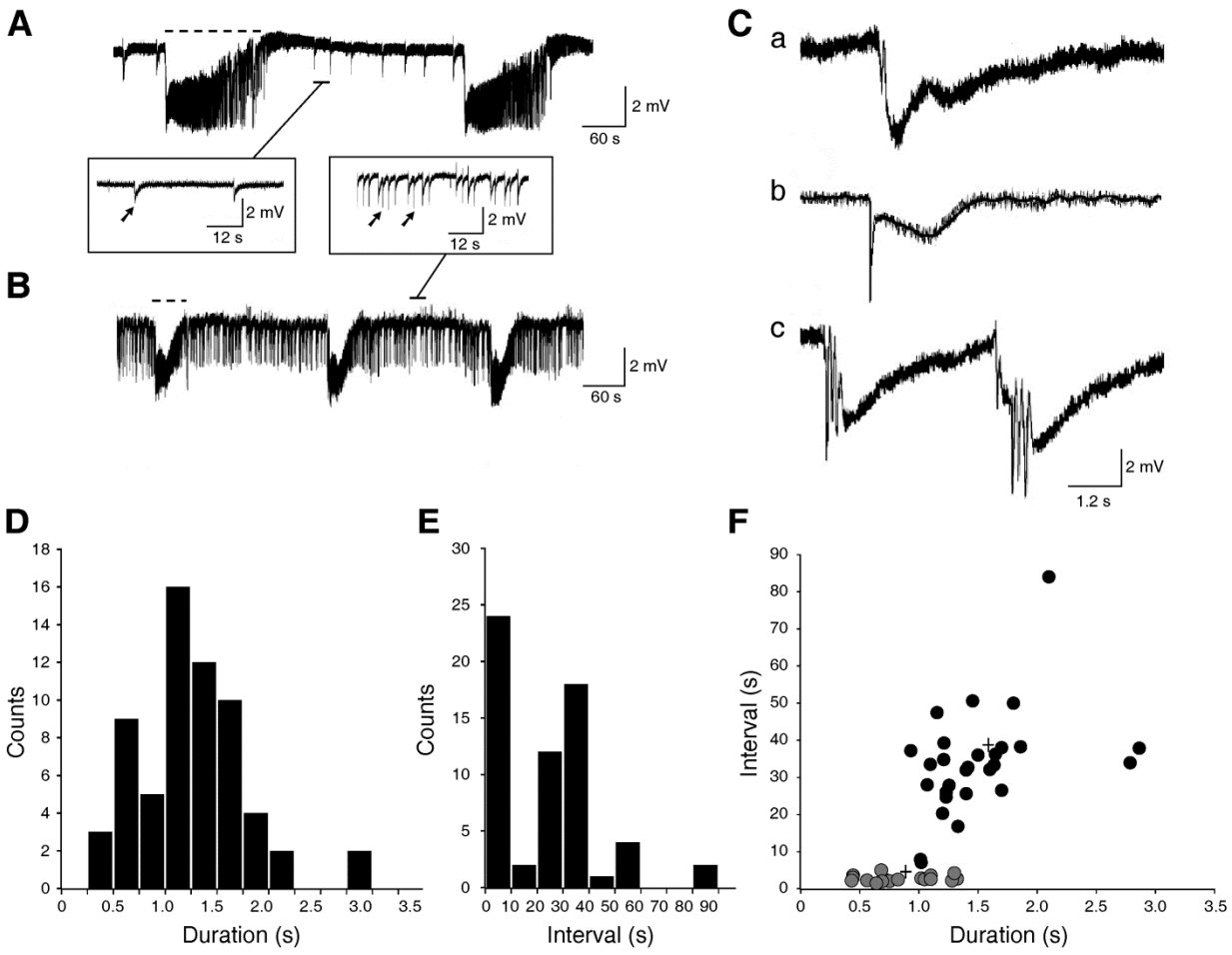

Synchronous epileptiform activity recorded *in vitro* from the EC. A and **B:** Interictal (arrows) and ictal (dotted lines) discharges recorded from the EC of two "intact" brain slices during application of 4AP. Note that the rate of the interictal discharges recorded in these two experiments is either slowly (**A**) or frequently occurring (**B**). **C:** Expanded interictal events occurring at a slow pace – also termed ISISs – consist of an initial fast transient followed by a biphasic (a) or monophasic (b) slow wave of negative polarity, while those occurring frequently (c) are characterized by a negative slow transient with multiple population spikes (termed FPIDs). **D** and **E:** Histograms of the mean duration and interval of occurrence of the interictal discharges. **F:** Plot of the duration versus the respective interval of occurrence of interictal activity recorded from these experiments; K-mean cluster analysis identifies two distinct groups (crosses).

Figure 2-2

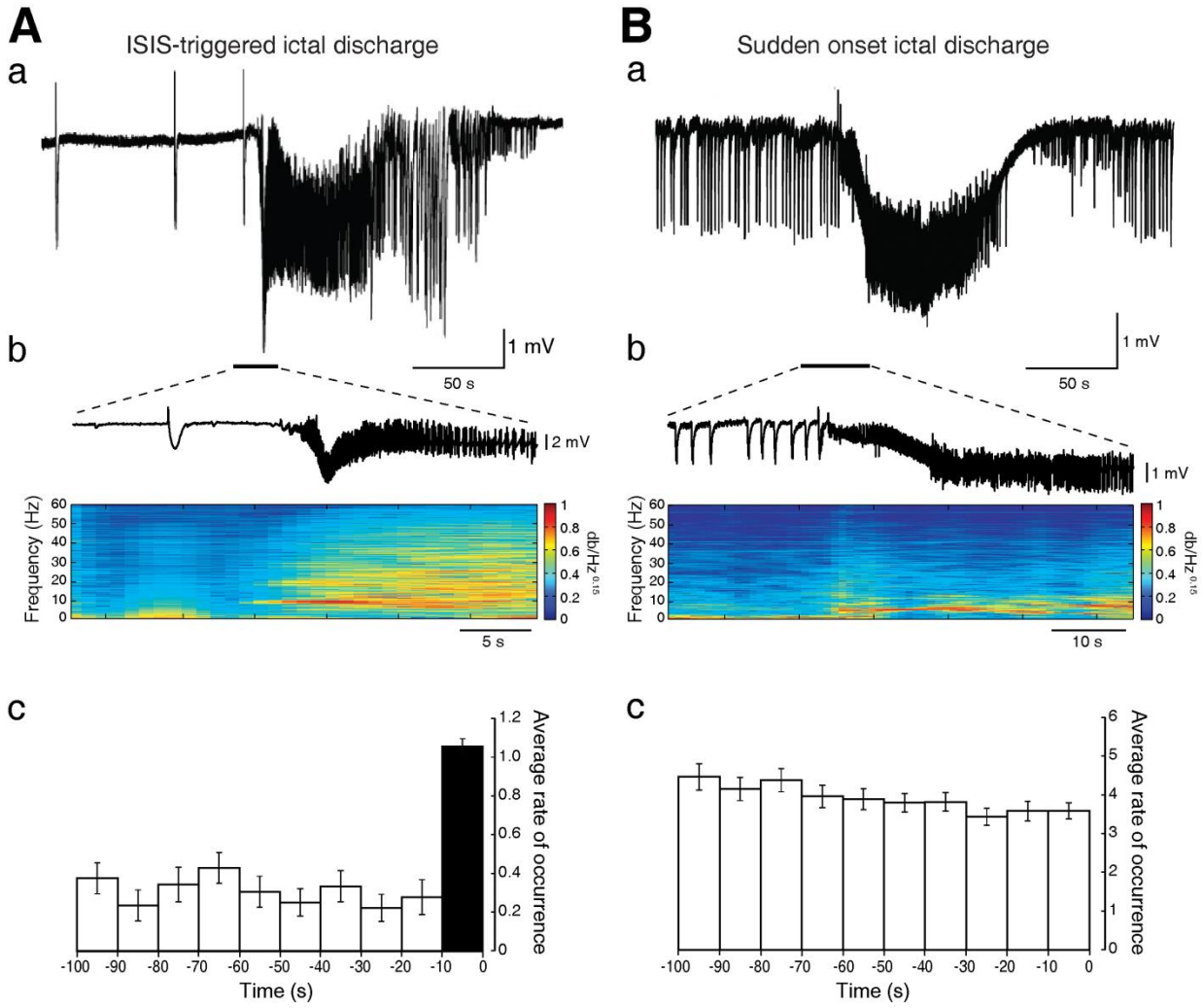
A
ISIS-triggered ictal discharge
a
b
1 mV
50 s
2 mV
Frequency (Hz)
60
50
40
30
20
10
0
1
0.8
0.6
0.4
0.2
0
db/Hz 0.15
5 s
c
1.2
1.0
0.8
0.6
0.4
0.2
0
Average rate of occurrence
-100 -90 -80 -70 -60 -50 -40 -30 -20 -10 0
Time (s)
B
Sudden onset ictal discharge
a
b
1 mV
50 s
1 mV
Frequency (Hz)
60
50
40
30
20
10
0
1
0.8
0.6
0.4
0.2
0
db/Hz 0.15
10 s
c
6
5
4
3
2
1
0
Average rate of occurrence
-100 -90 -80 -70 -60 -50 -40 -30 -20 -10 0
Time (s)

Interictal activity and ictal discharge initiation. A: Ictal discharge recorded in a brain slice that generated ISISs is shown at two time bases in a and b. In panel b, both the field potential and the power spectrogram corresponding to the onset of the ictal discharge are shown. In this experiment an ISIS occurs approx. 7 s before the ictal onset which is characterized by low-voltage oscillations at 10 Hz. In c, frequency distribution histogram showing the occurrence of ISISs 100 s before the onset of the ictal discharge (n=22 slices). **B:** Ictal discharge recorded in a brain slice that generated FPIDs is shown at two time bases in a and b. In panel b both the field potential and the power spectrogram of the onset of the ictal discharge are shown. Note that the ictal discharge onset occurs suddenly from an interictal background that does not show any change in frequency. In c, frequency distribution histogram showing the occurrence of interictal discharges 100 s before the onset of FPIDs (n=13 slices).

Figure 2-3

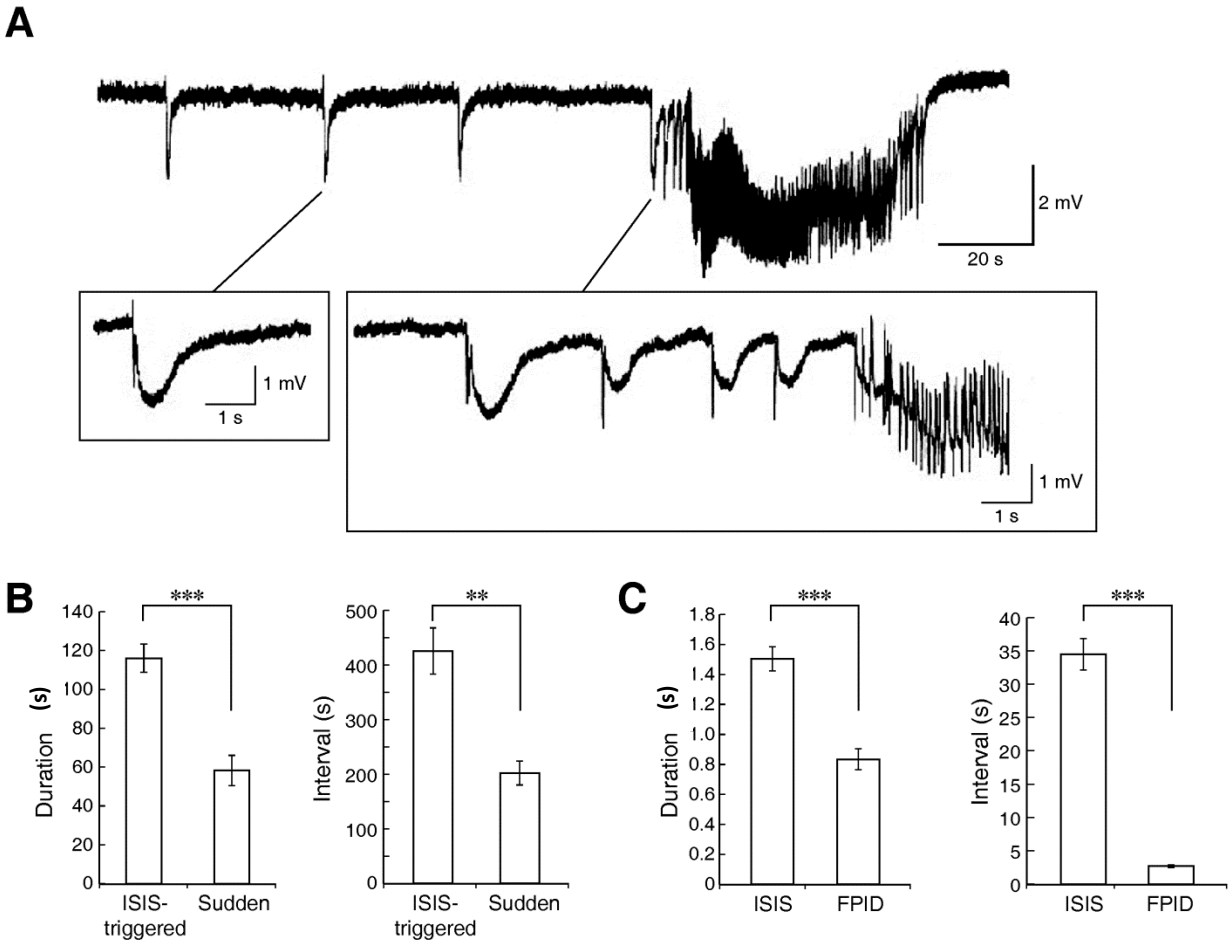
A
2 mV
20 s
1 mV
1 s
1 mV
1 s
B
Duration (s)
***
ISIS-triggered
Sudden
Interval (s)
**
ISIS-triggered
Sudden
C
Duration (s)
***
ISIS
FPID
Interval (s)
***
ISIS
FPID

Interictal activity and ictal discharge initiation. A: Recording of one of the 4 slices generating ISISs that accelerate before ictal discharge onset. In b and c are the events indicated in panel a, shown at faster time scale. **B:** Plots of the duration and interval of occurrence of ISIS-triggered and sudden onset ictal discharges; note that the former type has longer duration and interval of occurrence. **C:** Plots of the duration and interval of occurrence of ISIS and FPIDs. Note that both duration and the interval of occurrence of ISISs are higher than those of FPIDs.

Figure 2-4

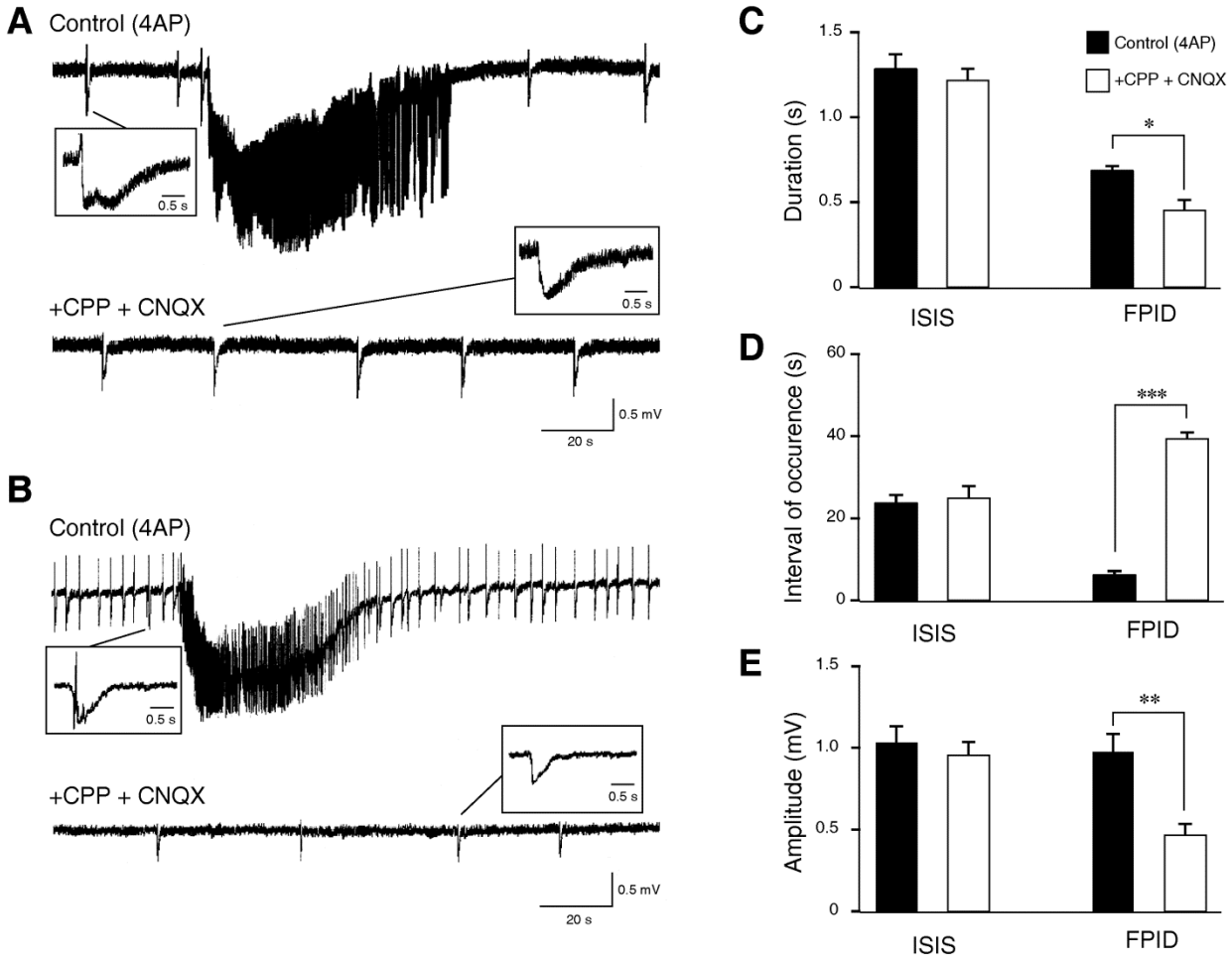
A
Control (4AP)
0.5 s
+CPP + CNQX
0.5 s
0.5 mV
20 s
B
Control (4AP)
0.5 s
+CPP + CNQX
0.5 s
0.5 mV
20 s
C
Control (4AP)
+CPP + CNQX
Duration (s)
1.5
1.0
0.5
0
*
ISIS
FPID
D
Interval of occurence (s)
60
40
20
0
***
ISIS
FPID
E
Amplitude (mV)
1.5
1.0
0.5
0
**
ISIS
FPID

Effects induced by blockade of glutamatergic transmission in brain slices generating ISIS-triggered and suddenly occurring ictal discharges. A: Concomitant application of CNQX and CPP abolishes ISIS-triggered ictal discharges while ISISs continue to occur with characteristics similar to those seen under control (4AP) conditions. **B:** The same pharmacological procedure blocks ictal discharges that occur suddenly during FPIDs but also reduce the frequency and the amplitude of the latter events. **C–E:** Quantification of the effects induced by CNQX+CPP on the two types of interictal discharge. Note that the duration and the amplitude of the events recorded from slices generating ISISs under control conditions are longer and higher than those observed in slices in which the control interictal activity was characterized by FPIDs.

Figure 2-5

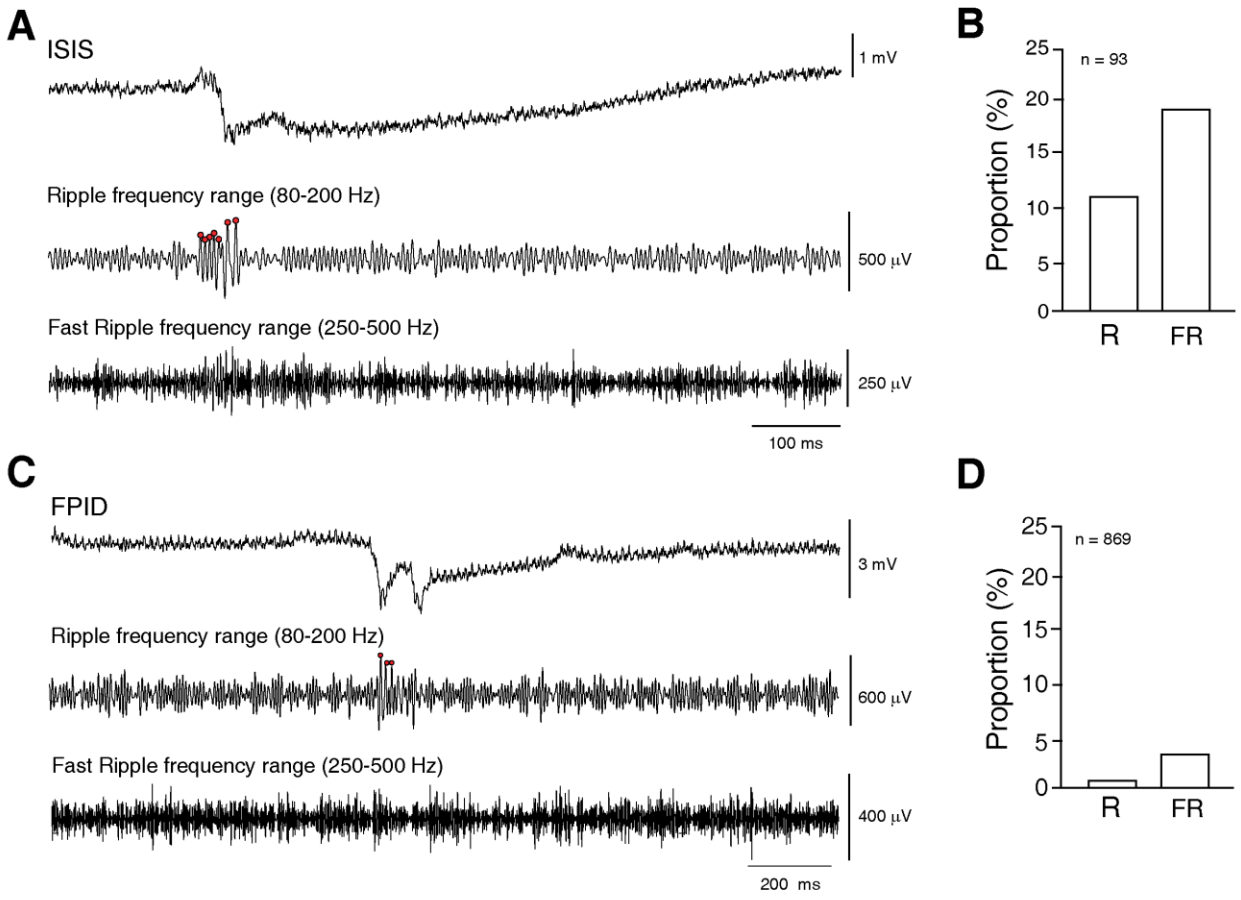
A
ISIS
1 mV
Ripple frequency range (80-200 Hz)
500 µV
Fast Ripple frequency range (250-500 Hz)
250 µV
100 ms
B
n = 93
Proportion (%)
25
20
15
10
5
0
R
FR
C
FPID
3 mV
Ripple frequency range (80-200 Hz)
600 µV
Fast Ripple frequency range (250-500 Hz)
400 µV
200 ms
D
n = 869
Proportion (%)
25
20
15
10
5
0
R
FR

HFOs and interictal discharges. A: ISIS recorded in EC showing activity in the ripple frequency range (red dots). **B:** Proportion of slow interictal spikes co-occurring with ripples (R) and fast ripples (FR) showing that ISISs are more often related to ripples and fast ripples compared to FPIDs (cf. panel D). **C:** FPID recorded from EC showing activity in the ripple frequency range (red dots). **D:** Proportion of FPIDs co-occurring with ripples (R) and fast ripples (FR).

Figure 2-6

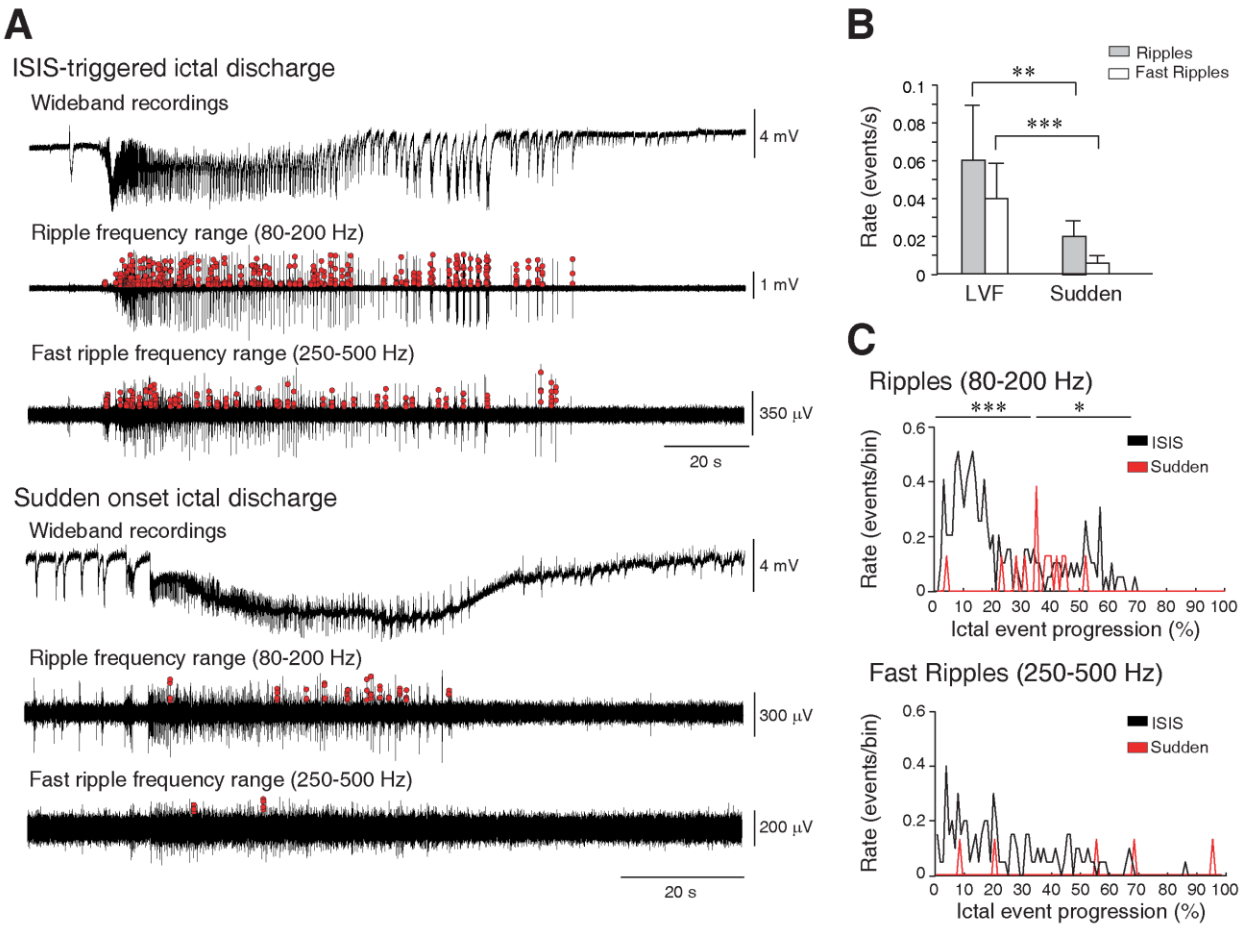
A
ISIS-triggered ictal discharge
Wideband recordings
4 mV
Ripple frequency range (80-200 Hz)
1 mV
Fast ripple frequency range (250-500 Hz)
350 µV
20 s
Sudden onset ictal discharge
Wideband recordings
4 mV
Ripple frequency range (80-200 Hz)
300 µV
Fast ripple frequency range (250-500 Hz)
200 µV
20 s
B
Ripples
Fast Ripples
**
***
Rate (events/s)
0.1
0.08
0.06
0.04
0.02
0
LVF
Sudden
C
Ripples (80-200 Hz)
***
*
ISIS
Sudden
Rate (events/bin)
0.6
0.4
0.2
0
0 10 20 30 40 50 60 70 80 90 100
Ictal event progression (%)
Fast Ripples (250-500 Hz)
ISIS
Sudden
Rate (events/bin)
0.6
0.4
0.2
0
0 10 20 30 40 50 60 70 80 90 100
Ictal event progression (%)

HFOs and ictal discharges. A: Representative recordings from the EC showing an ISIS-triggered and a sudden onset ictal discharge with activity in the ripple (80–200 Hz) and fast ripple (250–500 Hz) frequency ranges. HFOs are marked by red dots on each peak of detected oscillations. **B:** Average rate of occurrence of ripples and fast ripples during each ictal discharge type. ISIS-triggered ictal discharges contain more HFOs than sudden onset ictal discharges. **C:** Occurrence of HFOs over time during ictal discharges in the ripple and fast ripple frequency ranges. Ictal discharges were normalized from 0 (start of the ictal discharge) to 100 (end of the ictal discharge) to account for different durations. The first and middle parts of ISIS-triggered ictal discharges showed significantly more ripples compared to sudden onset ictal discharges. No significant differences were observed for fast ripples. * $P<0.05$, ** $P<0.005$, *** $P<0.001$.

3. SUBICULUM-ENTORHINAL CORTEX INTERACTIONS DURING *IN VITRO* ICTOGENESIS

By Herrington R, Lèvesque M, Avoli M

Accepted for publication in Seizure, 2015

3.1. Rationale and Objective

We determined that LVF and sudden ictal onset patterns are associated with different interictal patterns characterized by distinct underlying mechanisms in the entorhinal cortex; however, seizures occurring in para-hippocampal structures can be modified by inputs originating from the hippocampal formation. Considering that the entorhinal cortex is extensively connected to the hippocampus (reviewed in section 1.3) and that inputs from the hippocampus can modulate epileptiform synchronization, we sought to determine the contribution of local circuits between the entorhinal cortex, the major input structure to the hippocampus, and the subiculum, the major output structure. To this end, we performed cut experiments to determine whether local connections between the EC and subiculum were capable of modulating the two types of ictal onset patterns and their associated interictal discharges.

3.2. Abstract

Purpose: Our aim was to establish the contribution of neuronal networks located in the entorhinal cortex (EC) and subiculum to the generation of interictal and ictal onset patterns recorded *in vitro*.

Methods: We employed field potential recordings of epileptiform activity in rat brain slices induced with the application of the K^+ channel blocker 4-aminopyridine. Local connections between the EC and subiculum were severed to understand how EC-subicular circuits contribute to patterns of epileptiform synchronization.

Results: First, we found that ictal discharges occurred synchronously in these two structures, initiating from either the EC or subiculum, and were characterized by *low voltage fast* (LVF) or *sudden* onsets (*cf.*, Avoli et al., *Neurobiol Dis*, 52, 168-176, 2013). Second, sudden onset ictal events initiated more frequently in the EC whereas LVF onset ictal discharges appeared more likely to initiate in the subiculum ($P<0.001$). In both structures, polyspike interictal discharges occurred in brain slices generating sudden onset ictal events while isolated slow interictal discharges were recorded in experiments characterized by LVF onset ictal activity. Third, severing the connections between

subiculum and EC desynchronized both interictal and ictal discharges occurring in these two regions, leading to a significant decrease in ictal duration (regardless of the onset type) along with blockade of polyspike interictal activity in subiculum.

Conclusions: These findings highlight the contribution of EC-subicular interactions to epileptiform synchronization and, specifically, to ictogenesis in this *in vitro* model.

3.3. Introduction

Focal seizures can be classified according to their region of onset as well as to their onset pattern. Studies performed in temporal lobe epilepsy patients have revealed the existence of two main types of seizure onset patterns that have been termed hypersynchronous and low voltage fast (LVF) (Perucca et al., 2014, Velasco et al., 2000). These seizure onset patterns, which have also been observed in animal models of temporal lobe epilepsy *in vivo* (Bragin et al., 2005; Lévesque et al., 2012), may reflect the contribution of distinct mechanisms of ictogenesis. Moreover, *in vitro* studies performed in rodent brain slices comprising the hippocampus and the entorhinal cortex (EC) during application of the K^+ channel blocker 4-aminopyridine (4AP) have revealed the presence of LVF or sudden ictal onset patterns in the EC (Avoli et al., 2013). Hypersynchronous onset discharges were detected in the EC as well, but this pattern was limited to only a few cases (Avoli et al., 2013).

In this study, we analyzed for the first time the contribution of the interactions between the EC and the subiculum to the synchronous epileptiform activity induced by 4AP *in vitro*. The EC is implicated as one of the possible seizure onset regions in temporal lobe epilepsy (Lévesque et al., 2012; Toyoda et al., 2013), and presents with epileptogenic changes in both humans and animal models mimicking this disorder (Bertram, 2009; Du et al., 1993). In contrast to the EC, the subiculum of temporal lobe epileptic patients presenting with hippocampal sclerosis shows little to no neuronal damage (Andrioli et al., 2007; Bertram, 2009; Du et al., 1993). In addition, *in vivo* studies have demonstrated its involvement in seizure onset in models of temporal lobe epilepsy (Toyoda et al., 2013). Finally, tissue resected from the subiculum of patients with temporal lobe epilepsy generates spontaneous interictal-like (from hereafter termed interictal) discharges (Huberfeld et al., 2008), but it is unable to generate spontaneously occurring ictal discharges (Huberfeld et al., 2011). Using the *in vitro* 4AP model of epileptiform synchronization, we employed in this study field potential recordings to investigate the involvement of the subiculum in the ictogenic processes that lead to the generation of LVF or sudden ictal onset patterns in the EC.

3.4. Methods

Slice preparation and maintenance – All procedures were performed in accordance with and approved by the Canadian Council of Animal Care and the McGill Animal Care Committee. All efforts were made to minimize the suffering and number of animals used. Male Sprague-Dawley rats (175-250 g; Charles River Laboratories, Saint Constant, Qc, Canada) were decapitated under isoflurane anaesthesia (Baxter Corporation, Mississauga, ON, Canada). The brain was quickly removed and placed in ice cold, oxygenated artificial cerebrospinal fluid (ACSF) with the following composition: 124 mM NaCl, 2 mM KCl, 2 mM CaCl2, 2mM MgSO4, 1.25 mM KH2PO4, 26 mM NaHCO3, and 10 mM D-glucose. The ACSF was continuously bubbled with an O_2/CO_2 (95/5%) gas mixture to maintain the pH at 7.4. The cerebellum was severed and the brain was mounted for slicing. Slices with a thickness of 450 μm were obtained with a vibratome (VT1000S; Leica, Concord, ON, Canada) and transferred to an interface chamber. Slices were maintained between warm (32 ± 1°C) ACSF (pH 7.4, 305 mOSM/kg) and humidified gas (O_2/CO_2, 95%/5%). Following a recovery period of at least 1 hour, epileptiform activity was induced by continuous bath application of 4AP (50 μM; Sigma-Aldrich, Oakville, ON, Canada) at a flow rate of 2 mL/min.

The EC and subiculum were continuously recorded during 4AP application for a period of up to 90 min. In cut experiments, a scalpel blade mounted on a micromanipulator was used to sever the connections between the EC and subiculum. NMDA receptor mediated signalling was blocked by applying 10 μM 3-(2-carboxypiperazin-4-yl) propyl-1-phosphonic acid (CPP; Tocris Bioscience, Ellisville, MO, USA). Recordings were analyzed beginning 30 min following 4AP application, immediately following the recovery of spontaneous epileptiform activity after cut experiments, and 10 min following CPP application.

Field potential recordings - Field potential recordings were obtained with ACSF-filled glass pipettes (1B150F-4; World Precision Instruments, Sarasota, FL, USA; tip diameter <10μm; resistance 5-10 MΩ) pulled by a Sutter P-97 electrode puller (Sutter, Novato, CA, USA). Signals were fed to an AI 401 amplifier and a CyberAmp 380 (Molecular Devices, Silicon Valley, CA, USA). Traces were digitized using a Digidata 1322A (Molecular Devices). Signals were sampled at 5 kHz and cut off at 1 kHz.

Statistics and analysis – Analysis of field potential recordings were performed offline with CLAMPFIT 8.2 (Molecular Devices) and reviewers were blind to the regions being analyzed and

treatment applied to the slice. Throughout this study, we arbitrarily termed as 'ictal' or 'interictal' the synchronous epileptiform events longer or shorter than 3 s, respectively (*cf.* Traub et al., 1996). The normal distribution of data was tested with Skewness and Kurtosis tests. Data were analysed with either two-way ANOVA followed by Tukey's multiple comparisons test, or with Student's t-test. Fisher's Exact Test was used to determine whether non-random associations existed between two categorical variables. Throughout the text, n indicates the number of slices studied, unless otherwise specified. Results are expressed as mean ± standard error of the mean. Results were considered to be significantly different at $P< 0.05$.

Sudden onset discharges arose abruptly from a frequent polyspike interictal background (arrows in Fig. 1A) while LVF events initiated with a pattern of low-voltage fast activity occurring at approx. 10-20 Hz (arrows in Fig. 1B) (*cf.*, Avoli et al., 2013). The onset of the interictal events was determined to be the first deflection from the baseline. To determine the delays occurring between the EC and subiculum during ictal or interictal events, while blind to the region, cursors were placed at the onset of the respective ictal events. The time delay was then calculated by built-in software provided by CLAMPFIT 8.2. Following analysis, delays were reassigned based on the regions of onset with negative values arbitrarily defined to initiate from the subiculum and positive values to initiate from the EC.

3.5. Results

4AP induced ictal discharges - A total of 84 ictal events from 31 brain slices were recorded simultaneously from the EC and subiculum (Fig. 1A and B). Forty-six of these ictal events appeared to initiate in the subiculum, 38 in the EC, and one had simultaneous onset in both regions (Fig. 1C). When ictal events initiated from the EC, ictal duration averaged 73.8 ± 5.6 s in the EC and 66.3 ± 4.3 s in the subiculum (n= 46 events) (Fig. 1D). When events initiated from the subiculum, ictal duration averaged 87.3 ± 5.4 s in the EC and 76.8 ± 5.3 s in the subiculum (n = 38 events) (Fig. 1D). There was no significant difference between these values.

To understand the relationship between regions and patterns of ictal onset, we categorized ictal discharges by their onset pattern. From the total number of ictal events recorded, 51 were characterized as sudden onset events (n= 17 slices); 33 of these ictal discharges were found to initiate from the EC while 18 appeared to initiate from the subiculum. A total of 33 LVF onset ictal discharges (n= 13 slices) were recorded; 9 were found to initiate from the EC and 24 from the

subiculum (Fig. 1E). Both sudden and LVF onset events could be recorded from slices obtained from a single animal, but ictal onset patterns remained constant within a given slice.

Overall, suddenly arising ictal events were more likely to initiate in the EC area while LVF onset ictal events most frequently initiated from the subiculum (Fisher's Exact Test; $P > 0.001$). The average delay between the start of ictal activity in the EC and subiculum based on the type of ictal onset, irrespective of the region where the ictal event was first detected, was 162.1 ± 136.2 ms for sudden onset ictal events (n= 51 discharges) and -517.4 ± 340.5 ms for LVF onset events (n= 33 discharges). These values were found to be significantly different from each other thus reinforcing the evidence that the EC was more likely to initiate sudden onset ictal events whereas the subiculum was more frequently initiating LVF onset events ($P<0.001$) (see also Fig. 2E).

Interictal patterns preceding ictal events **-** Two patterns of interictal activity were closely associated with the two ictal onset patterns (Fig.2A and B) (Avoli et al., 2013). In both cases, interictal events occurred at the same frequency and with similar duration in the EC and subiculum within a given slice; therefore, data were pooled together. Suddenly arising ictal discharges were accompanied by frequent polyspike interictal discharges, which were characterized by an average duration of 0.7 ± 0.1 s and an average interval of 2.7 ± 0.6 s (n= 17 slices) (Fig. 2C). LVF onset ictal events were associated with isolated slow interictal discharges, which were characterized by longer durations (1.2 ± 0.2 s; $P = 0.017$) and intervals of occurrence (26.0 ± 4.8 s; $P = 4.8$ E-5) (n=13 slices) compared to frequent polyspike interictal discharges (Fig.2C).

The delays detected between the initiation of interictal events in the EC and subiculum were less pronounced compared to the initiation delays associated with the ictal onset. In the interictal event preceding the start of the ictal discharge, fast polyspike interictal discharge delays were distributed around 0 whereas isolated slow interictal delays were shifted toward more negative values (Fig. 2D); such negative values indicated that the onset of slow interictal discharges, like their associated ictal events, were more likely to initiate around the subiculum. To better understand the dynamics of jittering between the EC and subiculum, we assessed the delays for a period of 50 s in 10 s bins before the last interictal event preceding ictal onset (Fig. 2E). On average, isolated slow interictal discharge delays were found to be more negative compared to fast polyspike interictal discharge delays, further suggesting that isolated slow discharges were more likely to initiate in the subiculum. Compared to the ictal onset, interictal delays remained more closely around 0. We also expanded the 10 s epoch leading up to the ictal event in cases of sudden onset discharges to see

whether changes existed on a smaller scale (inset in Fig. 2E) but we could not find any predictive changes in interictal delay times that herald the onset of the ictal event. However, we saw that these delays jittered around 0 in a pattern that was characterized by a frequency of approximately 0.2 Hz. Overall, interictal delays did not appear to be predictive of ictal onset and ictal onset delays were longer than those associated with interictal delays.

Surgical cut between entorhinal cortex and subiculum - In a subset of 8 slices, the connections between the EC and subiculum were severed following 30 minutes of control recordings (Fig. 3C). In slices characterized by suddenly arising ictal discharges (n = 5 slices), cutting the connections desynchronized the epileptiform synchronous events occurring in these two structures (Fig. 3A). In 2 of 5 slices, ictal events disappeared from the subiculum while they continued to occur in the EC but with a marked reduction in duration compared to control (P = 0.034) (Fig. 3A, +Cut, panel a). In the remaining experiments (n = 3) a series of continuous spikes at 1 to 1.5 Hz lasting for several tens of seconds could be recorded from the subiculum following isolation from the EC (Fig. 3A, +Cut, identified by a dotted line in panel b); it should be emphasized that this continuous spike pattern lacked any tonic-clonic component as identified in typical ictal discharges and, in contrast to what observed before the cut, they were characterized by positive-going electrographic elements. The duration and the interval of occurrence of sudden onset ictal discharges recorded in the EC under control conditions and following the cut are plotted in Fig. 3D and E.

LVF onset ictal discharges were also influenced by severing the connections between the EC and subiculum (n = 3 slices) (Fig. 3B). After the cut, ictal events with LVF onset characteristics continued to occur in the EC with shorter duration ($P<0.05$) but at non-significantly different rates of occurrence compared to control (Fig. 3B, +Cut, panel a). In contrast, ictal discharges were abolished in the subiculum where they were replaced by a pattern of continuous positive-going spikes at 1 to 1.5 Hz similar to what is seen in brain slices generating sudden onset ictal activity following cut (Fig. 3B, +Cut, identified with a dotted line in panel b). The duration and the interval of occurrence of LVF onset ictal discharges recorded in the EC under control conditions and following the cut are plotted in Fig. 3D and E.

As illustrated in Fig. 4, following the cut, interictal events recorded in the EC and subiculum were also desynchronized (Fig. 4A and B). In slices generating sudden onset ictal discharges, the duration of interictal events in the subiculum increased after cut (n= 5 slices; $P< 0.001$) but did not significantly change in the EC (Fig. 4C). The interval between interictal events increased after the cut

in both the EC and subiculum (n= 5 slices; P<0.001), but the increase was greatest in the subiculum (P<0.001) (Fig. 4D). Furthermore, while frequent polyspike interictal discharges persisted in the EC following the cut, they disappeared in the subiculum and were replaced by slow interictal discharges similar to those recorded from brain slices generating LVF onset patterns (Fig 4A, double arrow). In slices characterized by LVF onset ictal discharges, the duration of interictal discharges in the EC increased after the cut (n= 3 slices; P<0.001) while in the subiculum there was not significant change (Fig. 4C). Moreover, as illustrated in Fig. 4D, the interval of occurrence of the interictal events recorded from the EC and subiculum decreased following the cut (n= 3 slices; P<0.001) (Fig. 4D). Overall, these findings indicate that the EC is able to sustain both polyspike and long-lasting interictal discharges whereas the subiculum can only sustain long lasting interictal discharges when the two regions are disconnected.

Application of an NMDA receptor antagonist - Finally, to establish the role of NMDA receptor mediated signalling in epileptiform activity recorded from the EC and subiculum following the severance of connections between the two regions, we applied 10 μM CPP to brain slices that were generating either sudden or LVF onset ictal discharges before the cut. Ictal events remaining in the EC as well as the trains of positive-going spikes at 1 to 1.5 Hz persisting in the subiculum after the cut were abolished by CPP (not illustrated). Therefore, we focused on the analysis of the changes induced by this NMDA receptor antagonist on interictal activity generated by the isolated EC and subiculum.

In brain slices that were characterized by sudden onset ictal discharges, CPP did not change the duration of the polyspike interictal discharges in the EC (Fig. 5C) while their interval of occurrence increased significantly and became irregular (n= 5; P<0.05) thus disrupting the rhythmicity of this type of interictal pattern (Fig. 5D); in addition, in these experiments field oscillations at approx. 2 Hz, which followed each interictal discharge, emerged during NMDA receptor antagonism (arrows and insert in Fig. 5A, +CPP). In the subiculum, the interval of occurrence and the duration (n= 3; P<0.05) of the long lasting interictal events increased significantly in the presence of CPP (Fig. 5C-D). In those brain slices in which LVF onset seizures occurred before the cut, CPP did not change the duration of the interictal events recorded in EC but significantly increased their interval of occurrence (n= 3; P<0.05) (Fig. 5C and D); in addition, we found in these experiments that CPP decreased the duration of the long-lasting interictal events

recorded in the subiculum (n= 3; P<0.001) without significantly affecting their interval of occurrence (Fig. 5C and D).

3.6. Discussion

The main findings of this study can be summarized as follows. First, in intact brain slices suddenly arising ictal events predominantly initiate in the EC whereas LVF onset ictal events often appear to initiate from the subiculum. Second, in spite of such apparent subicular initiation of LVF ictal activity, severing the connections between EC and subiculum abolishes ictogenesis in the latter structure. Third, we confirmed the application of the NMDA receptor antagonist CPP could block the occurrence of both sudden and LVF onset ictal events in the EC as well as the fast trains of spikes generated by the isolated subiculum after cut. Fourth, CPP disrupted the rhythmicity of fast polyspike interictal discharges in the EC following cut.

Contribution of entorhinal cortex-subiculum interactions to ictogenesis - Within the limbic system, the subiculum holds a strategic position as an interface between the hippocampus proper and parahippocampal structures. It serves as the major output structure of the hippocampus, receiving extensive projections from the CA1 hippocampal region (Finch and Babb, 1981; Witter and Groenewegen, 1990) and projecting towards both extralimbic and limbic areas including the thalamus (Witter et al., 1990; Canteras and Swanson, 1992), perirhinal cortex (Witter and Groenewegen, 1990), amygdala (Canteras and Swanson, 1992) and EC (Witter et al., 1989). While the subiculum acts as the output structure of the hippocampus, the EC provides afferents to the hippocampus via the perforant path (Hjorth-Simonsen, 1972; Witter and Groenewegen, 1984). The perforant pathway plays an important role in epileptic disorders but there also exists an additional entorhinal input to the subiculum (Van Groen and Lopes da Silva, 1986; Shao and Dudek, 2011). This short EC-subicular, subicular-EC circuit through temporoammonic pathway, is functionally active thus suggesting that hippocampal inputs and outputs can be modulated locally between these two regions (Steward and Scoville, 1976; Van Groen and Lopes da Silva, 1986).

In the current study, we found evidence suggesting that this local EC-subicular circuit plays an important role in the synchronization and maintenance of ictal activity while in a previous study from our laboratory, the subiculum was found to function as the gating structure acting between the hippocampus proper and the EC (Benini and Avoli, 2005). According to these early experiments, as long as $GABA_A$ receptor-mediated signaling was maintained, the subiculum effectively "blocked"

the further propagation of CA3-driven interictal discharges to the EC, and it generated interictal events that occurred synchronously with those recorded in the CA1-CA3 subfields (Benini and Avoli, 2005). These different results may depend on slightly different slicing procedures such as the angle of approx. 10° used to orient the brain tissue before obtaining horizontal slices (*cf.*, Avoli et al. 1996; Benini and Avoli, 2005). This view is supported by the fact that in these early studies the majority of the epileptiform patterns recorded from the EC during 4AP application consisted of isolated, long lasting interictal discharges along with LVF onset ictal events while the sudden onset pattern described here (as well as in Avoli et al., 2013) was rarely seen. Another factor contributing to the ability of subicular networks to generate and actually initiate LVF ictal events may rest on the spacing of specific subicular area targeted for obtaining extracellular signals; in fact in the experiments by Benini and Avoli (2005) recording microelectrodes were placed in the subiculum adjacent to the CA1, whereas in the current study, they were positioned more rostrally and closer to the medial EC. If this is the case, it may be suggested that the subiculum receives either a gradient of or distinction between local inputs from the CA1 and the EC (Naber et al., 2001). Finally, one cannot exclude the possibility that signals recorded from the subiculum were contaminated by far field effects, namely volume-conducted synchronous neuronal events generated in the EC or other limbic areas comprised in the brain slice (Inaba and Avoli, 2006).

Our results also show that sudden onset ictal events most likely initiate in the EC, whereas those with LVF onset features appear to initiate from close subiculum-EC interactions. However, after cutting the connections between subiculum and EC, both types of ictal events continued to occur in the EC (though with shorter duration than in control) while they either disappeared in the subiculum altogether or manifested as trains of positive going spikes. This discrepancy suggests that the regional specificity is either an oversimplification of the size of the network involved in generating the ictal event, or the spatial resolution of our field recordings was insufficient to catch the 'true' ictal onset region.

Because ictal discharges are modified in both limbic structures, it can be hypothesized that a local EC-subicular circuit plays a role in generating and sustaining ictal activity. Why then, when the circuit is intact, is the EC more likely to initiate sudden onset ictal events whereas the subiculum is more likely to initiate LVF onset events? This propensity is possibly related to the homeostatic drive exerted by the CA1 on the subiculum to attenuate hyperexcitable activity (Sah and Sikdar, 2013). Feed forward inhibition during the hyperexcitable state can be characterized by inhibitory post-synaptic potentials in pyramidal cells and bursting activity in local fast-spiking interneurons (Sah and

Sikdar, 2013). This inhibitory drive could increase the likelihood to generate LVF compared to sudden onset events; however, to fully understand the role of EC-subicular interactions in ictogenesis, studies investigating single cell firing dynamics of interneurons and pyramidal cells simultaneously recorded from both regions are required. These studies have the potential to reveal the contribution of different cell types to different onset patterns and identify the region in which cell firing is most correlated to the epileptiform activity identified with field recordings. This approach has been successfully implemented *in vivo* by Toyoda et al. (2013, 2015) in a rat model of temporal lobe epilepsy; it is, however, difficult at this time to extrapolate from these data, which were obtained from a chronic model of epilepsy, to our findings that derive from brain slices acutely treated with convulsant drugs.

Interictal discharges in subiculum and entorhinal cortex and the role of NMDA receptors - Cutting the connections between EC and subiculum blocked the generation of polyspike discharges in the latter, further suggesting that they are driven by the activity of EC neuronal networks (Lopantsev and Avoli, 1998b). This effect was accompanied by the appearance in the subiculum of slow interictal events similar to those recorded between LVF onset seizures. Previous studies have shown that these slow interictal events are largely contributed by $GABA_A$ receptor-mediated currents caused by the release of GABA from interneuron terminals (Avoli et al., 1996; Lopantsev and Avoli, 1998b). This finding is in keeping with the ability of cortical networks to generate synchronous activity reflecting the postsynaptic activation of GABA receptors as reported to occur in human brain slices of the neocortex and subiculum during application of normal medium (Köhling et al., 2000; Cohen et al 2002; Huberfeld et al., 2011).

As expected (Avoli et al., 1996; Lopantsev and Avoli, 1998a; *cf.*, Avoli and de Curtis, 2011), blockade of NMDA-receptor mediated signalling prevented ictogenesis in the isolated EC. In addition, during such pharmacological treatment, fast polyspike interictal events were no longer observed and interictal events that were remaining occurred in a less regular pattern. This evidence demonstrates that NMDA receptor signalling plays an important role in ictogenesis as well as in the maintenance of the rhythmicity of fast polyspike interictal activity.

Conclusive remarks - Overall, our study demonstrates that the reciprocal circuitry between the EC and subiculum plays an important role in sustaining ictogenesis *in vitro*. When these connections are disrupted, ictal discharges cannot be sustained as efficiently as when EC-subicular connectivity is

intact. It is important to emphasize that both sudden- and LVF-onset ictal discharges are equally dependant on reciprocal connections between the subiculum and EC. To better understand the local contribution of the EC-subicular circuit in ictogenesis, further studies should be aimed at analyzing the single unit activity generated by specific cell types in both regions.

3.7. Figures

Figure 3-1

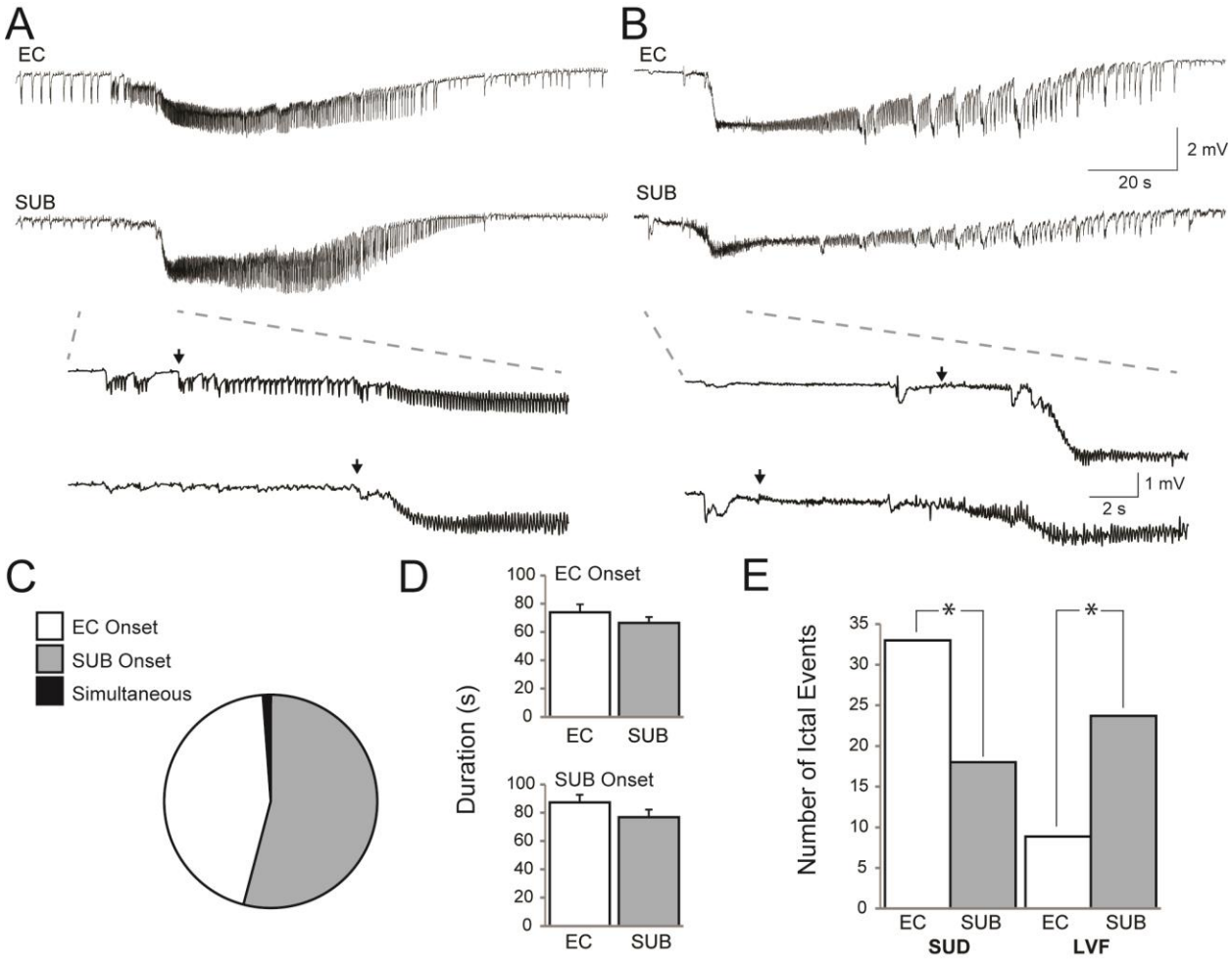

Figure 1: Different ictal onset patterns recorded from the EC and subiculum. (A) Example of a sudden onset ictal event with the onset period expanded below. Single arrows represent ictal onset points. **(B)** Example of an LVF onset ictal event, again with the onset period expanded below. **(C)** Pie chart representing the proportion of ictal events initiating in subiculum, EC, or simultaneously in both regions. **(D)** Bar graphs showing the duration of ictal events in the EC and subiculum based on the region in which they were first detected. **(E)** Proportion of sudden onset and LVF onset ictal events that appeared to initiate in either the EC (white) or subiculum (grey). (*$P<0.001$, Fisher's Exact Test)

Figure 3-2

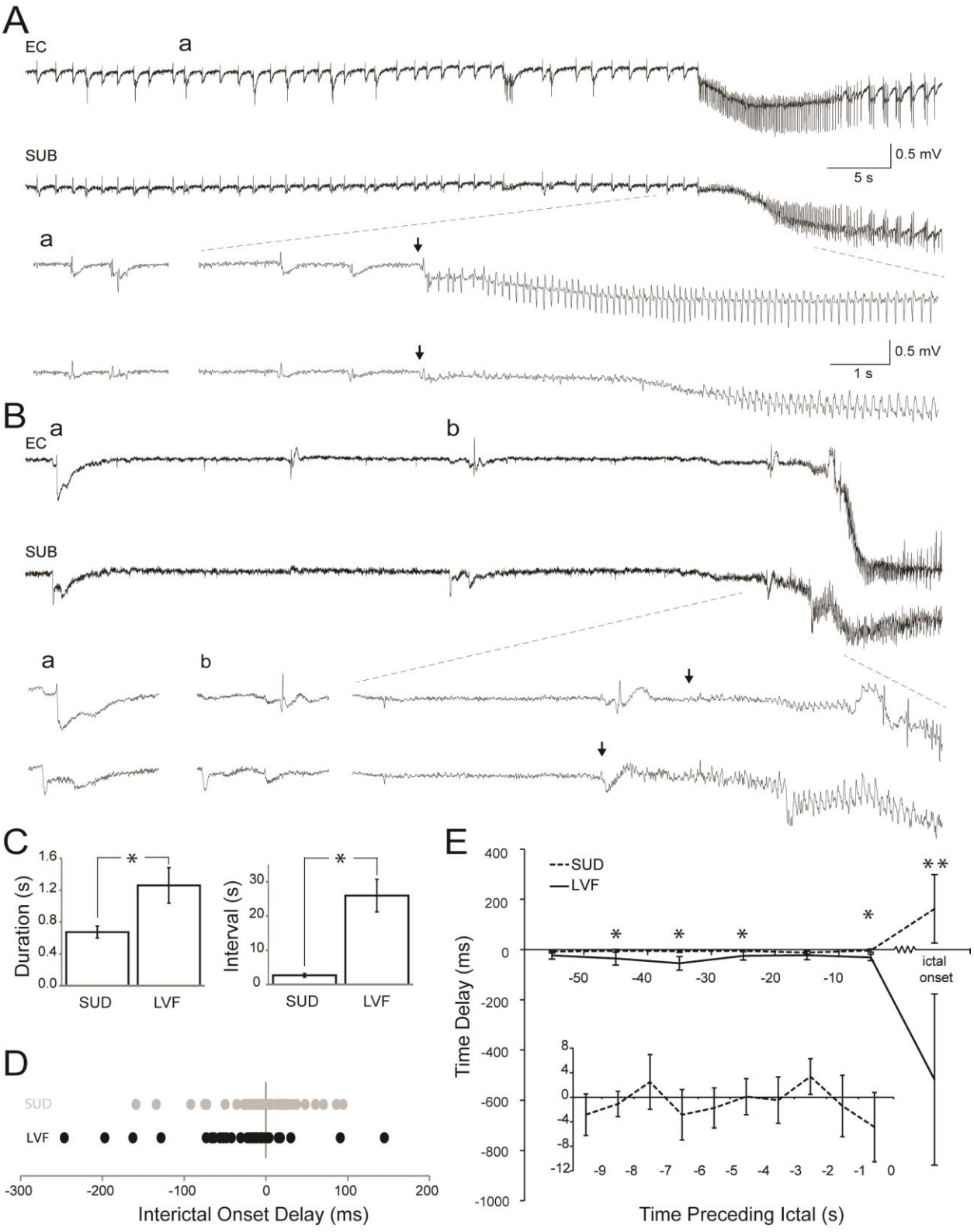
A
EC
a
SUB
0.5 mV
5 s
a
0.5 mV
1 s
B
EC
a
b
SUB
a
b
C
Duration (s)
1.6
1.2
0.8
0.4
0.0
*
SUD
LVF
Interval (s)
30
20
10
0
*
SUD
LVF
D
SUD
LVF
-300
-200
-100
0
100
200
Interictal Onset Delay (ms)
E
SUD
LVF
Time Delay (ms)
400
200
0
-200
-400
-600
-800
-1000
*
*
*
*
**
ictal onset
-50
-40
-30
-20
-10
8
4
0
-4
-8
-12
-9
-8
-7
-6
-5
-4
-3
-2
-1
0
Time Preceding Ictal (s)

Figure 2: Delays between interictal discharges in relation to the time preceding sudden and LVF ictal onset patterns. (A) Frequent polyspike interictal discharges precede a sudden onset ictal event. Single arrows represent ictal onset points. **(B)** Interictal discharges preceding an LVF onset ictal event. **(C)** Bar graphs showing the duration and the interval of occurrence of interictal events based on the ictal onset pattern they are associated with. **(D)** Chart showing the distribution of time delays between the entorhinal cortex and subiculum at the interictal event immediately preceding the ictal event. Negative values indicate that the subiculum leads the entorhinal cortex whereas positive values indicate that the entorhinal cortex leads the subiculum. Each dot represents a single interictal event. **(E)** Line graph depicting average delays between synchronized interictal events in 10 s time bins preceding the ictal event. Time 0 represents the interictal event immediately preceding the ictal event. Positive values indicate that the event initiates in the entorhinal cortex and negative values indicate that the event initiates in the subiculum. The inset shows an expansion of the time bin preceding ictal onset for sudden onset events only. (*$P<0.05$; **$P<0.001$)

Figure 3-3

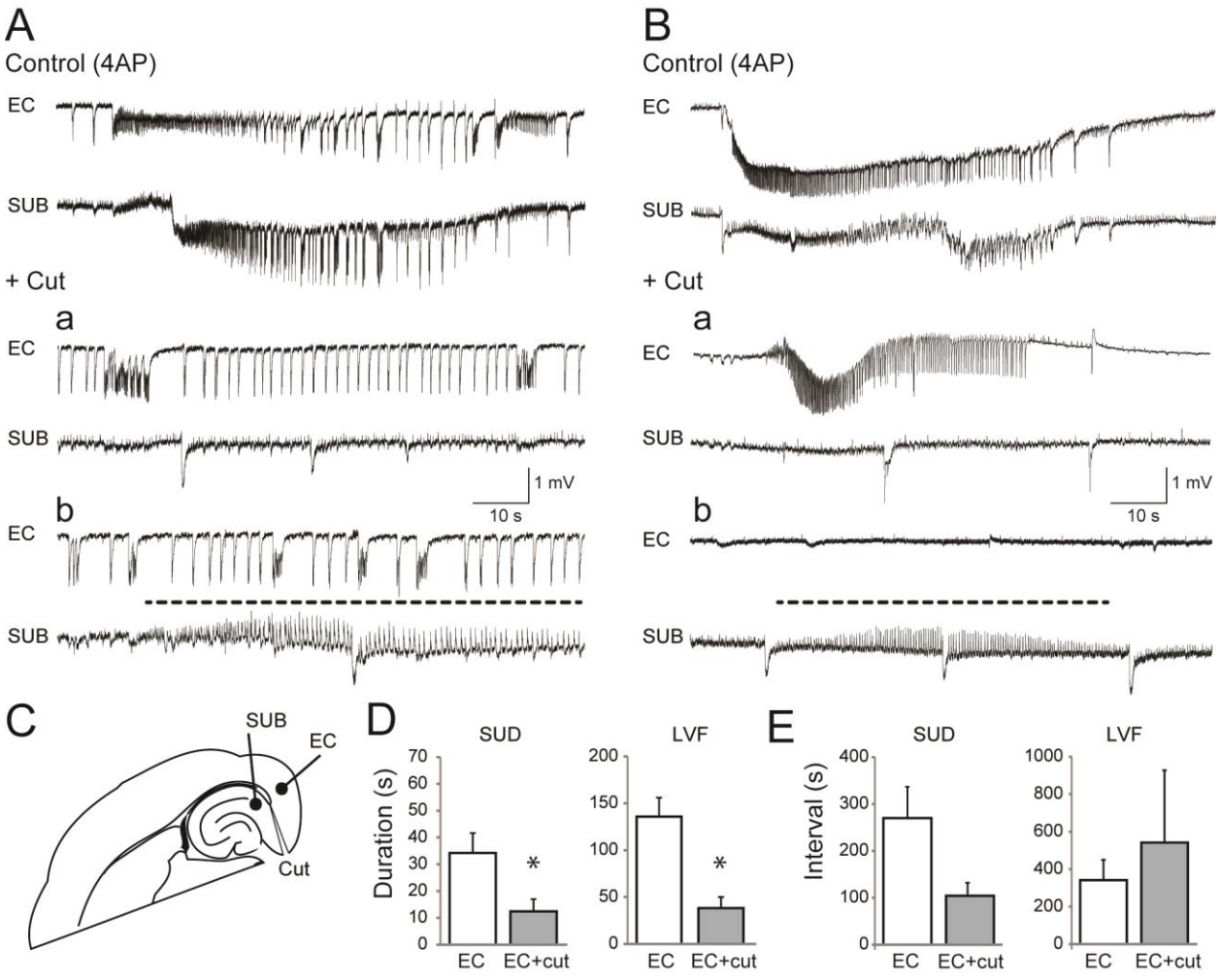
A
Control (4AP)
EC
SUB
+ Cut
a
EC
SUB
1 mV
10 s
b
EC
SUB
B
Control (4AP)
EC
SUB
+ Cut
a
EC
SUB
1 mV
10 s
b
EC
SUB
C
SUB
EC
Cut
D
SUD
LVF
Duration (s)
70
60
50
40
30
20
10
0
200
150
100
50
0
*
*
EC
EC+cut
EC
EC+cut
E
SUD
LVF
Interval (s)
400
300
200
100
0
1000
800
600
400
200
0
EC
EC+cut
EC
EC+cut

Figure 3: Ictal synchronization between structures. Synchronicity between the entorhinal cortex and subiculum can be manipulated by severing connections between the regions. **(A)** Traces of a sudden onset ictal event during control (4AP only) conditions and after cutting the connections between the subiculum and entorhinal cortex. **(B)** Traces depicting the change in synchronisation between the entorhinal cortex and subiculum in a slice characterized by LVF ictal events. In both panels **A** and **B**, the dotted line highlights the trains of positive-going spikes that occur in the subiculum after the cut. **(C)** Schematic showing the location of the "cut" and the electrode placement. **(D)** Bar graphs indicating the change in duration of ictal events following the cut in slices characterized by either sudden or LVF onset patterns. **(E)** Bar graphs showing the change in interval between either sudden onset or LVF ictal events following the cut. (*$P<0.05$)

Figure 3-4

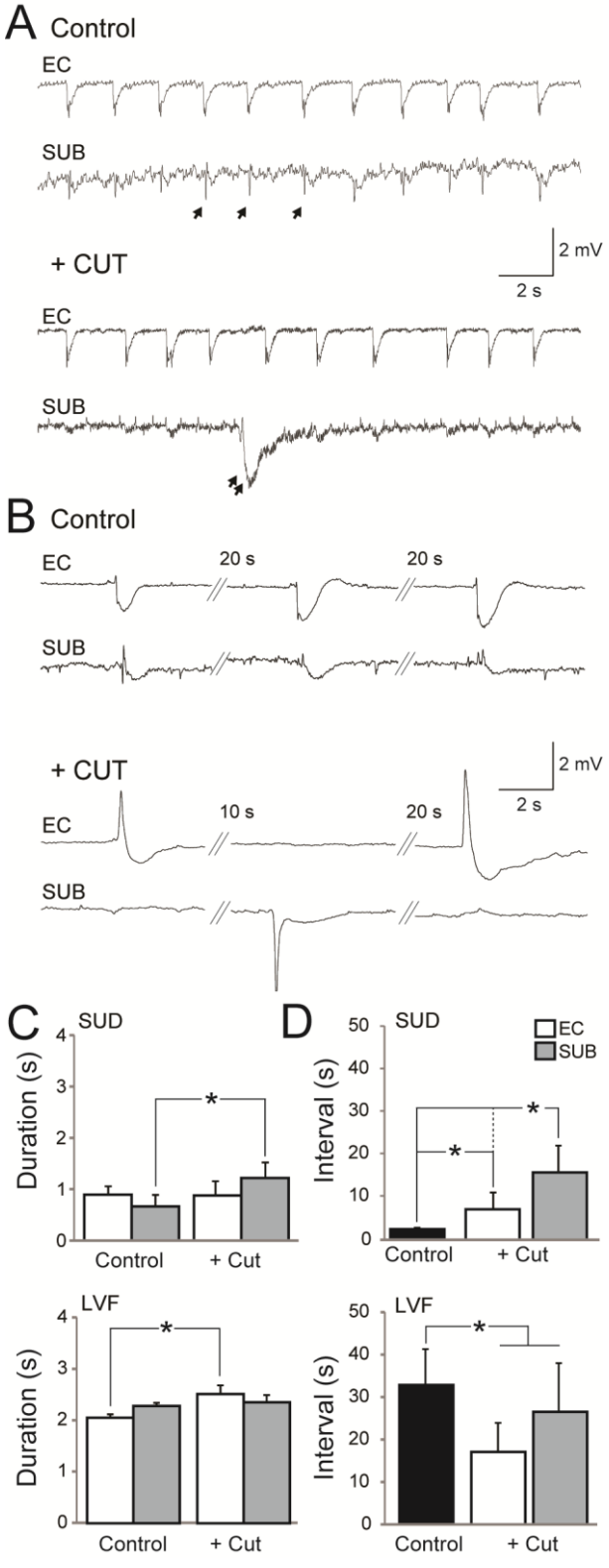
A Control
EC
SUB
+ CUT
2 mV
2 s
EC
SUB
B Control
EC
20 s
20 s
SUB
+ CUT
2 mV
2 s
EC
10 s
20 s
SUB
C
SUD
Duration (s)
Control
+ Cut
LVF
Duration (s)
Control
+ Cut
D
SUD
EC
SUB
Interval (s)
Control
+ Cut
LVF
Interval (s)
Control
+ Cut

Figure 4: Interictal synchronization between structures. Synchronicity between interictal events recorded in the subiculum and entorhinal cortex can be modulated by severing connections. **(A)** Representative traces of interictal events recorded during control (4AP) conditions and after cutting the connections between the subiculum and entorhinal cortex in a slice characterized by sudden onset ictal events. Single arrows point to fast polyspike interictal discharges and double arrows point to long lasting interictal discharges. **(B)** Interictal events recorded from a slice characterized by LVF ictal events. **(C & D)** Bar graphs showing the change in duration and interval, respectively, of interictal events recorded from slices characterized by LVF or sudden onset ictal events. (*$P<0.001$)

Figure 3-5

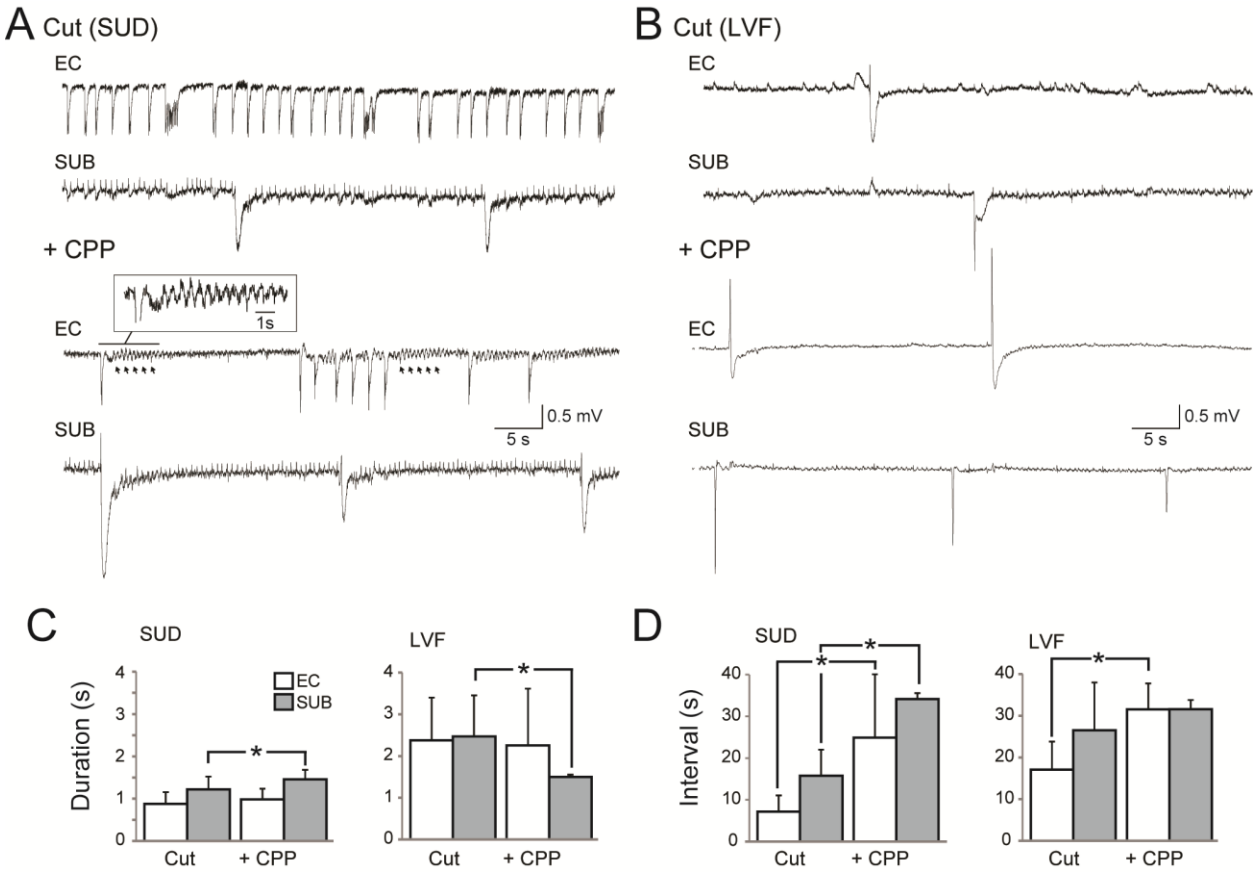
A Cut (SUD)
EC
SUB
+ CPP
1s
EC
0.5 mV
5 s
SUB
B Cut (LVF)
EC
SUB
+ CPP
EC
0.5 mV
5 s
SUB
C
SUD
LVF
Duration (s)
EC
SUB
Cut
+ CPP
Cut
+ CPP
D
SUD
LVF
Interval (s)
Cut
+ CPP
Cut
+ CPP

Figure 5: Blockade of NMDA-receptor mediated signalling. Glutamatergic activity plays an important role in epileptiform synchronization. **(A and B)** Representative traces showing the effects of CPP on slices where connections between EC and subiculum are severed. In panel **A**, the expanded inset shows activity that occurs at approximately 2 Hz which can be revealed with the application of CPP. **(C & D)** Bar graphs showing the changes in duration and interval in slices before (4AP + Cut) and after the application of CPP. (*$P<0.05$)

4. NEUROSTEROIDS MODULATE EPILEPTIFORM ACTIVITY AND ASSOCIATED HIGH-FREQUENCY OSCILLATIONS IN THE PIRIFORM CORTEX

By Herrington R, Lèvesque M, Avoli M

Published in Neuroscience, 2014

4.1. Rationale and Objective

We found that different ictal onset types may be characterized by different underlying mechanisms. Specifically, LVF ictal onset events appeared to be contributed by a more pronounced GABAergic component compared to sudden onset ictal events. Since GABA receptor agonists constitute a major class of AEDs, we tested how the positive modulation of $GABA_A$ receptor-mediated signalling can modulate patterns of epileptiform synchronization correlated with greater GABAergic contributions. To this end, we employed two different concentrations of THDOC, a neurosteroid that physiologically occurs at low levels in the brain. Furthermore, we shifted our interest from the entorhinal cortex to the anterior and posterior piriform cortices. These regions were of interest for three reasons. First, the anterior piriform cortex is more strongly connected to the olfactory bulb whereas the posterior piriform cortex is highly connected to structures in the limbic system (Illig, 2005). This allowed us to compare two regions that were presumably connected to the hippocampus but by different degrees. Second, local GABAergic signalling is stronger in the posterior compared to the anterior piriform cortex, which could have important implications for the neurosteroidal effect (Vismer et al., 2015). Third, the anterior piriform cortex contains the *area tempestas*, which is region that is highly susceptible to the generation of epileptiform activity (Piredda and Gale, 1985). Thus, elucidating how neurosteroids can differentially modulate epileptiform activity in these two regions can provide insight into the idiosyncrasies associated with different degrees of GABAergic contribution and hippocampal connectivity.

4.2. Abstract

Allotetrahydrodeoxycorticosterone (THDOC) belongs to a class of pregnane neurosteroidal compounds that enhance brain inhibition by interacting directly with $GABA_A$ signaling, mainly through an increase in tonic inhibitory current. Here, we addressed the role of THDOC in the modulation of interictal- and ictal-like activity and associated high-frequency oscillations (HFOs, 80-

500 Hz; ripples: 80-200 Hz, fast ripples: 250-500 Hz) recorded in vitro in the rat piriform cortex, a highly excitable brain structure that is implicated in seizure generation and maintenance. We found that THDOC: (i) increased the duration of interictal discharges in the anterior piriform cortex while decreasing ictal discharge duration in both anterior and posterior piriform cortices; (ii) reduced the occurrence of HFOs associated to both interictal and ictal discharges; and (iii) prolonged the duration of 4-aminopyridine-induced, glutamatergic independent synchronous field potentials that are known to mainly result from the activation of $GABA_A$ receptors. Our results indicate that THDOC can modulate epileptiform synchronization in the piriform cortex presumably by potentiating $GABA_A$ receptor-mediated signaling. This evidence supports the view that neurosteroids regulate neuronal excitability and thus control the occurrence of seizures.

4.3. Introduction

The piriform cortex is a highly excitable region that extends over the ventrolateral forebrain in rodents (Galvan et al., 1982; Loscher and Ebert, 1996; Luskin and Price, 1983). This three-layered cortical area projects to several limbic structures including the amygdala, lateral entorhinal cortex, and subiculum (Haberly, 2001; Luskin and Price, 1983). With regards to connectivity, the piriform cortex can be divided into the anterior and posterior subregions (Haberly, 1998). Along these subregions, GABAergic inputs are asymmetrically arranged, with the strength of interneuron-to-pyramidal cell contact increasing along the rostro-caudal axis or from the anterior subregion towards the posterior (Luna and Pettit, 2010). Therefore, the anterior piriform cortex is presumably more excitable when compared to the posterior piriform.

Neuronal excitability can be modulated by neurosteroids, a class of compounds that act on ion channels and membrane receptors (Akk et al., 2009; Mellon and Griffin, 2002). By modulating the efficacy of $GABA_A$ receptor function, allotetrahydrodeoxycorticosterone (THDOC) enhances brain inhibition and acts as a broad spectrum anticonvulsant, protecting against seizures induced by pilocarpine, kindling, and $GABA_A$ receptor antagonists in animal models of epilepsy *in vivo* (Reddy, 2004b, 2011; Rupprecht et al., 1996; Stell et al., 2003). Furthermore, *in vitro* studies performed in rat hippocampal slices have shown that neurosteroids produce a concentration dependent suppression of the epileptiform activity induced by 4-aminopyridine (4AP) and picrotoxin (Salazar et al., 2003). Finally, the induction of neurosteroid synthesis in rats following pilocarpine treatment can delay epileptogenesis *in vivo* (Biagini et al., 2009).

High frequency oscillations (HFOs, ripples: 80-200 Hz, fast ripples: 250-500 Hz) are recorded in the EEG of epileptic patients and in animal models of temporal lobe epilepsy (Engel and da Silva, 2012; Jefferys et al., 2012). HFOs occur in limbic structures such as the hippocampus and entorhinal cortex as well as in the neocortex, they are thought to reflect the activity of dysfunctional neural networks, and they are used to localize seizure onset zones (Bragin et al., 2004; Ibarz et al., 2010; Jacobs et al., 2009, 2010; Jiruska et al., 2010; Lévesque et al., 2011, 2012; Wu et al., 2010). Using sagittal and coronal brain slices maintained *in vitro*, Panuccio et al. (2012) have recently reported that HFOs coincide with the onset of ictal discharges induced by 4AP in the piriform cortex. Here, we further investigated the role of the piriform cortex in generating 4AP-induced epileptiform activity *in vitro* by addressing the impact of the neurosteroid THDOC on the epileptiform activity and associated HFOs in both anterior and posterior subregions. To improve access to both anterior and posterior aspects of the piriform cortex, which may differentially express epileptiform activity, we used horizontal rat brain slices that are known to better maintain rostro-caudal association fiber connections (Demir et al., 2001).

4.4. Methods

***In Vitro* Preparation -** Horizontal brain slices with a thickness of 450 μm were obtained from male Sprague-Dawley Rats weighing 250-275g (Charles River Laboratories, Saint Constant, Quebec, Canada). Animals were anesthetized with isoflurane and decapitated. Their brains were then quickly removed and chilled for 3 min in ice-cold artificial cerebrospinal fluid (ACSF) with the following composition (mM): 124 NaCl, 2 KCl, 2 $CaCl_2$, 2 $MgSO_4$, 1.25 KH_2PO_4, 26 $NaHCO_3$, 10 D-glucose. The ACSF was continuously bubbled with O_2/CO_2 (95/5%) gas mixture to maintain pH at ~ 7.4. Slices were prepared with a Vibratome (VT1000S; Leica, Concord, Ontario, Canada) and directly transferred to an interface chamber where they laid between warm (31-33 ºC) ACSF (pH ~7.4, ~305 mOsm/kg) and humidified gas (O_2/CO_2, 95/5%). Slices were allowed to recover for at least 1 hour before initiating the continual bath application of 4AP (50 μM) at a flow rate of ~2 ml/min. All pharmaceuticals were bath applied and obtained from Sigma-Aldrich Canada, Ltd. (Oakville, Ontario, Canada) or from Tocris Bioscience (Ellisville, Missouri, USA). All procedures were carried out in compliance with the guidelines of the Canadian Council on Animal Care and the McGill Animal Care Committee to minimize the suffering and number of animals.

Field Potential Recordings **-** Field potential recordings were obtained with ACSF filled glass pipettes (1B150F-4; World Precision Instruments, Sarasota, Florida, USA; tip diameter <10 μm, resistance 5-10 MΩ) that were pulled with a Sutter P-97 puller (Sutter, Novato, California, USA). Electrodes were placed in the anterior and posterior piriform cortices at a distance of approximately 1.5 mm. Signals were fed to an AI 401 amplifier and a CyberAmp 380 (Molecular Devices, Silicon Valley CA, USA), then digitized using the Digidata 1322A (Molecular Devices). Signals acquired with the CyberAmp 380 were sampled at 5 KHz and cut-off at 1 KHz.

Detection and analysis of high-frequency oscillatory events **-** To study HFOs, time-periods containing ictal and interictal discharges recorded from the piriform cortex were extracted and analysed offline using Matlab (The Mathworks, Natick, MA, USA). A multiparametric algorithm using routines based on standardized functions (Signal Processing Toolbox) was used. Recordings were first band-pass filtered in the 80-200 Hz and 250-500 Hz frequency ranges using a finite impulse response (FIR) filter. Zero phase digital filtering was used to avoid phase distortion. Each recording was then normalised using a 10 s artefact-free period. To be considered as an HFO candidate, oscillatory events in the 80-200 Hz and in the 250-500 Hz frequency range had to show four consecutive peaks at three standard deviations (SDs) above the mean as determined by the reference period.(Salami et al., 2012) The time lag between consecutive peaks varied from 5 to 12.5 ms for ripples and from 2 to 4 ms for fast ripples (Salami et al., 2012). HFOs were kept for analysis only if the oscillatory event was visible in either the 80-200 Hz or 250-500 Hz range. Overlapping events, which may be caused by the filtering of sharp spikes (Bénar et al., 2010), were excluded from the analysis. HFO rates were obtained for each ictal discharge and interictal discharge in the anterior and posterior subregions of the piriform cortex.

Statistical Analysis **-** Offline analysis of the duration and interval of occurrence of ictal and interictal discharges was performed using the software CLAMPFIT 8.2 (Molecular Devices). Specifically, in both cases, we measured the duration as the time span between the first deflection of the discharge from baseline to its return to baseline. Interval was measured as the time occurring between the onsets of consecutive discharges. Amplitude was measured from peak to peak. Time lag was measured as the difference in time onset between field potential recorded in the anterior and posterior subregion. Arbitrarily, discharges leading from the anterior piriform cortex were assigned a negative value and discharges originating in the posterior subregion were assigned positive value.

When no difference was detected, a value of 0 was assigned. All visual analyses were conducted blind to the subregion of the piriform cortex being analyzed and the concentration of THDOC present in the ACSF.

Distributions were tested for skewness and kurtosis. Data were analyzed with two-way ANOVAs followed by the Tukey post hoc test, as appropriate. To account for the variability in ictal discharge duration between slices, Z-values were assigned to each discharge within a given experiment, allowing us to test the group effect of THDOC. HFOs occurrence was analyzed using the non-parametric Mann-Whitney rank sum test followed by the Bonferroni correction for multiple comparisons since values were not normally distributed.

When analysing the dynamics of HFO occurrence, in order to account for differences in duration, ictal discharges were first transformed into a time scale from 1 (start of the ictal event) to 100 (end of the ictal event). The ictal period was then divided in three equal parts and rates of ripples and fast ripples in each subregion of the piriform cortex (anterior and posterior) were compared using non-parametric Wilcoxon signed rank tests followed by Bonferroni-Holm corrections for multiple comparisons. This allowed us to evaluate if ripples or fast ripples predominated at specific moments of the ictal event in each piriform cortex subregion. Throughout the text, *n* indicates the number of slices studied, unless otherwise specified. Results were considered significantly different if $p < 0.05$ and are expressed as mean ± standard error of the mean (SEM).

4.5. Results

Interictal and ictal discharges induced by 4-aminopyridine **-** Figure 1A shows examples of interictal and ictal activity induced by 4AP. Interictal discharges occurred synchronously in the anterior and posterior piriform cortex (Fig 1Ab) at an average interval of 9.6 ± 3.5 s, and lasted on average 297.3 ± 7.2 ms in the anterior piriform cortex and 322.6 ± 8.3 ms in the posterior piriform cortex (n= 19, 1171 events). These values were not significantly different. Moreover, interictal events were likely to initiate equally from the anterior and posterior subregions of the piriform cortex as shown by the time lag histograms (Fig 1B).

Ictal discharges occurred at average rate of 20 ± 2.4 events per hour (n= 19, 152 events), with all discharges in the anterior piriform cortex co-occurring with a discharge in the posterior piriform cortex (Fig 1A). Ictal discharges were characterized by an initial negative shift followed by the appearance of oscillations at approximately 15 Hz (spectrograms in Fig 1A). The average duration of ictal discharges in the anterior and posterior piriform cortex was 66.8 ± 6.0 s and 69.6 ±

6.4 s, respectively. These values were determined to be not significantly different. Ictal events were equally likely to initiate from either the anterior or the posterior piriform cortex as indicated by the time lag histograms (Fig 1B).

In 5 separate experiments ranging from 55 to 90 min, the duration and interval of interictal events were analyzed at five min intervals throughout the recording (Fig. 1C). Time 0 represents the onset of the first recorded ictal event. Interictal parameters were assessed during the first interictal interval following the time stamp. Overall, there were no significant changes in duration and interval over the recorded period in the slices analyzed. The time of the onset of each ictal event was then plotted with the corresponding ictal duration. Over the recorded period, duration and interval of ictal discharges remained constant over time.

Neurosteroids modulate 4-aminopyridine-induced interictal activity **-** Figure 2A shows examples of interictal discharges in the anterior and posterior piriform cortex under control conditions and during the application of 0.1 μM THDOC (n= 7) and 5 μM of THDOC (n= 6). Following the application of 0.1 μM THDOC, the duration of interictal events in the anterior piriform cortex increased significantly ($p< 0.05$) compared to those seen under control conditions only (Fig 2B). With 5 μM of THDOC (n= 6), the duration of interictal discharges further increased compared to the 0.1 μM condition ($p< 0.05$) (Fig 2B). In contrast, interictal discharge duration in the posterior piriform cortex exhibited no change (Fig 2B). However, in both anterior and posterior subregions, 0.1 μM THDOC significantly increased the interval between interictal discharges ($p<0.05$) from 4AP control, and 5 μM THDOC further increased the interval between discharges ($p <0.05$) (Fig 2C). Moreover, compared to the 4AP control condition, 0.1 μM and 5 μM THDOC increased interictal amplitude in the anterior piriform cortex but did not induce a corresponding change in the posterior subregion (Fig 2D). Following a 1.5 hour wash out period, there was no full recovery to control conditions, possibly due to the hydrophobic nature of THDOC. Consistent with the 4AP control condition, interictal discharges during 4AP and THDOC were likely to originate from either the anterior or posterior piriform cortices.

Neurosteroidal modulation of 4AP-induced ictal activity **-** Figure 3A shows ictal discharges recorded during the application of 4AP as well as following the addition of 0.1 μM and 5 μM THDOC. Application of 0.1 μM THDOC induced a decrease in ictal discharge duration compared to the control condition in recordings simultaneously performed in anterior piriform cortex ($p<0.05$)

and posterior piriform cortex ($p<0.05$) (Fig 3B). 5 μM THDOC also significantly reduced the duration of ictal events in both anterior ($p< 0.05$) and posterior piriform cortex ($p< 0.05$) (Fig 3A and B). Moreover, 5 μM of THDOC led to a larger decrease in duration of ictal discharges compared to 0.1 μM condition ($p< 0.05$) (Fig 3B). Neither the 0.1 μM nor the 5 μM THDOC concentration affected the interval of ictal events (Fig 3C) although a trend toward an increase in interval length was observed. In 2 of 6 experiments ictal events were completely abolished 40 min following the application of 5 μM THDOC with only interictal events remaining. Finally, as reported for interictal discharges, THDOC application (both 0.1 μM and 5 μM) did not affect the "initiation jittering" observed by simultaneously recording ictal discharges from the anterior and posterior piriform subregions.

***Effects of THDOC on high-frequency oscillations* -** Figure 4A shows examples of a ripple (Fig 4Aa) and a fast ripple (Fig 4Ab) occurring in the anterior piriform cortex in coincidence with interictal events induced by 4AP. Under this condition, only 1.9 % (23/1235) of interictal spikes recorded in the anterior subregion co-occurred with ripples, whereas 16.5 % of them (204/1235) co-occurred with fast ripples (n= 19 slices) (Fig 4Ba). Thus, fast ripples occurred more frequently than ripples ($p<0.05$). In the posterior subregion, HFO occurrence was markedly lower than the anterior subregion with only 1% of interictal discharges co-ocurring with either ripples or fast ripples (11 of 1047 interictal events, n = 19) (Fig 4Bb). In both anterior and posterior subregions, HFOs occurring outside of interictal discharges were negligible.

Application of 0.1 μM THDOC induced a significant decrease in the occurrence of fast ripples associated with interictal spikes in the anterior piriform cortex (44/665 events, n= 7 slices) ($p < 0.01$) while ripple occurrence did not change significantly (3/665 events, n= 7 slices) (Fig 4Ba). Following application of 5 μM THDOC, fast ripples were virtually abolished (633 events, n= 7 slices) ($p < 0.05$) and the occurrence of ripples remained low (2/633 events, n= 7 slices) (Fig 4Ba). In the posterior piriform cortex HFO rates remained low during the application 0.1 μM or 5 μM THDOC (Fig 4Bb). Thus, THDOC can significantly reduce the proportion of fast ripples associated to interictal discharges in the anterior subregion of the piriform cortex.

Next, we analyzed the incidence of ripples and fast ripples during ictal discharges recorded from the anterior and posterior piriform cortices during 4AP application (Fig 5A). Throughout the duration of ictal discharges, fast ripples occurred at higher rates compared to ripples in both anterior and posterior subregions. Fast ripple occurrence in the pre-ictal period was higher in the anterior

than the posterior piriform cortex. During the ictal period, ripple and fast ripple occurrence was higher in the anterior piriform cortex. In the post-ictal period, fast ripple rates remained higher compared to those in the posterior region (Fig 5B).

We also established the proportion of ictal discharges containing ripples and fast ripples in the anterior and posterior piriform cortices under control conditions and following application of 0.1 μM and 5 μM THDOC. In the anterior piriform cortex, ripples and fast ripples were detected in 47.7% (71/149) and in 48.3% (72/149), respectively, of the ictal discharges occurring in the 4AP control condition (149 events, n= 19) (Fig 5C). In both subregions, treatment with 0.1 μM THDOC (n= 7) led to a higher proportion of ictal discharges containing ripples (70%) while those containing fast ripples remained constant (50%). During the application of 5 μM THDOC (n = 6), although the total proportion of ictal discharges containing ripples and fast ripples decreased, there was still a higher number of discharges that contained ripples (30%) than fast ripples (10%). A similar pattern was observed in the posterior region. Thus, THDOC increased the probability for an ictal discharge to contain HFOs in the ripple frequency range (if they contained HFOs at all) compared to the fast ripple frequency range, despite fast ripples occurring at a greater rate.

We then considered only those ictal discharges where HFOs were detected in order to determine the change in occurrence of ripples and fast ripples induced by THDOC. In the anterior piriform cortex, there was an average of 14.6 ± 2.2 ripples and 45.1 ± 7.6 fast ripples per discharge under control conditions; application of 0.1 μM or 5 μM THDOC led to a significant decrease of HFO occurrence ($p< 0.01$ in both cases) (Fig 5C). In the posterior piriform cortex, an average of 7.6 ± 1.13 ripples and 14.1 ± 2.2 fast ripples were detected per ictal event under 4AP; addition of 0.1 μM THDOC or 5 μM THDOC did not affect significantly HFO occurrence as the counts were low to begin with (Fig 5C).

To rule out the possibility that the reduced occurrence of ripples and fast ripples during THDOC application was due to the decrease in ictal duration, we normalized the duration of ictal discharges, ripple occurrence, and fast ripple occurrence and compared their respective degree of change by assigning z-scores to values in each group. In the anterior piriform cortex, both 0.1 and 5 μM THDOC induced a decrease in ripple and fast ripple occurrence that was greater than the decrease in ictal duration ($p<0.05$) (Fig 5D). However, in the posterior piriform cortex, ripple and fast ripple occurrence changed at a similar degree when compared to ictal discharge duration (Fig 5D).

Pharmacologically isolated synchronous events **-** Finally, we pharmacologically blocked glutamatergic transmission with CPP and NBQX to analyze the effects of THDOC on the 4AP-induced synchronous, presumably GABAergic, events that are recorded under these conditions. As shown in Fig 6A, CPP and NBQX (10 μM each) abolished the spontaneous epileptiform discharges, revealing the recurrence of slow field events with a duration of 1.4 ± 0.1 s in the anterior piriform cortex (331 events, n = 4) and 1.2 ± 0.1 s in the posterior piriform cortex (288 events, n = 4); these values, however, were not significantly different from each other. In both the anterior and posterior piriform cortices, the average interval between these slow field events was 24.0±1.2 s (n=4, 368 events). HFOs were virtually abolished by the application of CPP and NBQX.

In the anterior piriform cortex, adding 0.1 μM or 5μM THDOC to medium containing 4AP, CPP, and NBQX increased the duration of the isolated slow events to 1.7 ± 0.1 s or 1.8 ± 0.05 s, respectively ($p < 0.05$) (Fig 6B). These values were however not significantly different from each other. In the posterior piriform cortex, application of 0.1 μM THDOC the duration of the field events averaged 1.4 ± 0.1 s (not significant from control) and 2.1 ± 0.1 s following application of 5μM THDOC (significant from control $p<0.05$; not significant from 5 μM in anterior piriform) (Fig 6B). THDOC application failed to induce a change in interval and amplitude of these slow field events.

4.6. Discussion

The main findings of our study can be summarized as follows. First, the neurosteroid THDOC increases the duration of 4AP-induced interictal discharges in the anterior subregion of the piriform cortex. Second, THDOC reduces the duration of ictal discharges in both subregions of the piriform cortex. Third, THDOC decreases the occurrence of HFOs associated to interictal and ictal discharges in the anterior piriform cortex. Fourth, THDOC induces an increase in the duration of pharmacologically isolated synchronous GABAergic events.

THDOC modulation of 4AP-induced interictal and ictal activity **-** We have found that THDOC increases the duration of interictal discharges in the anterior piriform cortex. This could be due to the fact that THDOC modulates $GABA_A$ receptor signaling, which is known to participate in the generation of interictal events (Avoli and de Curtis, 2011). The different responsiveness to THDOC in the anterior and posterior piriform cortices could be due to the weaker interneuron-to-pyramidal cell connections in the anterior compared to the posterior piriform cortex (Luna and

Pettit, 2010) and the different patterns of connectivity that characterize these two regions. It is known that the anterior piriform cortex receives sensory information directly from the olfactory tract (Murthy, 2012), whereas the posterior piriform cortex receives projections from the entorhinal, perirhinal, amygdala, prefrontal and anterior piriform regions (Haberly, 2001). The anterior piriform cortex may be thus more sensitive to neurosteroids compared to the posterior piriform cortex due to differential levels of inhibition and different preservation of local networks following slicing (Suzuki and Bekkers, 2011).

Ictal discharge duration was also significantly reduced following THDOC application and in one third of experiments, ictal discharges were even completely abolished. Since THDOC potentiates $GABA_A$ receptor activity, with a greater preference to act on tonic currents (Ferando and Mody, 2012; Reddy, 2010), an increased level of "inhibitory tone" provided by THDOC during 4AP induced hypersynchronous activity could have reduced the capacity for the maintenance of ictal discharges.

The effects of THDOC in the 4AP model are congruent with studies investigating the anticonvulsant nature of neurosteroids in *in vivo* models of epilepsy and in human studies; however, these results must be duplicated in other models of epileptiform hyperexcitabilty such as low Mg^{2+} or high K^+. The replication of these studies will provide a more thorough understanding of the role of neurosteroids in epilepsy. In rodent models of epilepsy, neurosteroidal compounds are effective in protecting against $GABA_A$ receptor antagonist induced seizures, pilocarpine induced limbic seizures and kindled seizures (Salazar et al., 2003; Reddy, 2010). In epileptic patients, finasteride, which inhibits neurosteroid synthesis, was recently shown to enhance seizure susceptibility (Pugnaghi et al., 2013). Moreover, the synthetic analogue of anti-convulsant neurosteroids, ganaxolone, significantly reduced seizure frequency in patients with medically refractory partial epilepsy (Laxer et al., 2000).

Interictal and ictal HFOs can be modulated by neurosteroids - We have also discovered that THDOC decreases HFO occurrence (ripples and fast ripples) associated with both 4AP-induced interictal and ictal discharges. The occurrence of HFOs associated with interictal discharges was modulated with THDOC to a greater degree than the rate of interictal discharges, supporting the hypothesis that interictal spikes and HFOs may reflect different underlying neural mechanisms (Demont-Guignard et al., 2012; Wendling et al., 2012; Zijlmans et al., 2009). Regarding ictal discharges and associated HFOs, we found that discharges are more likely to contain ripples than

fast ripples when THDOC is applied. This suggests that ripples might be more related to interneuron firing and their corresponding IPSPs recorded on principal cells compared to fast ripples (Buzsáki et al., 1992; Ylinen et al., 1995). However, when considering only those ictal events during which HFOs were detected, THDOC induced a decrease in HFO occurrence without influencing ictal discharge frequency. Moreover, HFO rates decreased independently of a decrease in ictal discharge duration following THDOC. This evidence suggests that neurosteroids can affect interneuronal synchronization underlying the occurrence of ripples (Buzsáki et al., 1992; Ylinen et al., 1995) as well as the pyramidal cell synchrony that is presumed to contribute to fast ripple generation (Bragin et al., 2011; Dzhala and Staley, 2004; Engel Jr et al., 2009). This effect may be related to the ability for THDOC to potentiate tonic and phasic $GABA_A$ receptor mediated currents (Wohlfarth et al., 2002). By doing so, the shunting of excitatory inputs would reduce cell firing and synchrony (Farrant and Nusser, 2005) and thus the capacity of neuronal networks to maintain epileptiform activity over time.

Neurosteroidal modulation of synchronous GABAergic events **-** Slow GABA receptor-dependent potentials were isolated in 4AP treated slices with the blockade of glutamatergic signalling using NMDA and non-NMDA receptor antagonists. These slow discharges result from synchronous interneuronal network firing, leading to the postsynaptic activation of principal cells (Avoli and de Curtis, 2011; Avoli et al., 1996a; Lamsa and Kaila, 1997; Michelson and Wong, 1994). Similar results were described in sagittal and coronal slices of the piriform cortex (Panuccio et al., 2012), insular cortex, perirhinal cortex, hippocampal networks, and entorhinal cortex (Avoli and de Curtis, 2011).

In addition, we found that THDOC prolonged the duration of these synchronous events. Our findings substantiate previous reports on the importance of interneuronal networks in driving neuronal populations toward hypersynchronous states in the temporal lobe (Avoli and de Curtis, 2011) and additionally show that neurosteroids can be important modulators of interictal activity.

Conclusions **-** Neurosteroids act as a class of broad spectrum anticonvulsants, which can be implicated in catamenial epilepsy, stress-induced changes in seizure susceptibility, alcohol withdrawal epilepsy, and temporal lobe epilepsy when their endogenous levels are reduced (Reddy, 2010). Our findings demonstrate that THDOC can modulate interictal and ictal events as well as HFOs in the piriform cortex, although these effects are differentially expressed in the anterior and posterior

subregions. To the best of our knowledge, this is the first study showing an effect of neurosteroids on HFOs and it supports the hypothesis that these compounds may modulate the overall excitability of the central nervous system thus playing relevant roles in both ictogenesis and epileptogenesis. However, the relationship between HFOs and epileptogenesis is complex and it remains to be established whether a drug that alters HFOs can be used as an effective treatment for the control of seizure occurrence. Clinical EEG studies in epileptic patients link HFOs to the seizure generating capacity of the recorded tissue, concomitantly HFOs increase in frequency with a reduction of antiepileptic drugs (Jacobs et al., 2012). Based on this evidence, neurosteroids could be a potential antiepileptic agent; however, further studies must be conducted to confirm these claims. This is important for providing new avenues of treatment for epilepsy, since ripples and fast ripples are thought to reflect the underlying pathological network activity that contribute to the generation and maintenance of ictal activity.

4.7. Figures

Figure 4-1

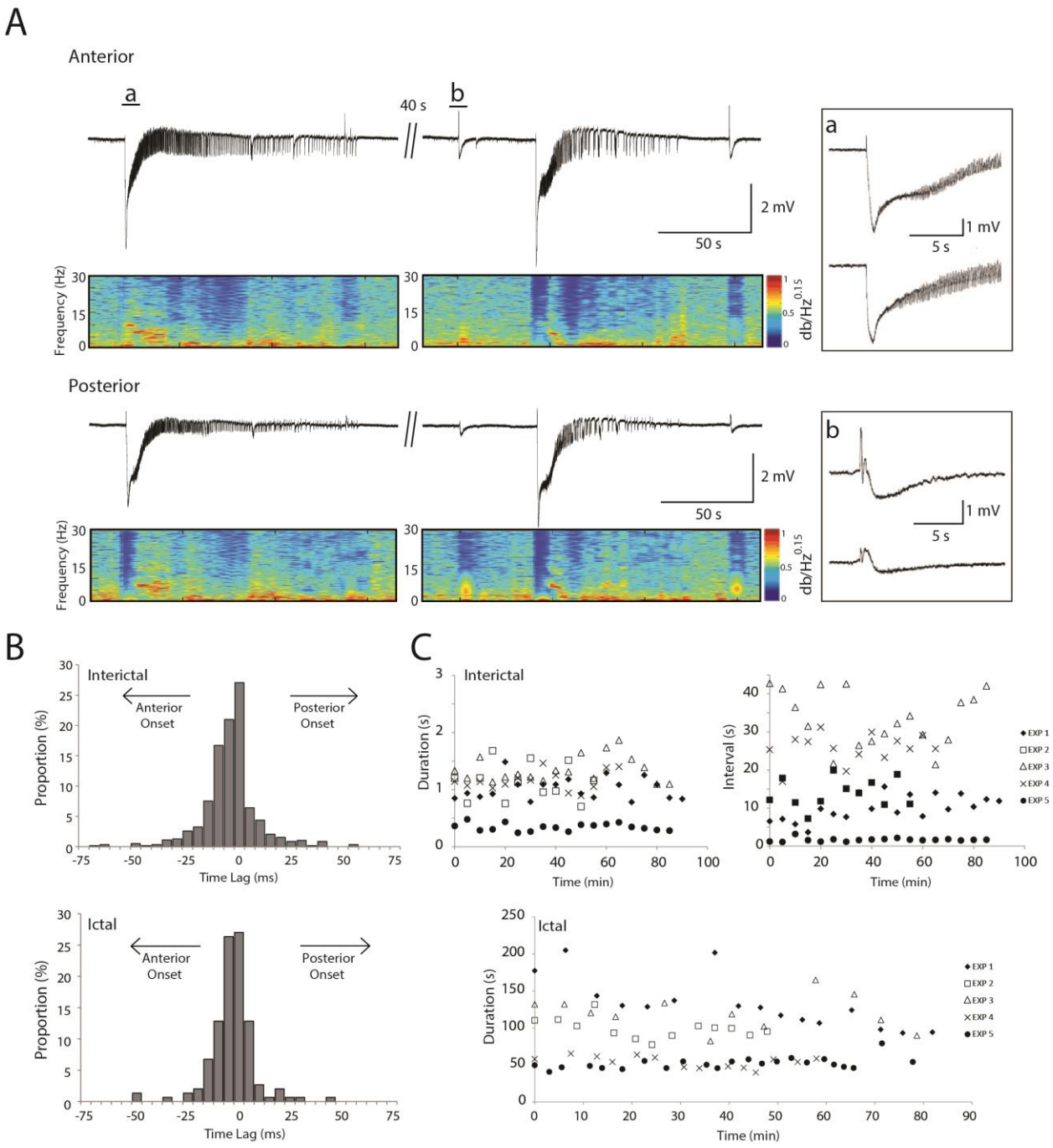

Interictal and ictal discharges in the piriform cortex. (A) Epileptiform discharges recorded from the anterior and posterior piriform cortices of an intact brain slice following the application of 4AP. The spectrograms show the initial negative shift followed by oscillations in the 10–20 Hz range characterizing the ictal event. The ictal onset and an interictal discharge are expanded in insets a and b, respectively. **(B)** Time delay histograms between the anterior and posterior regions calculated for interictal and ictal discharges. These are pooled data from 19 slices. Note the jittering in the region of onset, as no event initiated in one region in particular. Events in the anterior piriform cortex are used as the reference (time 0). **(C)** Epileptiform activity does not change over time during 4AP application (n = 5 slices). Upper panels show the duration and interval of occurrence of interictal events over time, respectively while lower panels show the duration and interval of occurrence of ictal events; data were averaged in epoques lasting 5 min. Time 0 represents the time of appearance of spontaneous epileptiform activity.

Figure 4-2

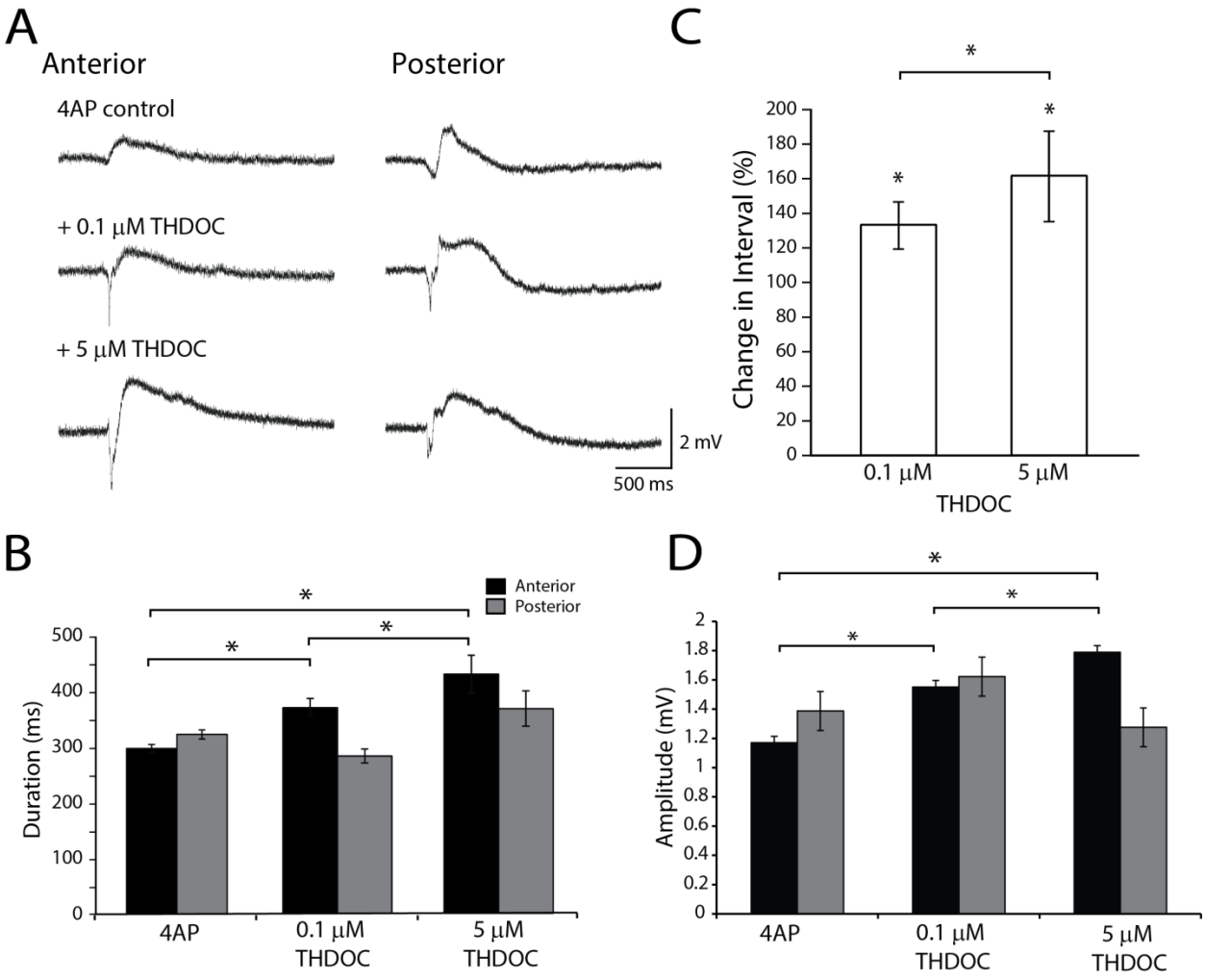
A
Anterior
Posterior
4AP control
+ 0.1 μM THDOC
+ 5 μM THDOC
2 mV
500 ms
C
Change in Interval (%)
0.1 μM
5 μM
THDOC
B
Anterior
Posterior
Duration (ms)
4AP
0.1 μM THDOC
5 μM THDOC
D
Amplitude (mV)
4AP
0.1 μM THDOC
5 μM THDOC

Modulation of Interictal discharges by THDOC. (A) Representative examples of interictal events in the 4AP control, 4AP + 0.1 μM THDOC and the 4AP + 5 μM THDOC condition. **(B)** Bar graph showing the average duration of 4AP-induced slow events. THDOC induced a significant increase in duration of these slow events in the anterior region. **(C)** Bar graph showing the change in interval of interictal events normalized to the 4AP control condition (100%). THDOC induced a significant increase compared to 4AP. **(D)** Change in amplitude of interictal events, note that THDOC induced a significant increase of amplitude compared to 4AP. (*$P < 0.05$; 4AP pooled data from n = 13 slices, 0.1 μM THDOC n = 7 slices, 5 μM THDOC n = 7 slices).

Figure 4-3

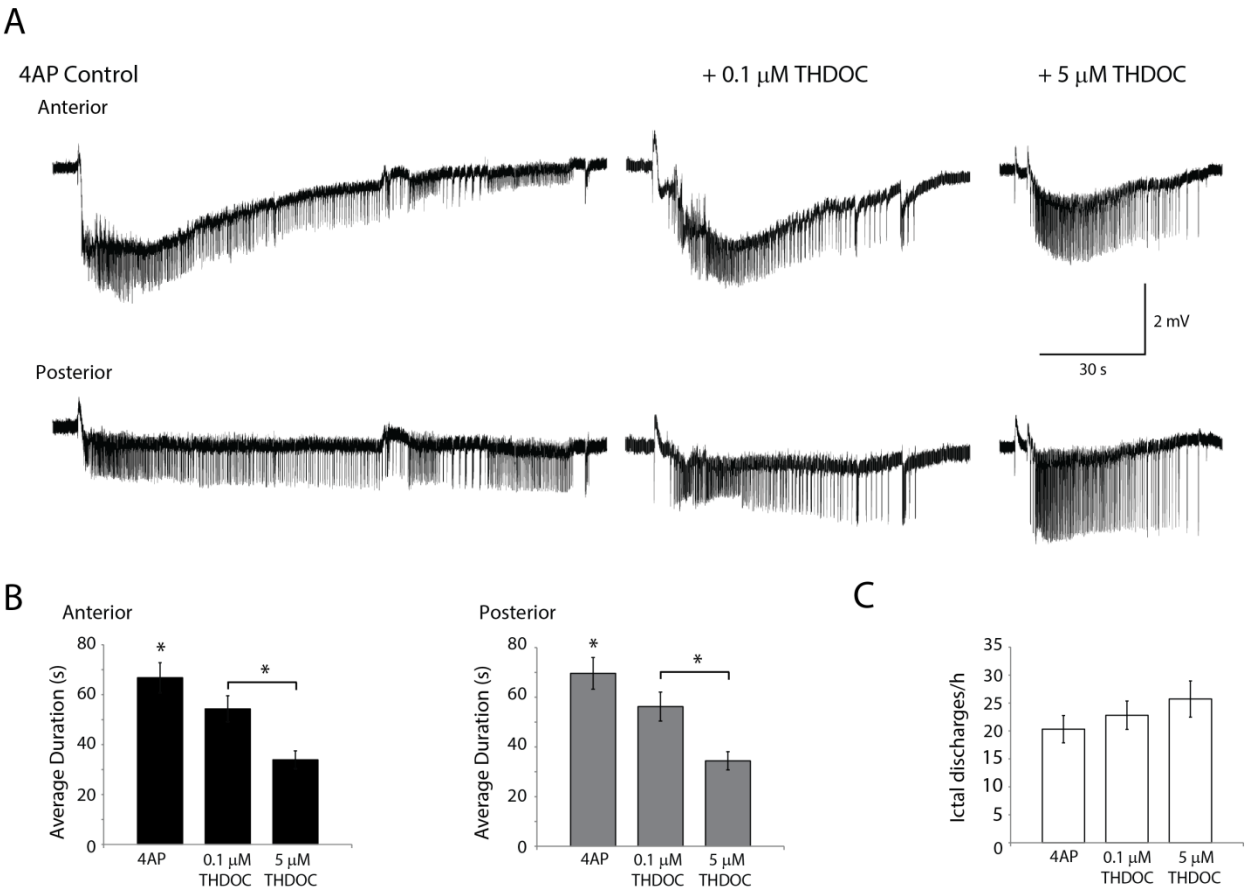
A
4AP Control
+ 0.1 μM THDOC
+ 5 μM THDOC
Anterior
2 mV
30 s
Posterior
B
Anterior
Average Duration (s)
80
60
40
20
0
*
*
4AP
0.1 μM THDOC
5 μM THDOC
Posterior
Average Duration (s)
80
60
40
20
0
*
*
4AP
0.1 μM THDOC
5 μM THDOC
C
Ictal discharges/h
35
30
25
20
15
10
5
0
4AP
0.1 μM THDOC
5 μM THDOC

Effect of THDOC on Ictal-like events. (A) Representative examples of ictal discharges in the 4AP control condition, 4AP + 0.1 μM THDOC and the 4AP + 5 μM THDOC condition. **(B)** Bar graph showing the average duration of ictal discharges following the application of 4AP and THDOC. THDOC induced a significant decrease in ictal discharge duration compared to 4AP in both the anterior and posterior regions of the piriform cortex. **(C)** Number of ictal discharges per hour following in the 4AP control condition, 4AP + 0.1 lM THDOC and 4AP + 0.5 lM. The frequency of ictal discharges did not change significantly following the application of THDOC. (*P < 0.05; 4AP pooled data n = 13, 0.1 μM THDOC n=7, 5 μM THDOC n=7).

Figure 4-4

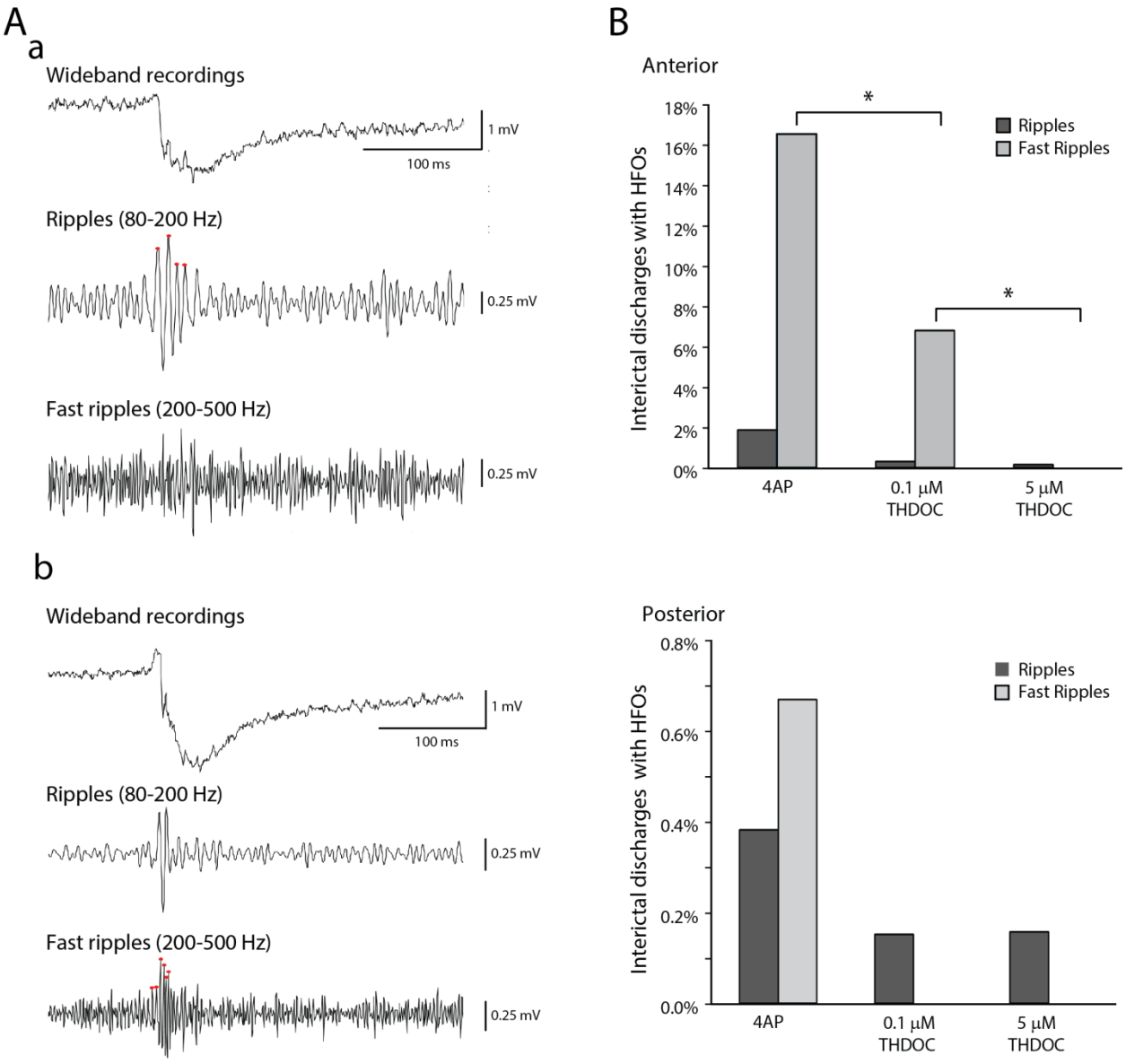
A
a
Wideband recordings
1 mV
100 ms
Ripples (80-200 Hz)
0.25 mV
Fast ripples (200-500 Hz)
0.25 mV
b
Wideband recordings
1 mV
100 ms
Ripples (80-200 Hz)
0.25 mV
Fast ripples (200-500 Hz)
0.25 mV
B
Anterior
Interictal discharges with HFOs
18%
16%
14%
12%
10%
8%
6%
4%
2%
0%
*
*
Ripples
Fast Ripples
4AP
0.1 μM THDOC
5 μM THDOC
Posterior
Interictal discharges with HFOs
0.8%
0.6%
0.4%
0.2%
0.0%
Ripples
Fast Ripples
4AP
0.1 μM THDOC
5 μM THDOC

HFOs during interictal discharges. (A) Example of an interictal discharge co-occurring with a ripple (a) or with a fast ripple (b) in the anterior piriform cortex under 4AP bath application. Note in b that the fast ripple is visible on the descending phase of the spike. **(B)** Bar graph showing the proportion of interictal events, in the anterior and posterior piriform cortex, co-occurring with HFOs in the 4AP control (anterior: n = 19, events = 1235; posterior: n = 19, events = 1047), 4AP + 0.1 μM THDOC (anterior: n = 7, events = 665; posterior: n = 7, events = 659) and the 4AP + 5 μM THDOC (anterior: n = 6, events = 633; posterior: n = 6, events = 636) condition. The application of THDOC induced a significant decrease in the proportion of interictal spikes co-occurring with HFOs, mainly in the fast ripple frequency range and in the anterior region. (*P < 0.05) Note that the proportion of interictal spikes co-occurring with HFOs in the posterior region of the piriform cortex is almost negligible.

Figure 4-5

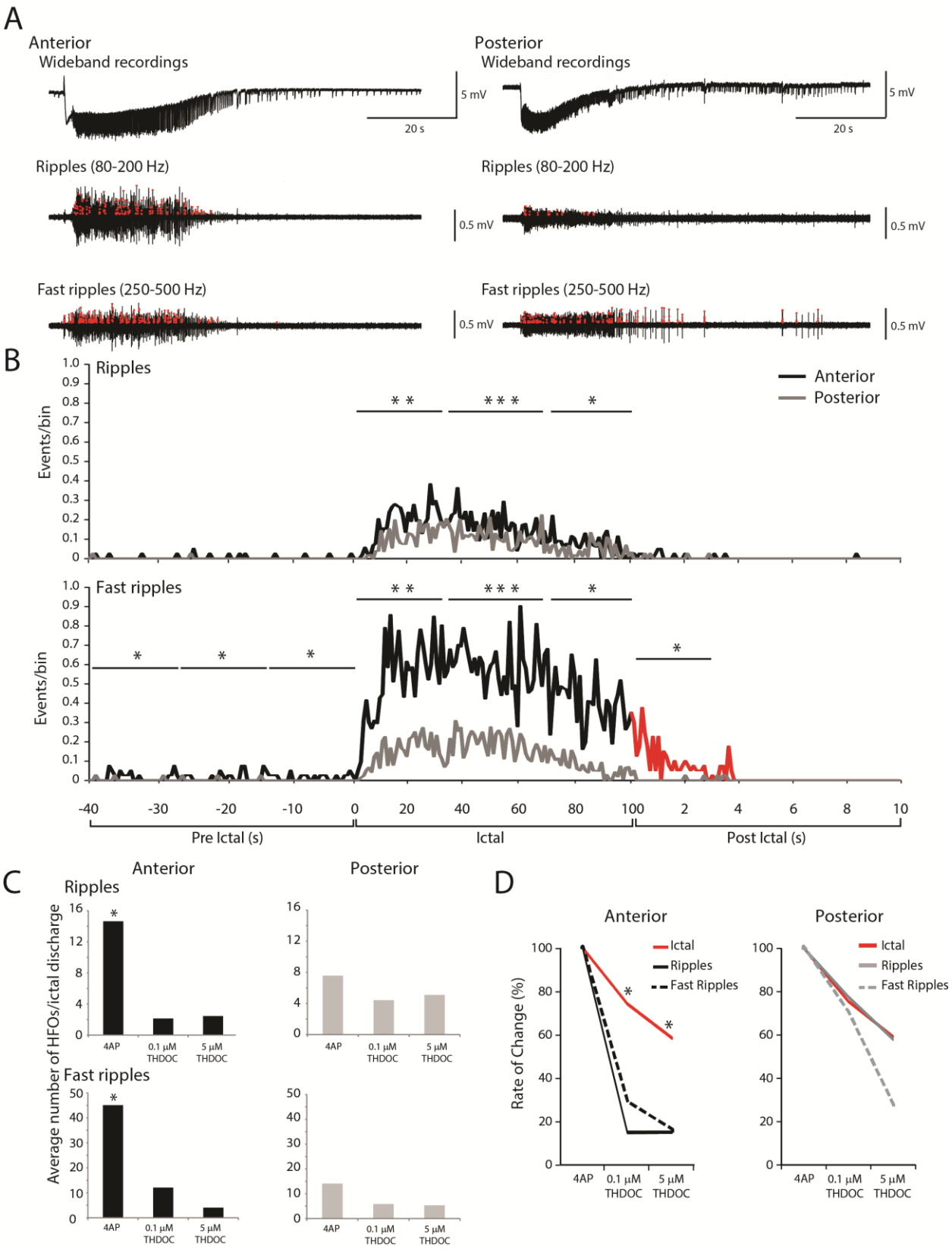
A
Anterior
Wideband recordings
5 mV
20 s
Posterior
Wideband recordings
5 mV
20 s
Ripples (80-200 Hz)
0.5 mV
Ripples (80-200 Hz)
0.5 mV
Fast ripples (250-500 Hz)
0.5 mV
Fast ripples (250-500 Hz)
0.5 mV
B
Ripples
Anterior
Posterior
Events/bin
Fast ripples
Events/bin
Pre Ictal (s)
Ictal
Post Ictal (s)
C
Anterior
Posterior
Ripples
Fast ripples
Average number of HFOs/ictal discharge
4AP
0.1 µM THDOC
5 µM THDOC
D
Anterior
Posterior
Ictal
Ripples
Fast Ripples
Rate of Change (%)

HFOs during ictal discharges. (A) Representative 4AP-induced ictal discharge from the anterior and posterior piriform cortex, with filtered traces showing HFOs (red circles) in the ripple and fast ripple frequency ranges. **(B)** Rates of ripples and fast ripples over time during 4AP induced ictal discharges in the anterior and posterior regions (data pooled from n = 19 slices). Note that ripples and fast ripple rates are significantly higher in the anterior compared to the posterior region. During the pre- and post-ictal periods, rates of fast ripples are also significantly higher in the anterior region of the piriform cortex compared to the posterior region. **(C)** Bar graphs showing the average number of HFOs per ictal discharge following the application of 4AP (n = 13), 0.1 μM (n = 7 slices) and 5 μM THDOC (n = 6 slices). Application of THDOC induced a significant decrease in the occurrence of HFOs in the anterior region, but not in the posterior region. **(D)** Line graph showing the change in ictal duration compared to the change in HFO rate following the application of either 0.1 or 5 μM THDOC. All events are normalized to the 4AP control condition. (*P < 0.05, **P < 0.01, ***P < 0.001).

Figure 4-6

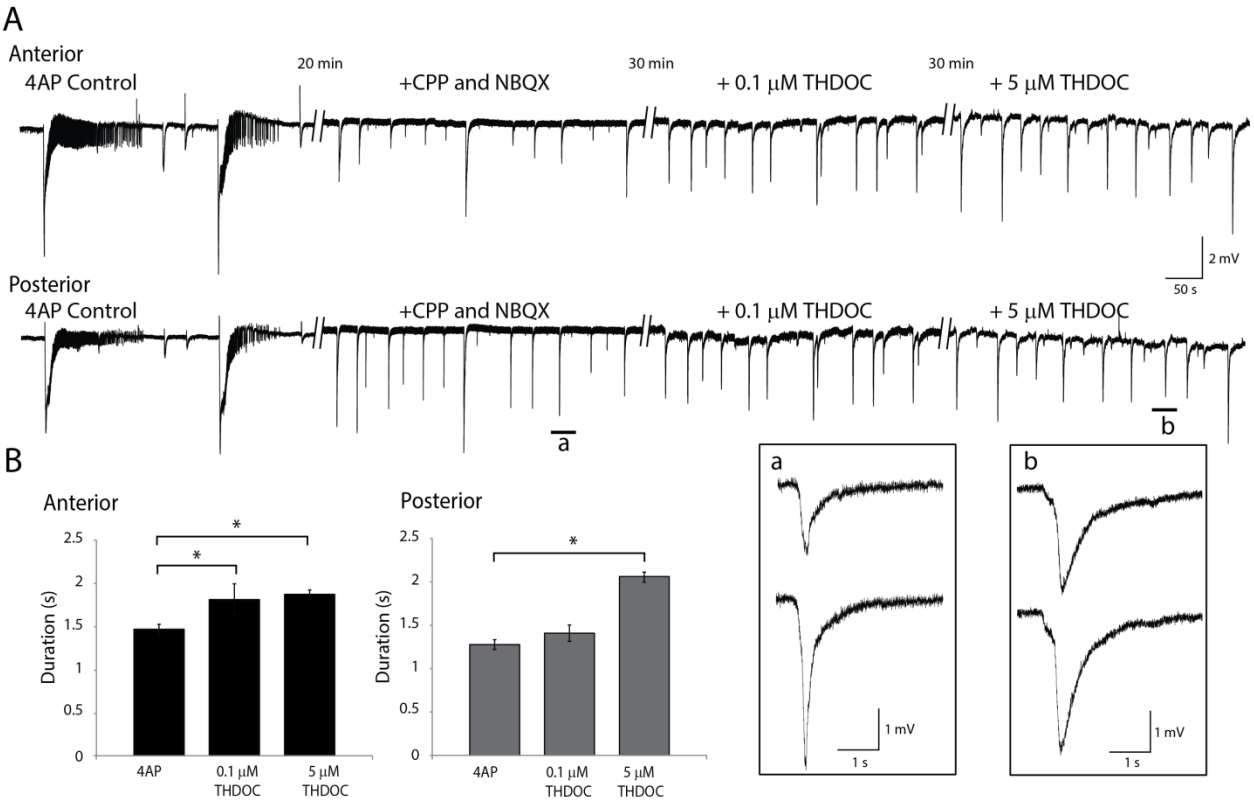
A
Anterior
4AP Control
20 min
+CPP and NBQX
30 min
+ 0.1 μM THDOC
30 min
+ 5 μM THDOC
2 mV
50 s
Posterior
4AP Control
+CPP and NBQX
+ 0.1 μM THDOC
+ 5 μM THDOC
a
b
B
Anterior
Duration (s)
2.5
2
1.5
1
0.5
0
4AP
0.1 μM THDOC
5 μM THDOC
Posterior
Duration (s)
2.5
2
1.5
1
0.5
0
4AP
0.1 μM THDOC
5 μM THDOC
a
1 mV
1 s
b
1 mV
1 s

Fig. 6. Effects of THDOC on slow events (A) Recording of 4AP control activity, followed by the application of CPP and NBQX, 0.1 μM THDOC and then 5 μM THDOC in the anterior and posterior piriform cortex. Insets a and b show an example of a slow event on an expanded time scale. **(B)** Bar graphs showing the change in duration of these slow spikes in the 4AP + 0.1 μM (n = 4 slices) and 4AP + 5 μM (n = 4 slices) THDOC. Duration is expressed as the change from the 4AP control condition. (*$P < 0.05$).

5. NEUROSTEROIDS DIFFERENTIALLY MODULATE FAST AND SLOW INTERICTAL DISCHARGES IN THE HIPPOCAMPAL CA3 AREA

By Herrington R, Lèvesque M, Avoli M

Published in European Journal of Neuroscience, 2014

5.1. Rationale and Objective

After establishing that neurosteroids differentially affect the anterior and posterior piriform cortex, we returned our focus to the hippocampus proper in order to address whether the two distinct types of epileptiform activity recorded CA3 could also be differentially modulated by the neurosteroid THDOC. *Fast* and *slow* interictal events recorded from the hippocampus proper during the bath application of 4AP have been found to be contributed by different GABAergic/glutamatergic components. This has important implications because different types of interictal discharges can be recorded in epileptic patients, in *in vivo* and in *in vitro* models of epilepsy. It could be possible that depending on the type of discharge that predominates, different drugs will prove to be more effective in attenuating the epileptiform activity.

5.2. Abstract

Two types of spontaneous interictal discharge, identified as fast and slow events, can be recorded from the hippocampal CA3 area in rat brain slices during application of 4-aminopyridine (4AP) (50 μm). Here, we addressed how neurosteroids modulate the occurrence of these interictal events and of the associated high-frequency oscillations (HFOs) (ripples, 80-200 Hz; fast ripples, 250-500 Hz). Under control conditions (i.e. during 4AP application), ripples and fast ripples were detected in 12.3 and 17.5% of fast events, respectively; in contrast, the majority of slow events (> 98%) did not co-occur with HFOs. Application of 0.1, 1 or 5 μM allotetrahydrodeoxycorticosterone (THDOC) to 4AP-treated slices caused a dose-dependent decrease in the duration of the fast events and an increase in the occurrence of ripples, but not fast ripples; in contrast, the duration of slow events increased. THDOC potentiated the slow events that were recorded during pharmacological blockade of glutamatergic transmission, but had no effect on interictal discharges occurring during $GABA_A$ receptor antagonism. These results demonstrate that

potentiation of $GABA_A$ receptor-mediated signaling by THDOC differentially affects slow and fast interictal discharges; these differences may provide insights into how hyperexcitable activity is influenced by neurosteroids.

5.3. Introduction

Excitatory and inhibitory mechanisms contribute to two types of interictal discharges that are recorded in the CA3 subfield in *in vitro* preparations during application of the K^+ channel blocker 4-aminopyridine (4AP) (Perreault and Avoli, 1991, 1992; reviewed in Avoli and de Curtis, 2011). The first type consists of brief epileptiform discharges, also termed *fast* interictal events, that are associated with intracellular paroxysmal depolarizing shifts and are mainly contributed by excitatory synaptic currents (Avoli and de Curtis, 2011); accordingly these f*ast* events are abolished by ionotropic glutamatergic receptor antagonists (Perreault and Avoli, 1991, 1992). The second type is characterized by long-lasting *slow* events that are thought to arise from the periodic synchronous activity of GABAergic interneurons, and continue to occur during application of glutamatergic receptor antagonists but are abolished by $GABA_A$ receptor antagonists (Avoli and de Curtis, 2011; Perreault and Avoli, 1992). These two types of interictal discharge have been correlated with both protective and precipitating roles in the generation of ictal discharges that occur outside the CA3 (Engel et al., 1990; Avoli and de Curtis, 2011).

In addition to interictal discharges, high frequency oscillations (HFOs, 80-500 Hz) also represent potential biomarkers of epileptogenicity (Jefferys et al., 2012b). HFOs were initially identified as physiological events playing a role in consolidating synaptic plasticity and episodic memory (Axmacher et al., 2006; Buzsaki, 2009). Subsequently, however, HFOs have been recorded in the EEG of epileptic patients and in animal models of epilepsy, and were proposed to be specifically localized to regions of seizure onset (Engel Jr. and da Silva, 2012; Jacobs et al., 2008, 2010; Jefferys et al., 2012b). Pathological HFOs can be categorized into two frequency bands: ripples (80-200 Hz) and fast ripples (250-500 Hz). HFOs in the ripple band – like those recorded under physiological conditions – are thought to represent population IPSPs generated by principal neurons entrained by synchronously active interneuron networks, while those in the fast ripple band (250-500 Hz) presumably reflect the asynchronous firing of abnormally active principal cells, and are independent of inhibitory neurotransmission (Bragin et al., 2011; Engel et al., 2009; Ibarz et al., 2010).

Pregnane neurosteroids are potent positive allosteric modulators of $GABA_A$ receptor-mediated signaling and play an important role in modulating hippocampal excitability (Baulieu and Robel, 1990; Hosie et al., 2006; Mienville and Vicini, 1989; Reddy and Rogawski, 2012). Enzymes involved in the synthesis of these neurosteroids are strongly expressed in the CA3 region of the hippocampus (Agís-Balboa et al., 2006) and the dysregulation of neurosteroids, either an increase or decrease, can have a profound effect on hyperexcitable brain networks. To date, Salazar et al. (2003) have demonstrated that anticonvulsant neurosteroids such as allopregnanolone can reduce epileptiform bursting induced by either 4AP or picrotoxin (PTX) in hippocampal slices. Based on this evidence, along with the presence of two distinct types of interictal activity with differing GABAergic and glutamatergic contributions in the CA3 hippocampus, we sought to determine here how THDOC can differentially modulate fast and slow events. Furthermore, since (i) ripples and fast ripples should have distinct underlying mechanisms and (ii) neurosteroids modulate $GABA_A$ receptor mediated signaling, we expected that THDOC could also lead to selective changes in ripple and fast ripple occurrence. Thus, our study could contribute to understanding how neurosteroids differentially influence glutamatergic and GABAergic circuits in the CA3 area of the hippocampus.

5.4. Methods

In vitro preparation - Horizontal brain slices with a thickness of 450 μm were obtained from male Sprague-Dawley rats weighing 250–275 g (Charles River Laboratories, Saint Constant, Quebec, Canada). Animals were decapitated following anaesthesia with isoflurane (Baxter Corporation, Mississauga, Ontario), and their brains were then quickly removed and chilled for 3 min in ice-cold artificial cerebrospinal fluid (ACSF) with the following composition (mM): 124 NaCl, 2 KCl, 2 $CaCl_2$, 2 $MgSO_4$, 1.25 KH_2PO_4, 26 $NaHCO_3$, 10 D-glucose. The ACSF was continuously bubbled with O_2/CO_2 (95/5%) gas mixture to maintain pH at 7.4. Slices were obtained with a Vibratome (VT1000S; Leica, Concord, Ontario, Canada) and directly transferred to an interface chamber where they laid between warm (31–33° C) ACSF (pH 7.4, 305 mOsm/kg) and humidified gas (O_2/CO_2, 95/5%). Brain slices were allowed to recover for at least 1 h before initiating continuous bath application of 4AP (50 μM) at a flow rate of 2 ml/min. All pharmaceuticals were bath applied and obtained from either Sigma–Aldrich Canada, Ltd. (Oakville, Ontario, Canada) or Tocris Bioscience (Ellisville, MO, USA). The care and handling of animals was in compliance with the guidelines of the Canadian Council on Animal Care to minimize the suffering and number of animals used, and all procedures were approved by the McGill University Animal Care Committee.

To assess overtime changes in spontaneous 4AP-induced epileptiform activity, the CA3 was continuously recorded during 4AP perfusion for a period of up to two hours. THDOC (Sigma–Aldrich) was applied to slices at concentrations of 0.1 μM, 1 μM or 5 μM in separate experiments 20 minutes following the appearance of 4AP induced spontaneous interictal discharges. THDOC data was analyzed following THDOC perfusion for a span of approximately 20 minutes. Glutamatergic antagonists NBQX and CPP (Sigma–Aldrich and Tocris Bioscience, respectively) were applied 20 minutes following the onset of 4AP-induced spontaneous interictal activity. PTX (Sigma–Aldrich) was applied 20 minutes following the onset of 4AP induced spontaneous interictal activity, for a period of 15 minutes, THDOC was also bath applied to brain slices. The benzodiazepine diazepam (CDMV, Canada) was bath applied 20 minutes following the onset of 4AP induced spontaneous events and recordings were analyzed 10 min following diazepam application.

Field potential recordings **-** Field potential recordings were obtained with ACSF-filled glass pipettes (1B150F-4; World Precision Instruments, Sarasota, Florida, USA; tip diameter <10 μm, resistance 5–10 MΩ) that were pulled with a Sutter P-97 puller (Sutter, Novato, CA, USA). A recording electrode was placed in the *stratum pyramidale* or *stratum radiatum* of the hippocampus CA3 subfield. Signals were fed to an AI 401 amplifier and a CyberAmp 380 (Molecular Devices, Silicon Valley CA, USA), then digitized using the Digidata 1322A (Molecular Devices). Signals were sampled at 5 kHz and cut-off at 1 kHz.

Detection and analysis of high-frequency oscillatory events **-** The same method as in Salami et al. (2012) was used to analyse HFOs co-occurring with interictal discharges and it will be described here. Time-periods containing interictal discharges recorded from the CA3 were extracted and analyzed offline using Matlab (The Mathworks, Natick, MA, USA). Recordings were first band-pass filtered in the 80–200 and 250–500 Hz frequency ranges using a finite impulse response (FIR) filter. The frequency band between 200-250 Hz was omitted in order to prevent over sampling of HFOs due to the properties of the filters. Zero phase digital filtering was used to avoid phase distortion. Each recording was then normalized using a 10 s artefact-free period. To be considered as an HFO candidate, oscillatory events in the 80–200 Hz and in the 250–500 Hz frequency range had to show four consecutive peaks at three standard deviations (SDs) above the mean as determined by the reference period. Overlapping events, which may be caused by the filtering of sharp spikes (Bénar et al., 2010), were excluded from the analysis. The mortlet wavelet transform was used to verify events

detected by band-pass analysis. HFO duration was measured as the time difference between the first and last peak of the oscillation in a given event. Cycles per event was considered to be the number of positive peaks in a given HFO. HFO amplitude was measured in the raw trace and reported as the average amplitude of the oscillations occurring in each ripple or fast ripple.

Statistical analysis **-** Offline analysis of the duration and interval of occurrence of *fast* and *slow* interictal discharges was performed using the software CLAMPFIT 8.2 (Molecular Devices). *Fast* and *slow* interictal events were identified using visual analysis based on duration and morphology of the field event (see Fig. 1A). *Slow* events were longer lasting and less 'sharp' compared to their *fast* counterparts. In both cases we measured the duration as the time span between the first deflection of the discharge from baseline to its return to baseline. Frequency was measured as the rate of onset of discharges occurring over a period of 100-200 s. Amplitude was measured from peak to peak. All visual analyses were conducted blind to the pharmacological manipulations of the slice.

Distributions were tested for skewness and kurtosis. Data were analyzed with either two-way analysis of variance (ANOVA) followed by Tukey's multiple comparisons test, or Student's t-test. HFO occurrence was analyzed using the non-parametric Mann–Whitney rank sum test followed by the Bonferroni correction for multiple comparisons since values were not normally distributed. Throughout the text, n indicates the number of slices studied, unless otherwise specified. Results are expressed as mean ± standard error of the mean (SEM) and considered significantly different if $P < 0.05$.

5.5. Results

Characteristics of interictal activity and HFOs **-** As reported in previous studies (Brückner and Heinemann, 2000; Perreault and Avoli, 1991, 1992; Voskuyl and Albus, 1985), 4AP (50 μM) induced in the CA3 subfield two types of interictal activity that were classified them as either *fast* or *slow* interictal discharges (Fig. 1A). On average, *fast* events lasted 121.2 ± 11.5 ms and *slow* events lasted 1428.0 ± 127 ms, (n= 15 slices, 657 *fast* and 157 *slow* events; Student's t-test; P= <0.001) (Fig. 1B). *Fast* interictal events occurred at a higher rate (1.8 ± 0.3 Hz; n= 15 slices) than *slow* interictal events (0.02 ± .004 Hz; n=15 slices) (Student's t-test; P= <0.001) (Fig. 1B). To verify our classification, we applied the k-mean cluster analysis and identified two distinct groups (Fig. 1C). As reported in previous experiments performed in the hippocampal slice preparation (Voskuyl and Albus, 1985; Perreault and Avoli 1991), *fast* interictal discharge polarity was inverse with respect to the polarity of

the *slow* discharges. As illustrated in Fig. 2, properties of *fast* and *slow* interictal events such as duration, frequency and amplitude remained constant for up to 90 min following the onset of epileptiform activity during continuous bath application of 4AP.

Fast interictal events were more likely to be associated with HFOs compared to *slow* events ($f_{1,59}$=30, P=0.0004; multiple comparison test, P<0.05, n=15 slices). The coincidence of fast ripples and *fast* events occurred at a higher rate (17.5% of discharges) compared to the coincidence of ripples and *fast* events (12.3% of discharges) (multiple comparison test; P<0.05) (Fig. 1D). Under control conditions, ripple duration was significantly higher than fast ripple duration at 29.4 ± 1.1 ms and 11.9 ± 0.8 ms, respectively (Student's t-test, P< 0.001; n=18 slices). On average, ripples had 4.5 ± 0.2 oscillations per event and fast ripples had 4.7 ± 0.2 oscillations per event. The amplitude of ripples and fast ripples were comparable at 245.8 ± 40.1 μV and 238.4 ± 37.2 μV, respectively. Both ripple and fast ripple occurrence associated with *slow* events was low (1.5 ± 0.1 %, for both HFO types; n=15 slices) (Fig. 1D).

THDOC differentially modulates interictal activity in CA3 - We then tested the effect induced by 0.1 μM, 1 μM or 5 μM THDOC (in a series of separate experiments) on the *fast* and *slow* interictal discharges recorded from the CA3 subfield (n=6 slices for each concentration) (Fig. 3A). Application of THDOC led to a dose-dependent ($f_{3,3504}$= 55.60, P<0.001; multiple comparisons test, P<0.05) decrease in the duration of *fast* interictal discharges (Fig. 3B). Concomitantly, THDOC application increased the duration of *slow* interictal events, with the greatest increase occurring during application of 5 μM ($f_{3,1107}$=55.11, P<0.001; multiple comparisons test, P<0.05). Analysis of *fast* interictal event duration at half the maximum amplitude (half-width), showed an increase from an average of 44 ± 4.6 ms in control conditions to 55 ± 4.9 ms following the application of 5 μM THDOC (Student's t-test, P<0.001; n=6 slices). There was no significant change in the half width of slow events following treatment with 5 μM THDOC (Fig. 3E). In addition, 5 μM THDOC led to a significant reduction in the frequency of *fast* interictal events ($f_{3,67}$=5.03, P=0.004) while there was no significant change in *slow* interictal event frequency at any of the concentrations tested (Fig. 3C). The amplitude of *fast* interictal events was not affected by the application of THDOC, but 1 and 5 μM THDOC significantly increased the amplitude of *slow* interictal events ($f_{3,51}$=32.48, P<0.001; multiple comparisons test, P<0.05).

THDOC effects on HFO properties - The co-occurrence of ripples associated to *fast* interictal events increased only during application of 5 μM THDOC (n= 6 slices; $f_{3,43}$=3.47, P=0.03) while levels of fast ripples were not significantly affected by any of the THDOC concentrations tested (Fig. 4A). We also measured the duration, number of oscillations, and amplitude of ripples and fast ripples associated with the *fast* interictal events induced by 4AP during application of 0.1 μM, 1 μM and 5 μM THDOC (Fig. 4B-D). The addition of THDOC failed to significantly change either the duration or number of oscillations of ripples and fast ripples (n=6 slices at each concentration). Only at the highest concentration of THDOC tested (i.e., 5 μM) was there an increase in the amplitude of ripples and fast ripples (ripples: 367.2 ± 42.9 μV, fast ripples: 477.3 ± 36.5 μV; P<0.05) compared to control ($f_{3,39}$=6.46, P=0.0019 for ripples; $f_{3,39}$=17.38, P<0.001 for fast ripples; multiple comparisons test, P<0.05). THDOC induced no changes in the occurrence of HFOs associated with *slow* events because they were virtually absent to begin with.

Network effects of THDOC - To understand whether neurosteroids affect the site of genesis and propagation of interictal events, adjacent electrodes were placed 1±0.5 mm apart to assess the dynamics of interictal firing in the CA3 before and after the application of 5 μM THDOC (Fig. 5A) (*fast* events, n = 118; *slow* events, n = 52). The delay between the onset of interictal events were measured between electrodes a-b and electrodes a-c. While there was no significant changes in delay of onset between 4AP only and THDOC treatment, the variability of the delay was increased following THDOC treatment in *fast* events (Fig. 5B). The same trend was not observed in *slow* events (Fig. 5C). Additionally, while HFOs showed similar rates of occurrence in each electrode, the co-occurrence of HFOs between the 3 recorded sites was low during 4AP application. Less than 1% of HFOs occurred simultaneously between adjacent electrodes (a-b or b-c) and virtually no HFOs co-occurred between distant electrodes (a-c). Following THDOC treatment, no HFOs were detected to co-occur between electrodes.

THDOC modulates pharmacologically isolated slow events - As reported in previous studies (see for review Avoli and de Curtis, 2011), pharmacologically isolated *slow* field potentials continued to occur in the presence of 4AP during blockade of ionotropic glutamatergic transmission with bath application of 10 μM CPP and 10 μM NBQX. CPP bath applied 20 min after the appearance of 4AP-induced synchronous activity led to a significant reduction in the duration of *slow* field events (n=6 slices; $f_{3,715}$=23.57, P<0.001; multiple comparisons test, P<0.05) (Fig.6A and B). NBQX was

then applied in addition to CPP and *fast* events were abolished. S*low* events were significantly reduced in duration (multiple comparisons test, $P<0.05$) and increased in frequency (n=6 slices; $f_{3,35}=3.15$, $P<0.001$; multiple comparisons test, $P<0.05$) compared to the 4AP control, but not compared to application of CPP and 4AP only.

The effect of 5 μM THDOC (the highest concentration previously applied; Fig. 3) was then tested on these isolated *slow* potentials (Fig.6A). Bathing CPP and NBQX treated slices with 5 μM THDOC led to an increase in the duration of the *slow* events (n=5, multiple comparisons test, $P<0.05$) (Fig.6B-D). 5 μM THDOC also reduced the frequency of isolated *slow* events, and increased their amplitude ($f_{3,195}=5.35$, $P=0.0016$; multiple comparisons test, $P<0.05$)(Fig.6D). CPP mediated blockade of NMDA receptors also led to a significant reduction of fast ripples occurrence in association with *fast* events compared to 4AP control conditions (n=6, $f_{3,35}=4.97$, $P=0.008$, multiple comparisons test, $P<0.05$) (Fig.6E). There was no significant effect of CPP, NBQX or THDOC on the occurrence of ripples or fast ripples associated with *slow* events, likely because their frequency of occurrence was almost negligible to begin with (Fig.6E).

To better understand the role of modulating $GABA_A$ receptor mediated activity in 4AP induced epileptiform activity, we also assessed the effect of 150 nM diazepam on *fast* and *slow* interictal activity. The reported EC50 of diazepam in the hippocampus is between 100-150 nM (Kapur and MacDonald, 1996; Aguayo et al., 1994). Overall, the effect of 150 nM diazepam was relatively modest. The duration, amplitude and frequency of *fast* events were not significantly modulated. The duration and amplitude of *slow* events also remained unchanged; however, their frequency of occurrence significantly increased (Student's t-test, $P= 0.0256$; n=5 slices). In two separate experiments, we tested whether a high concentration of diazepam was sufficient to abolish interictal events occurring in the CA3. In the presence of 50 μM 4AP, interictal events persisted even during the application of 70 μM diazepam over a period of at least 30 minutes.

Effects of THDOC following blockade of GABAergic transmission - In 5 slices we established the effects induced by high concentrations of the $GABA_A$ receptor antagonist PTX (100 μM) on 4AP-induced interictal activity. PTX application abolished *slow* interictal discharges and produced high amplitude (5.02 ± 0.81 mV) rhythmic events lasting 1.6 ± 0.1 ms in duration, occurring at an average frequency of 0.06 ± 0.02 Hz (Fig. 7 A-D). Additionally, fast ripple occurrence increased during PTX application ($f_{2,44}=7.30$, $P=0.0028$; multiple comparisons test, $P<0.05$), but ripple occurrence remained unchanged. Application of 5 μM THDOC failed to significantly modulate the

duration, frequency and amplitude of the PTX-induced epileptiform activity; however, the occurrence of fast ripples was decreased (multiple comparisons test, $P<0.05$).

5.6. Discussion

Our main findings can be summarized as follows. First, *fast* interictal discharges recorded from the CA3 subfield during bath application of 4AP are more likely to be associated with fast ripples than ripples while *slow* interictal events are virtually not accompanied by HFOs. Second, THDOC decreases the duration and frequency of *fast* interictal events while increasing the duration and amplitude of the *slow* events. Third, pharmacologically isolated *slow* events are sensitive THDOC. Finally, the occurrence of ripples does not increase with the addition of THDOC following PTX application. It should be emphasized that these effects are not time-dependent since the duration, amplitude and frequency of the 4AP-induced epileptiform activity remains constant over time suggesting that they are related to the pharmacological effects of THDOC.

Neurosteroidal modulation of interictal activity **-** THDOC application led to differential changes in the field properties of *fast* and *slow* interictal discharges generated in the CA3 area during 4AP application. *Fast* interictal events, which are known to be abolished by ionotropic glutamatergic receptor antagonists (see for review Avoli and de Curtis., 2011), became shorter in duration and occurred at a reduced frequency compared to control following THDOC application, possibly due to the potentiation of GABAergic conductances by THDOC in pyramidal cells. In contrast, *slow* interictal discharges occurred at longer durations and higher amplitudes following THDOC treatment and a similar trend was observed following the blockade of glutamatergic signalling. *Slow* field events can be recorded in all limbic areas following the application of 4AP (Avoli and de Curtis, 2011) and are mainly attributed to $GABA_A$ receptor mediated postsynaptic currents generated by pyramidal cells in response to GABA released from interneurons (Avoli et al., 1996a, 2002; Perreault and Avoli, 1991, 1992).

Enzymes involved in the synthesis of neurosteroids such as THDOC and allopregnanolone are strongly expressed in CA3 pyramidal cells (Agís-Balboa et al., 2006), the same cells that fire action potential bursts during *fast* interictal discharges (Perreault and Avoli, 1991, 1992); therefore, endogenous neurosteroids should regulate the excitability of pyramidal neurons in the CA3 in an autocrine fashion. Neurosteroids are also synthesized in glial cells (Jung-Testas et al., 1989; Robel

and Baulieu, 1994), so they can additionally control the tone of a given region through a paracrine mechanism (Lambert et al., 2003), influencing not only principal neurons but also interneurons.

THDOC has the ability to potentiate both tonic and phasic $GABA_A$ receptor mediated currents (Wohlfarth et al., 2002), so by hyperpolarizing the membrane potential or by shunting of excitatory inputs, THDOC can reduce cell firing and possibly the potential for the neuronal networks to maintain epileptiform activity over time (Farrant and Nusser, 2005). This mechanism may account for what appears to be the reduction in epileptiform activity in the CA3 following the application of THDOC to 4AP-treated slices.

In line with the evidence indicating that neurosteroids modulate $GABA_A$ receptor mediated currents, the non-competitive $GABA_A$ receptor antagonist PTX (Sivilotti and Nistri, 1991) effectively abolished the effect of THDOC on the duration, amplitude and frequency of epileptiform events. It is important to note that in the *in vitro* study conducted in the CA3 by Salazar et al., they found that the neurosteroid allopregnanolone produces concentration dependent suppression of epileptiform bursting induced by the application of either PTX (100 μM) or 4AP (55 μM) (2003). The differences between the aforementioned study and our study may be due to the effect of neurosteroids on 4AP alone and PTX alone, compared to 4AP and PTX together. Salazar et al. (2003) also investigated the effects of high concentrations of allopregnanolone and pregananolone (10-90 μM) whereas we used lower concentrations (0.1-5 μM) of THDOC. Those $GABA_A$ receptor channels that remain open in the presence of 100 μM of PTX maintain normal kinetics (Sivilotti and Nistri, 1991), but perhaps very high concentrations of neurosteroids are required to modulate these GABA receptors. These contrasts highlight the differences between more physiological versus therapeutically beneficial concentrations of neurosteroids and the role they play in controlling brain excitability.

Both THDOC and diazepam (at EC50) increased the frequency of occurrence of slow events occurring in the CA3; however, diazepam did not significantly modulate their amplitude and duration. Moreover, diazepam failed to significantly modulate fast interictal events occurring in the CA3. The differences observed between the effect of diazepam and THDOC may be accounted for by differences in the effective concentration. While diazepam was applied at the EC50, THDOC was applied at comparatively higher concentrations.

Interictal events in the CA3 were only minimally modulated by diazepam at the EC50 concentration and events persisted even in the presence of 70 μM diazepam. The persistence of interictal events may reflect the mechanism by which 4AP enhances epileptiform activity. Under the

application of 4AP, the release of both excitatory and inhibitory neurotransmitters is increased while $GABA_A$ receptors can mediate long lasting depolarizing potentials, which may still maintain a degree of inhibition through a shunting mechanism (Avoli and de Curtis, 2011). In this sense, increasing GABAergic transmission may not be sufficient to abolish 4AP induced epileptiform activity unless under the application of very high concentrations, as demonstrated by Salazar et al. (2003). Why then do interictal events persist whereas ictal events recorded in the piriform cortex can be abolished (50% of slices) over time following the application of 5 μM THDOC (Herrington et al., 2014)? This difference may illustrate the importance of shunting inhibition provided by $GABA_A$ receptor mediated currents in sustaining ictal event compared to interictal event occurrence.

Neurosteroidal modulation of HFOs - Our findings show that ripples and fast ripples are differently associated with *fast* and *slow* interictal discharges. Both ripples and fast ripples were more likely to co-occur with *fast* events compared to *slow* events; in addition, *fast* events were more likely associated with fast ripples, supporting the hypothesis that principal neuron firing is involved in the generation of fast ripples (Bragin et al., 2011; Engel et al., 2009; Ibarz et al., 2010). In line with this view, when we blocked GABAergic signaling with PTX, there was an increase in fast ripple occurrence but no change in ripple occurrence. Finally, in the presence of glutamatergic signaling blockers (CPP and NBQX) both ripple and fast ripple occurrence were virtually negligible. These findings reinforce the hypothesis that the interplay between interneuronal and principal neuron firing plays an important role in the maintenance of ripple and fast ripple activity (Jefferys et al., 2012b).

The application of THDOC to 4AP treated slices led to an increase in ripple occurrence that coincided with a decrease in interictal frequency, but without a concomitant change in fast ripple occurrence. It is known that THDOC leads to an increase in $GABA_A$ receptor mediated activity (Reddy and Rogawski, 2012); thus the increase in ripple but not fast ripple occurrence further supports the hypothesis that ripples may reflect the activity of synchronous GABAergic interneuronal activity entraining a population of principal neurons (Buzsáki et al., 1992; Demont-Guignard et al., 2012; Wendling et al., 2012; Ylinen et al., 1995; Zijlmans et al., 2009). When THDOC was applied to slices treated with glutamatergic antagonists, HFO occurrence remained low. Interestingly, when 5 μM THDOC was applied to 4AP and PTX treated slices, fast ripple occurrence decreased to control levels while parameters such as event duration, frequency and

amplitude of epileptiform activity remained unaffected. This may be related to changes induced by THDOC within local networks that can only be detected at the level of HFOs.

The duration of ripples and fast ripples, along with the number of oscillations per an event remained constant between the control condition (i.e., in the presence of 4AP only) and the application of THDOC. Whether changes in the duration and the number of oscillations per HFO can be observed with lower detection thresholds remains uncertain, but it seems that the most important parameter is the shift from higher frequency bands to lower frequency bands (fast ripples to ripples) with the application of THDOC. Ripple and fast ripple amplitude was also increased following the application of 5 μM THDOC, which may reflect an increased recruitment of synchronized pyramidal cells during interictal events regardless of whether this is mediated through interneurons or not; however, this hypothesis must be confirmed in future studies.

Concluding Remarks - Our study demonstrates that neurosteroids can modulate both *fast* and *slow* interictal discharges as well as HFOs associated with *fast* events recorded in the CA3. Although *fast* and *slow* discharges rely on predominantly different glutamatergic and GABAergic contributions, they are both modulated by the neurosteroid THDOC. We propose that the way these events are modulated can provide further insight into our understanding of how GABAergic mechanisms contribute to controlling epileptiform synchronization.

5.7. Figures

Figure 5-1

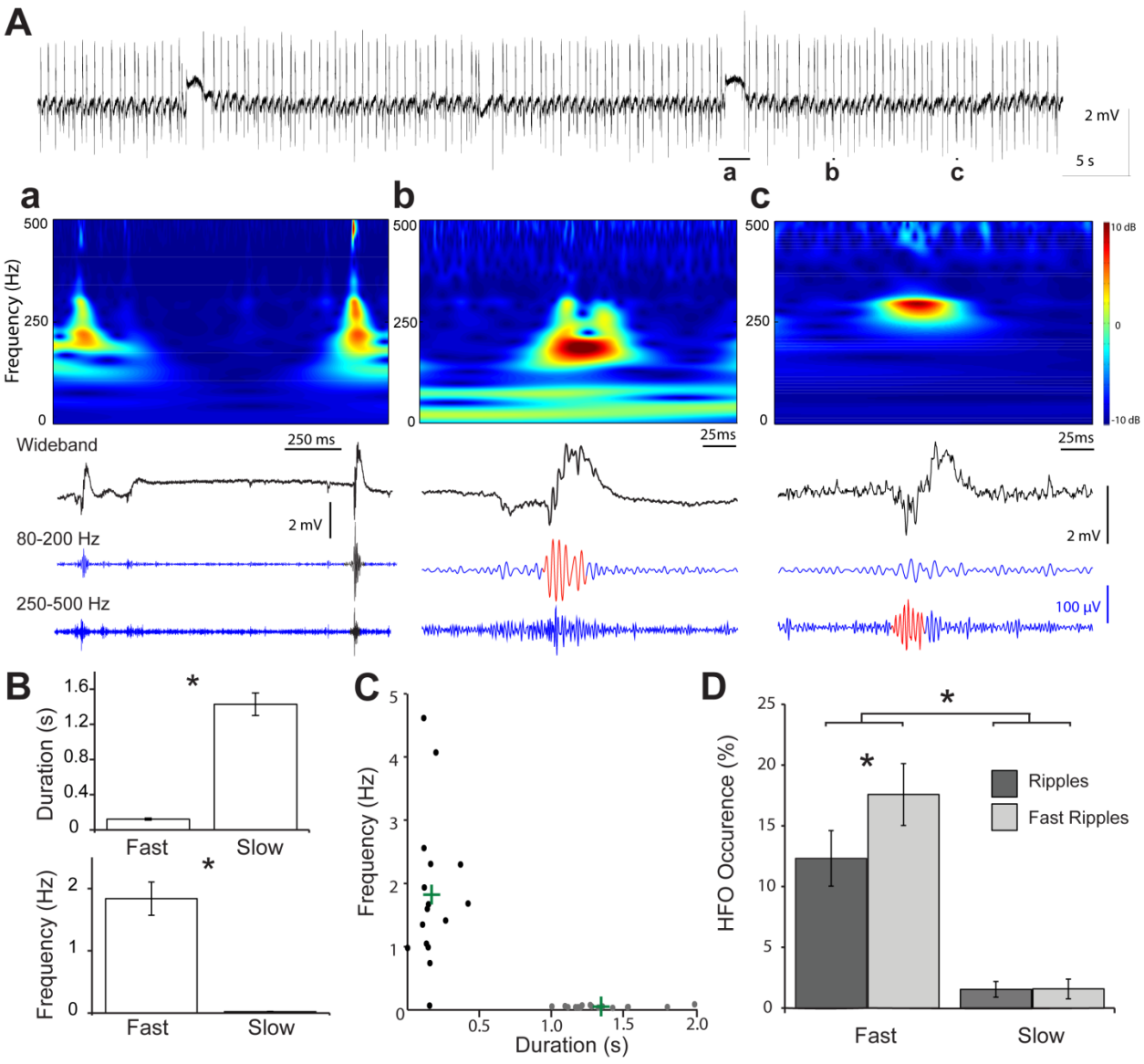

Interictal activity induced by 4AP bath application. (A) Epileptiform discharges recorded from the CA3 area of an intact brain slice following the application of 50 μM 4AP. Top – wavelet transform analysis was used to confirm the frequency components of the HFOs. The traces show the wideband recording along with filtered and normalized traces used for the detection of HFOs. The expanded trace on the left shows a slow interictal event without any corresponding HFO. Highlighted in black is an example of an overlapping event, which was omitted from the HFO analysis. The expanded traces on the right show two fast interictal events with a corresponding ripple and fast ripple, respectively. **(B)** Bar graphs showing the respective durations and frequencies of fast and slow events. **(C)** The mean frequencies and durations of fast (black) and slow (gray) events from 16 experiments are plotted on the scatter plot. The green crosses show the centers of the fast and slow clusters calculated by k-means clustering analysis. **(D)** Bar graph showing the occurrence of ripples and fast ripples associated with fast and slow events. Fast events were more likely to co-occur with fast ripples, and were more likely to be associated with HFOs in general than were slow events. *$P < 0.05$.

Figure 5-2

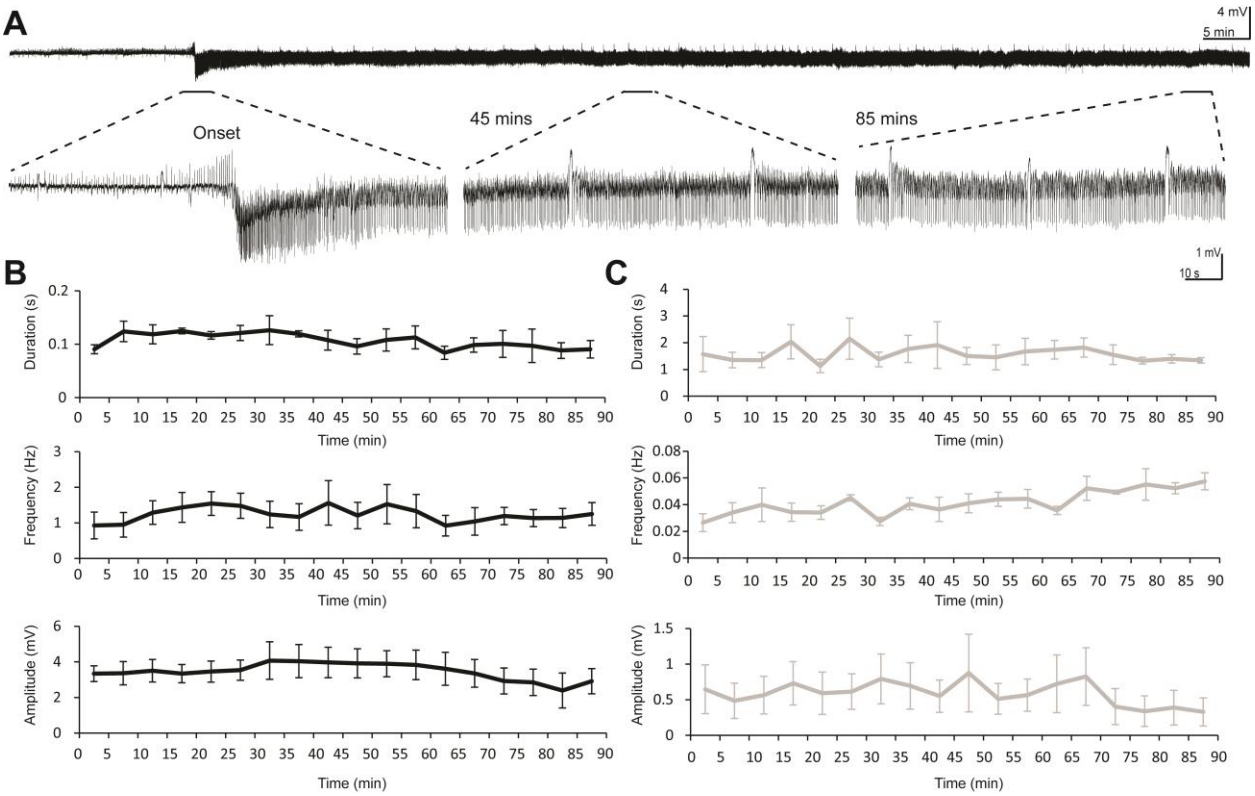
A
4 mV
5 min
Onset
45 mins
85 mins
B
C
1 mV
10 s
Duration (s)
Frequency (Hz)
Amplitude (mV)
Time (min)

4AP-induced epileptiform activity is maintained over time. (A) Example of a field recording of CA3 interictal activity that lasted for 90 min. Portions of the recording, indicated by the dashed lines, are expanded to show that the activity remains consistent over time. Bath application of 4AP began 20 min before the onset of the recording. **(C** and **D)** Graphs show the durations, frequencies and amplitudes of fast **(B)** and slow **(C)** interictal activity over time. Times are calculated from the 'onset' of 4AP application.

Figure 5-3

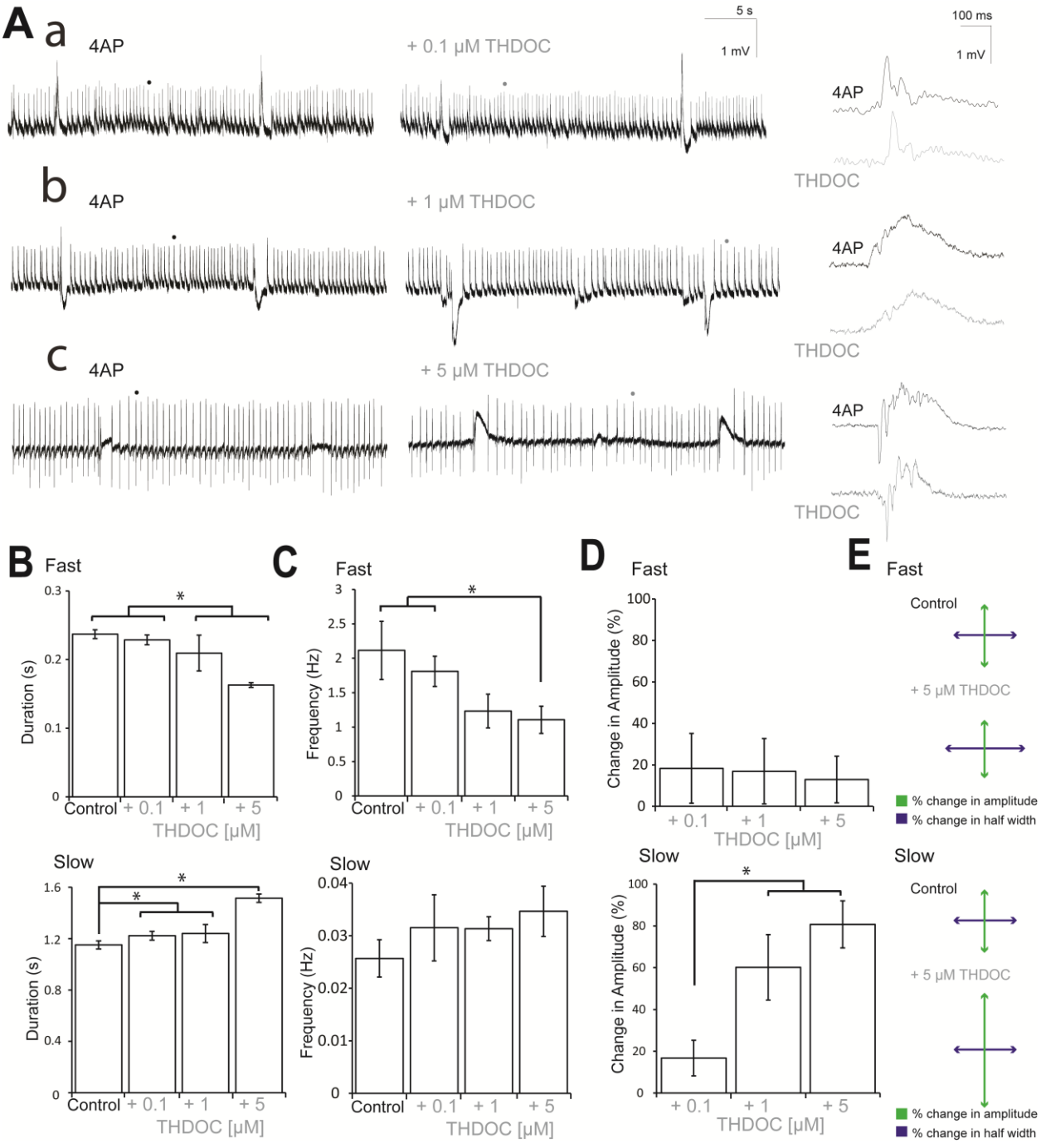
A
a
4AP
+ 0.1 µM THDOC
5 s
1 mV
100 ms
1 mV
4AP
THDOC
b
4AP
+ 1 µM THDOC
4AP
THDOC
c
4AP
+ 5 µM THDOC
4AP
THDOC
B
Fast
Duration (s)
Control
+ 0.1
+ 1
+ 5
THDOC [µM]
Slow
Duration (s)
Control
+ 0.1
+ 1
+ 5
THDOC [µM]
C
Fast
Frequency (Hz)
Control
+ 0.1
+ 1
+ 5
THDOC [µM]
Slow
Frequency (Hz)
Control
+ 0.1
+ 1
+ 5
THDOC [µM]
D
Fast
Change in Amplitude (%)
+ 0.1
+ 1
+ 5
THDOC [µM]
Slow
Change in Amplitude (%)
+ 0.1
+ 1
+ 5
THDOC [µM]
E
Fast
Control
+ 5 µM THDOC
% change in amplitude
% change in half width
Slow
Control
+ 5 µM THDOC
% change in amplitude
% change in half width

THDOC modulates interictal activity in the CA3 area. (A) Three different sets of experiments showing the effects of 0.1, 1 and 5 μM THDOC on fast and slow interictal events in the CA3 area. Fast events indicated below the dots are expanded on the right. **(B)** Summary of the effects of THDOC on the durations of fast and slow events. Note that, at the highest concentrations tested, THDOC reduced the duration of fast events and increased the duration of slow events recorded in the field ($P < 0.05$). **(C)** Summary of the effects of THDOC on the frequencies of occurrence of fast and slow events. Note that THDOC significantly reduced the frequency of fast events at 1 and 5 μM ($P < 0.05$), but had no significant effect on slow events. **(D)** Summary of the effects of THDOC on the amplitudes of fast and slow events. Note that THDOC failed to induce any changes in the amplitude of fast events, but increased the amplitude of slow events at 1 and 5 μM ($P < 0.05$). **(E)** Diagram showing the changes in half-width (blue) and amplitude (green) in slices treated with 5 μM THDOC as compared with the control (*$P < 0.05$).

Figure 5-4

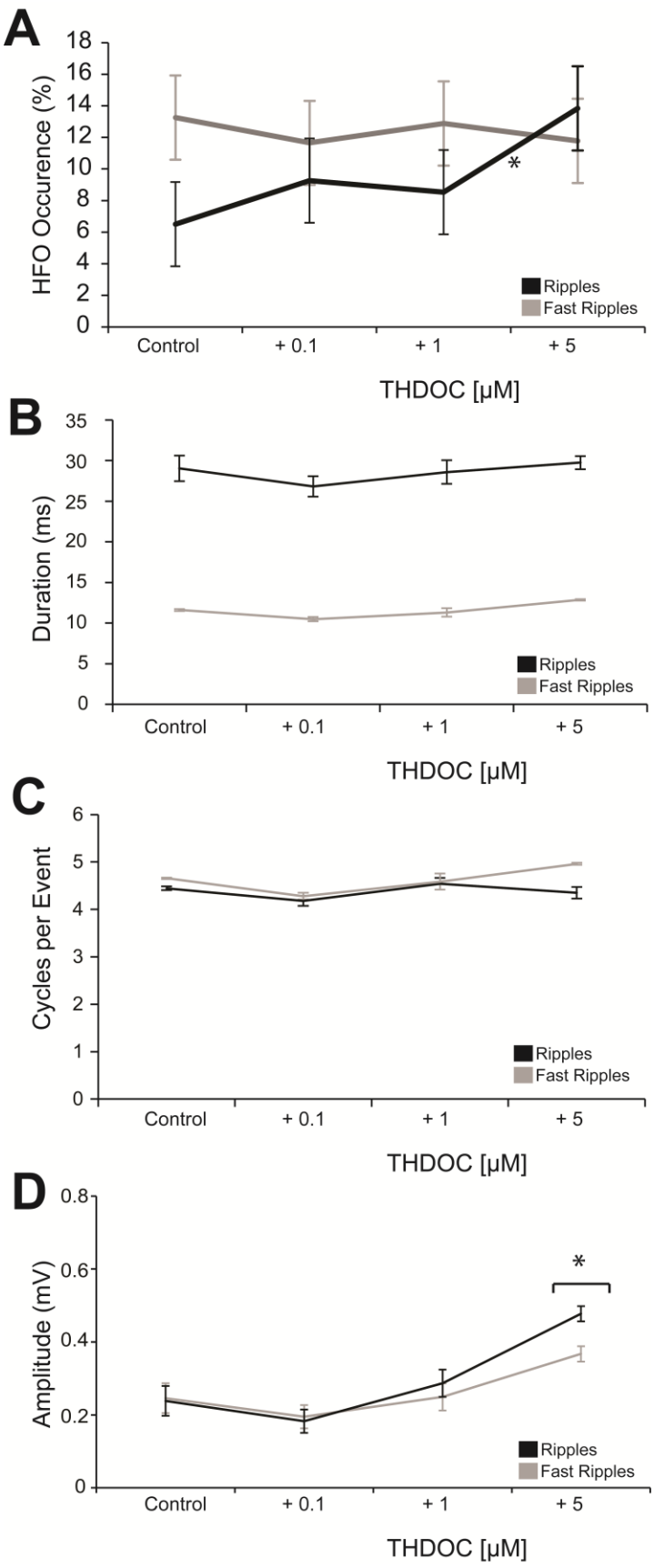
A
HFO Occurence (%)
18
16
14
12
10
8
6
4
2
0
*
Ripples
Fast Ripples
Control
+ 0.1
+ 1
+ 5
THDOC [μM]
B
Duration (ms)
35
30
25
20
15
10
5
0
Ripples
Fast Ripples
Control
+ 0.1
+ 1
+ 5
THDOC [μM]
C
Cycles per Event
6
5
4
3
2
1
0
Ripples
Fast Ripples
Control
+ 0.1
+ 1
+ 5
THDOC [μM]
D
Amplitude (mV)
0.8
0.6
0.4
0.2
0
*
Ripples
Fast Ripples
Control
+ 0.1
+ 1
+ 5
THDOC [μM]

Properties of HFOs following THDOC treatment. (A) Graphs showing the occurrence of HFOs under control conditions and during THDOC application. Note that ripple occurrence remained constant at the concentrations of THDOC tested; however, fast ripple occurrence increased with the highest concentration of THDOC. **(B–D)** Graphs showing the durations, cycle numbers and amplitudes of ripples and fast ripples associated with fast interictal events following THDOC treatment. Note that only 5 μM THDOC induced significant increases in the amplitudes of ripples and fast ripples (*$P < 0.05$).

Figure 5-5

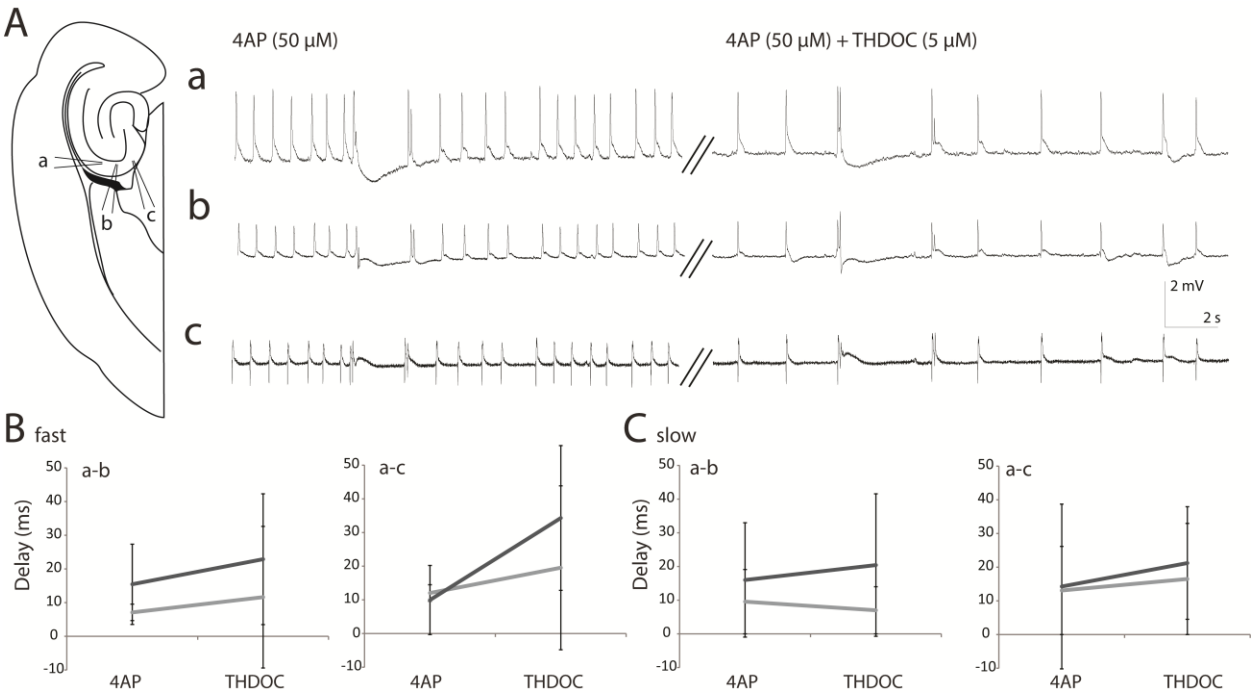
A
4AP (50 µM)
4AP (50 µM) + THDOC (5 µM)
a
b
c
2 mV
2 s
B fast
a-b
a-c
Delay (ms)
4AP
THDOC
C slow
a-b
a-c
Delay (ms)
4AP
THDOC

Network effects of THDOC. (A) Recordings from three adjacent electrodes placed within the CA3 area. **(B)** Graphs showing the delay between electrodes a and b and between electrodes a and c before and after treatment with THDOC in fast events in two sets of experiments. **(C)** Analysis of delay between a and b and between a and c in slow events for two sets of experiments.

Figure 5-6

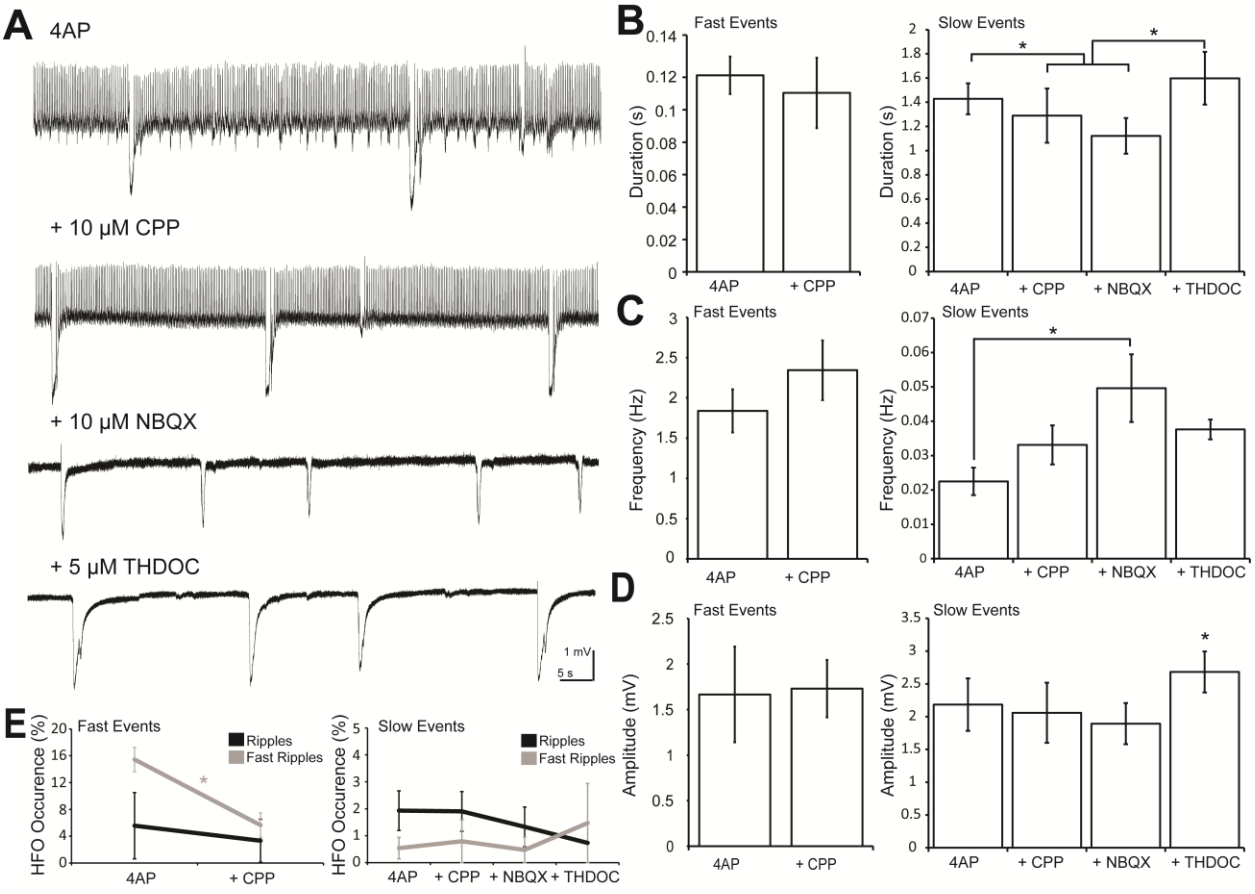
A
4AP
+ 10 μM CPP
+ 10 μM NBQX
+ 5 μM THDOC
1 mV
5 s
B
Fast Events
Duration (s)
4AP
+ CPP
Slow Events
+ NBQX
+ THDOC
C
Frequency (Hz)
D
Amplitude (mV)
E
HFO Occurence (%)
Ripples
Fast Ripples

THDOC modulates isolated slow events. (A) Field potential recordings of 4AP-induced interictal activity following CPP, NBQX and THDOC treatment in the CA3 area. **(B)** Summary of the durations of fast and slow events during application of CPP, NBQX, and THDOC (5 μM); note that fast events were abolished by NBQX treatment. **(C)** Summary of the frequencies of occurrence of fast and slow events under the different pharmacological conditions. **(D)** Summary of the changes in amplitudes of fast and slow events. **(E)** Ripple and fast ripple occurrence associated with fast (left) and slow (right) events. Note that ripple and fast ripple occurrence associated with slow events remained low throughout the pharmacological manipulations. *$P < 0.05$.

Figure 5-7

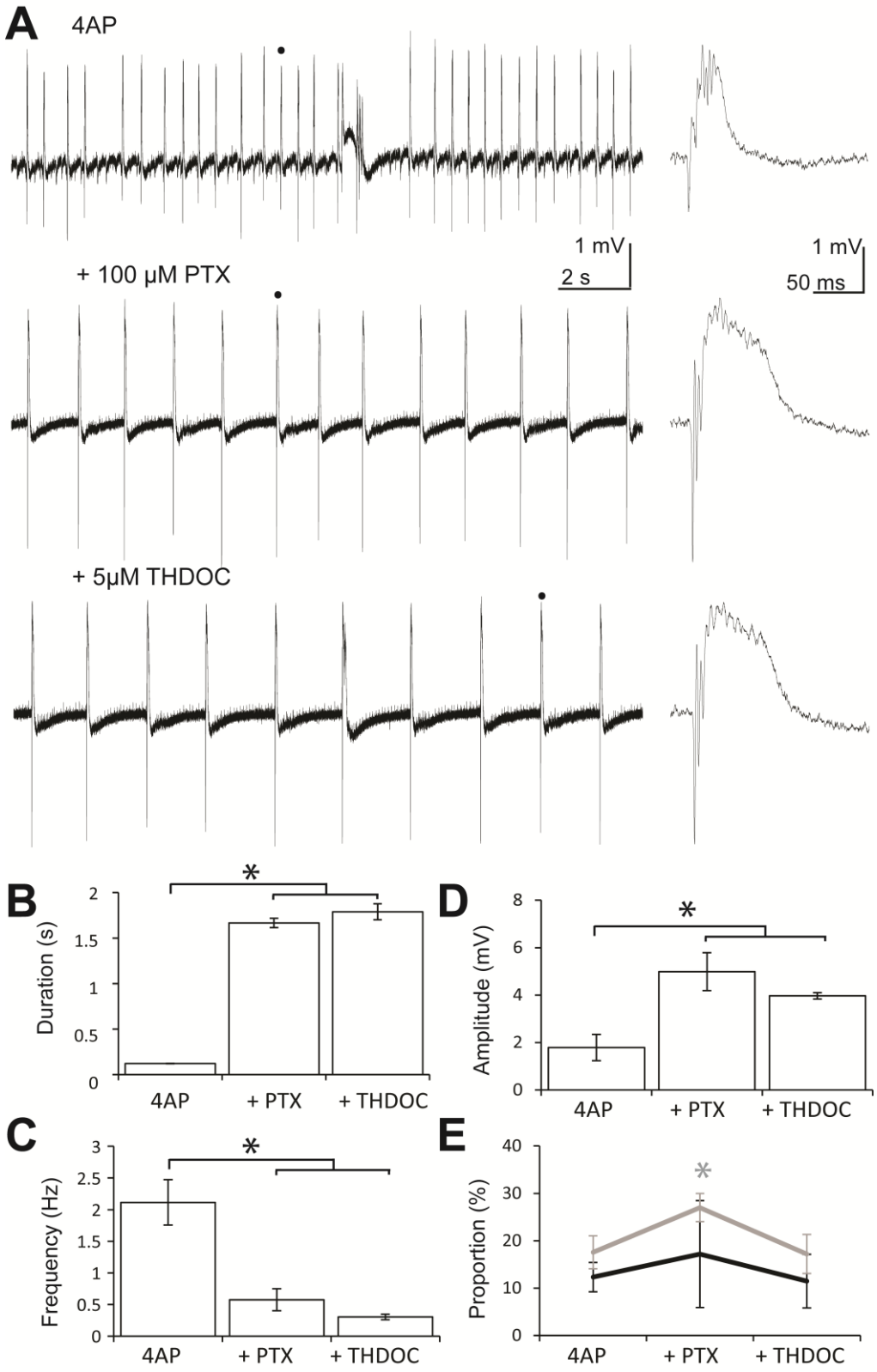
A
4AP
1 mV
2 s
1 mV
50 ms
+ 100 µM PTX
+ 5µM THDOC
B
Duration (s)
4AP
+ PTX
+ THDOC
C
Frequency (Hz)
4AP
+ PTX
+ THDOC
D
Amplitude (mV)
4AP
+ PTX
+ THDOC
E
Proportion (%)
4AP
+ PTX
+ THDOC

$GABA_A$ receptor-mediated activity blockade. (A) Field potential recordings of 4AP-induced epileptiform activity in the CA3 area during PTX and THDOC treatment. The event indicated under the dot is expanded on the right. **(B–D)** Graphs summarising the durations, frequencies and amplitudes of the epileptiform events occurring in slices treated with PTX and THDOC. Note that THDOC failed to significantly affect the epileptiform activity generated by PTX-treated slices. **(E)** Application of PTX increased fast ripple occurrence (gray) but did not affect ripple occurrence (black). $*P < 0.05$.

6. General Discussion

6.1. Ictal Onset Patterns

There is a growing body of evidence indicating that different ictal onset patterns can be mediated by distinct mechanisms, regions, and pathological substrates (Lévesque et al., 2012; Perucca et al., 2013; Shiri et al., 2015; Velasco et al., 2000). This has important implications for both the study and the treatment of epilepsy. Findings obtained in the experiments of *Chapter 2* have provided firm evidence of two specific ictal onset patterns that occur following the bath application of 4-aminopyridine (4AP): sudden and low voltage fast (LVF) onset. Sudden onset ictal events were not preceded by any changes in interictal firing pattern, whereas LVF events were preceded by a precipitating spike. On one hand, the findings of this study may suggest that changes in the dynamics of interictal event occurrence could predict seizure onset; however, to date there are no good electrophysiological biomarkers that are capable of reliably predicting the imminent occurrence of a seizure. High frequency oscillations have been found to increase before seizure occurrence (Lévesque et al., 2012), but the clinical significance of these findings are much more nuanced (Perucca et al., 2013).

Furthermore, while the *in vitro* findings showed a concise relationship between isolated slow interictal discharges and LVF onset ictal events, and between frequent polyspike interictal discharges and sudden onset ictal events; this relationship is not so clearly evident in *in vivo* models and in TLE patients. Part of the reason for this is that epileptiform activity is highly stereotyped and occurs at regular intervals in the 4AP model, whereas epileptiform activity is much more variable in *in vivo* models of epilepsy and in patients. Additionally, in TLE, hypersynchronous and LVF ictal onset types are the two major patterns detected, but hypersynchronous events make up a very small proportion of ictal onset types detected *in vitro* during the application of 4AP. This potentially limits the direct translatability of findings from the 4AP model; however, the broader implication of the study, which is to highlight the existence of different mechanisms underlying different ictal onset types, remains important. Future studies should take into account the type of ictal onset patterns that are generated, and if a model generates more than one ictal onset type then it is important these events are separated so the results can be interpreted in a clinically meaningful manner.

In the second study (*Chapter 3*), we looked at the contribution of subicular-entorhinal interactions to the generation of different patterns of epileptiform activity. The findings of this study were significant because we discovered that following the severance of subiculum-entorhinal cortex

connections, ictal activity was no longer sustained in the subiculum and ictal discharge properties were modified in the EC. With respect to the subiculum, previous studies looking at tissue excised from epileptic patients have found that while the region is capable of generating interictal events in the absence of manipulation of the perfusing media, the generation of ictal events, however, requires the application of a convulsant (Huberfeld et al., 2008; 2011). This phenomena could be related to the previously described GABAergic block in the subiculum (Benini and Avoli, 2005). It is important to emphasize that the subiculum should not be excluded as a possible culprit for the seizure onset zone. Evidence obtained from patients (Wozny et al., 2005) and *in vivo* studies (Lévesque et al., 2012) identify the area as a potential region from which seizures have been found to arise.

Specific aspects of the slice preparation must also be kept in mind while interpreting the results of the studies contained in this thesis. The *in vitro* slice preparation is a powerful tool that allows electrophysiological properties to be examined without contamination from prolonged anaesthetic and muscle relaxant use, and allows for the study of specific isolated circuits and brain networks. Researchers also have the advantage of visualizing brain structures, directly manipulating the recording environment, and locally applying pharmacological agents. However, there are certain limitations related to the use of *in vitro* brain slice preparations. First, neurons remain healthy only for a period lasting up to 4 hours (Fukuda et al., 1995). While our experiments are finished within 4 hours, the possibility for more subtle changes occurring in this timeframe cannot be excluded. Second, the slicing action itself can damage portions of brain tissue, particularly the top and bottom of the slice. This may be of particular importance with respect to the study contained in *Chapter 3*, after the surgical cut procedure a number of changes to the milieu of the slice environment and damage to neurons at the site of the cut could have affected our findings. Third, the ACSF does not mimic all the components present in the extracellular milieu of the brain.

6.1. HFOs and Patterns of Epileptiform Activity

The studies of *Chapters 2*, *4*, and *5* investigated the prevalence of ripples and fast ripples associated with different types of epileptiform activity. There is a degree of variability to these findings, but overall two general trends prevail. First, ictal events are associated with an increased rate of HFO occurrence compared to the interictal period in the piriform cortices and in the entorhinal cortex. Second, in the CA3, fast interictal events are most likely to be associated with HFOs and these HFOs have a greater tendency occur in the fast ripple frequency band.

The association between an increase in ripple occurrence and the onset of ictal LVF discharges was a more variable finding. While this phenomenon was evident in *Chapter 2,* in pilocarpine treated rats (Lévesque et al., 2012), and in patients (Perucca et al., 2013), this was not confirmed in the piriform cortex study of *Chapter 4*. Instead, in the piriform cortex, both ripples and fast ripples were found to increase at the onset of the ictal event. One reason for these differences could be the region of interest. The anterior piriform cortex (the region where HFOs were most prevalent) contains an area highly susceptible to the generation of epileptiform activity following the application of a chemoconvulsant whereas the other studies were conducted in the hippocampal and parahippocampal areas. The dominance of fast ripples over ripples in the piriform cortices could be related to the mechanisms underlying the propagation of seizures from the *area tempestas* (chemoconvulsant trigger zone) into the posterior piriform cortex and other limbic areas. It has been found that intact glutamatergic signalling is required (Halonen et al., 1994), while it is also suggested that fast ripples are mediated by glutamatergic mechanisms (Dzhala and Staley, 2004; Ibarz et al., 2010).

HFOs are considered to be mediated by local networks (Bragin et al., 2002; Staba et al., 2002), which are preserved during the slicing procedure; however, input and feedback loops can be lost in the preparation. In addition, the variability in the nature of the findings between studies suggests that while HFOs can be a powerful component of the arsenal of tools used to localize the seizure onset zone, they cannot be employed alone. HFOs can also be used to assess the glutamatergic and GABAergic contribution to a given epileptiform event, but again, these results should be interpreted with caution and verified with appropriate pharmacological manipulations. It is possible that pre-existing networks can predispose a given region to produce ripples over fast ripples or *vice versa*. Furthermore, it is important to note that ripples and fast ripples, at this point, only go so far as to describe the phenomena in a given frequency band. There needs to be more work on what constitutes a physiological ripple from a pathological ripple, whether an HFO occurring with an interictal event is mediated by different mechanisms than that occurring with an ictal event, and a universal definition of the frequency range encompassing these high frequency events should be developed to enhance the cohesiveness of the literature.

6.2. Neurosteroids and Patterns of Epileptiform Activity

The findings contained in *Chapters 4* and *5* indicate that neurosteroids exert differential effects depending on the region of interest and based on the mechanisms underlying the epileptiform event.

Neurosteroids are of particular interest because there is a large body of evidence linking the dysregulation of neurosteroids in the central nervous system, especially in the limbic structures, to epilepsy (Bauer et al., 2000; Belelli et al., 1989; Reddy, 2003). The nature of this dysregualtion can be different in males and females, but the manifestation of hyperexcitability is evident in both cases when neurosteroids are downregulated (Edwards et al., 2001; Herzog, 2002; Kim et al., 2010). Furthermore, in epileptic animals, endogenous neurosteroids have been found to keep seizure occurrence in check (Lawrence et al., 2010).

The effects of neurosteroids have been described for different types of epilepsies, but not for different types of epileptiform events. We sought to determine how neurosteroids can modulate events mediated predominantly by either glutamatergic or GABAergic mechanisms. These studies fail to distinguish between tonic and phasic components of the THDOC effect, which could have important implications in TLE where $GABA_A$ receptor subunit expression is modified. Furthermore, the concentrations of THDOC applied in these studies are on the high end of the spectrum. Concentrations of THDOC up to 100 nM are known to potentiate tonic currents and represent the upper limit of levels detected *in vivo* (Stell et al., 2003), whereas greater concentrations are necessary to control epileptic activity in chemoconvulsant models of epileptiform synchronization (Salazar et al., 2003).

Using neurosteroids to control epileptiform activity has proven to be beneficial in some cases because they do not lead to desensitization of the $GABA_A$ receptor (Glykys and Mody, 2007; Wohlfarth et al., 2002). Neurosteroids, however, are difficult to administer due to their highly hydrophobic nature and at high concentrations, they can be back-converted to their steroidal precursors. Synthetic neurosteroids (*e.g.* ganaxolone) that circumvent these obstacles have been developed for use in the clinic (Laxer et al., 2000). Overall, neurosteroids are important modulators of epileptiform activity and their effects can differ based on the mechanisms underlying a given event. Future studies should establish the network mechanisms underlying ictal onset types. Single unit studies employed in vitro could help elucidate when and how interneurons and principle cells contribute to patterns of epileptiform synchronization during the interictal, preictal, ictal, and postictal periods. In order to understand when neurosteroids should be employed, long term studies assessing the efficacy of these compounds with respect to ictal onset patterns should be conducted.

6.3. Concluding Remarks

The motivation behind the studies conducted in my thesis ultimately stems from the reality that concrete biomarkers pointing to the underlying cause of a specific epileptiform event and providing an indication for the best course of treatment are still missing. Understanding the mechanisms and neural connections involved in generating different patterns of ictal activity can contribute establishing better treatments for epilepsy. For instance, the best AED candidates could be identified earlier with less trial and error and classes of AEDs could be better employed based on regional specificity or predominant patterns of epileptiform activity. Additionally, because epilepsy can be a complex disease and the underlying cause of a given seizure can be multifaceted, it is also imperative to understand how a given AED can affect any given epileptiform event. The studies included in this thesis focus specifically on electrophysiological elements of ictogenesis; however, it is important to keep in mind that epilepsy can be investigated from behavioural, molecular, structural, hemodynamic, and immunological perspectives as well. Ultimately, epilepsy represents a disease that can be characterized by different underlying mechanisms, and the aim is to effectively identify these mechanisms so treatments can be appropriately employed.

REFERENCES

Acharya V, Acharya J, Lüders H (1998) Olfactory epileptic auras. *Neurology,* 51: 56–61.

Agís-Balboa RC, Pinna G, Zhubi A, Maloku E, Veldic M, Costa E, Guidotti A (2006) Characterization of brain neurons that express enzymes mediating neurosteroid biosynthesis. *Proc Natl Acad Sci USA*, 103: 14602–14607.

Aguayo LG, Pancetti FC, Klein RL, Harris RA (1994) Differential effects of GABAergic ligands in mouse and rat hippocampal neurons. *Brain Res*, 647: 97–105.

Akk G, Covey DF, Evers AS, Steinbach JH, Zorumski CF, Mennerick S (2009) The influence of the membrane on neurosteroid actions at $GABA_A$ receptors. *Psychoneuroendocrinology*, 34(Supplement 1): S59–S66.

Amaral DG, Insausti R, Cowan WM (1987) The entorhinal cortex of the monkey: I. Cytoarchitectonic organization. *J Comp Neurol,* 264: 326–355.

Amaral DG and Witter MP (1989) The three-dimensional organization of the hippocampal formation: A review of anatomical data. *Neuroscience*, 31: 571–591.

Andersen P, Bliss TVP, Skrede KK (1971) Lamellar organization of hippocampal excitatory pathways. *Exp Brain Res*, 13: 222–238.

Andrioli A, Alonso-Nanclares L, Arellano JI, DeFelipe J (2007) Quantitative analysis of parvalbumin-immunoreactive cells in the human epileptic hippocampus. *Neurosci*, 149: 131-143.

Avoli, M (1990). Epileptiform discharges and a synchronous GABAergic potential induced by 4-aminopyridine in the rat immature hippocampus. *Neurosci. Lett*. 117: 93–98.

Avoli M, Barbarosie M, Lucke A, Nagao T, Lopantsev V, Köhling R (1996) Synchronous GABA-mediated potentials and epileptiform discharges in the rat limbic system in vitro. *J Neurosci,* 16: 3912–3924.

Avoli M, D'Antuono M, Louvel J, Köhling R, Biagini G, Pumain R, D'Arcangelo G, Tancredi V (2002) Network and pharmacological mechanisms leading to epileptiform synchronization in the limbic system in vitro. *Prog Neurobiol*, 68: 167–207.

Avoli M and de Curtis M (2011) GABAergic synchronization in the limbic system and its role in the generation of epileptiform activity. *Prog Neurobiol*, 95(2): 104-32.

Avoli M, Louvel J, Kurcewicz I, Pumain R, Barbarosie M (1996b) Extracellular free potassium and calcium during synchronous activity induced by 4-aminopyridine in the juvenile rat hippocampus. *J Physiol,* 493 (Pt 3): 707–717.

Avoli M, Panuccio G, Herrington R, D'Anutono M, de Guzman P, Lévesque M (2013) Two different interictal spike patterns anticipate ictal activity in vitro. *Neurobiol Dis*, 52: 168-176.

Avoli M, Psarropoulou C, Tancredi V, Fueta Y (1993) On the synchronous activity induced by 4-

aminopyridine in the CA3 subfield of juvenile rat hippocampus. *J Neurophysiol*, 70: 1018–1029.

Axmacher N, Mormann F, Fernández G, Elger CE, Fell J (2006) Memory formation by neuronal synchronization. *Brain Res Rev*, 52: 170–182.

Ayala GF, Dichter M, Gumnit RJ, Matsumoto H, Spencer WA (1973) Genesis of epileptic interictal spikes. New knowledge of cortical feedback systems suggests a neurophysiological explanation of brief paroxysms. *Brain Res*, 52: 1–17.

Barbarosie M and Avoli M (1997) CA3-driven hippocampal-entorhinal loop controls rather than sustains in vitro limbic seizures. *J Neurosci*, 17: 9308–9314.

Bartolomei F, Wendling F, Régis J, Gavaret M, Guye M, Chauvel P (2004) Pre-ictal synchronicity in limbic networks of mesial temporal lobe epilepsy. *Epilepsy Res*, 61: 89–104.

Bauer J, Isojärvi JI, Herzog AG, Reuber M, Polson D, Taubøll E, Genton P, van der Ven H, Roesing B, Luef GJ, Galimberti CA, van Parys J, Flügel D, Bergmann A, Elger CE (2002) Reproductive dysfunction in women with epilepsy: recommendations for evaluation and management. *J Neurol Neurosurg Psychiatry*, 73: 121–125.

Bauer J, Stoffel-Wagner B, Flügel D, Kluge M, Schramm J, Bidlingmaier F, Elger CE (2000) Serum androgens return to normal after temporal lobe epilepsy surgery in men. *Neurology*, 55: 820–824.

Baulieu E-E and Robel P (1990) Neurosteroids: A new brain function? *J Steroid Biochem Mol Biol*, 37: 395–403.

Baulieu E-E (1998) Neurosteroids: A novel function of the brain. *Psychoneuroendocrinology*, 23: 963–987.

Beierlein M, Gibson JR, Connors BW (2000) A network of electrically coupled interneurons drives synchronized inhibition in neocortex. *Nat Neurosci*, 3: 904–910.

Belelli D, Bolger MB, Gee KW (1989) Anticonvulsant profile of the progesterone metabolite 5-alpha-pregnan-3 alpha-ol-20-one. *Eur J Pharmacol*, 166: 325–329.

Belelli D, Casula A, Ling A, Lambert JJ (2002) The influence of subunit composition on the interaction of neurosteroids with $GABA_A$ receptors. *Neuropharmacology*, 43: 651–661.

Bénar CG, Chauvière L, Bartolomei F, Wendling F (2010) Pitfalls of high-pass filtering for detecting epileptic oscillations: A technical note on "false" ripples. *Clin Neurophysiol* 121: 301–310.

Benini R and Avoli M (2005) Rat subicular networks gate hippocampal output activity in an in vitro model of limbic seizures. *J Physiol*, 566: 885–900.

Benini R, D'Antuono M, Pralong E, Avoli M (2003) Involvement of amygdala networks in epileptiform synchronization in vitro. *Neuroscience,* 120: 75–84.

Berg AT, Berkovic SF, Brodie MJ, Buchhalter J, Cross JH, van Emde Boas W, Engel J Jr, French J, Glauser TA, Mathern GW, Moshé SL, Nordli D, Plouin P, Scheffer IE (2010) Revised terminology and concepts for organization of seizures and epilepsies: report of the ILAE Commission on Classification and Terminology, 2005-2009. *Epilepsia*, 51: 676–685.

Bertram EH (2009) Temporal lobe epilepsy: where do the seizures really begin? *Epilepsy Behav,* Suppl 1: 32-37.

Biagini G, Longo D, Baldelli E, Zoli M, Rogawski MA, Bertazzoni G, Avoli M (2009) Neurosteroids and epileptogenesis in the pilocarpine model: evidence for a relationship between P450scc induction and length of the latent period. *Epilepsia*, 50:53–58.

Biagini G, Baldelli E, Longo D, Pradelli L, Zini I, Rogawski MA, Avoli M (2006) Endogenous neurosteroids modulate epileptogenesis in a model of temporal lobe epilepsy. *Exp Neurol*, 201: 519–524.

Blümcke I, Thom M, Wiestler OD (2002) Ammon's Horn Sclerosis: A Maldevelopmental Disorder Associated with Temporal Lobe Epilepsy. *Brain Pathol*, 12: 199–211.

Bragin A, Azizyan A, Almajano J, Wilson CL, Engel J (2005) Analysis of chronic seizure onsets after intrahippocampal kainic acid injection in freely moving rats. *Epilepsia*, 46: 1592–1598.

Bragin A, Benassi SK, Kheiri F, Engel J Jr (2011) Further evidence that pathologic high-frequency oscillations are bursts of population spikes derived from recordings of identified cells in dentate gyrus. *Epilepsia*, 52:45–52.

Bragin A, Engel J Jr, Wilson CL, Vizentin E, Mathern GW (1999) Electrophysiologic analysis of a chronic seizure model after unilateral hippocampal KA injection. *Epilepsia*, 40: 1210–1221.

Bragin A, Engel J Jr, Wilson CL, Fried I, Mathern GW (1999b) Hippocampal and entorhinal cortex high-frequency oscillations (100--500 Hz) in human epileptic brain and in kainic acid--treated rats with chronic seizures. *Epilepsia*, 40: 127–137.

Bragin A, Engel J Jr, Wilson CL, Fried I, Buzsáki G (1999c) High-frequency oscillations in human brain. *Hippocampus,* 9: 137–142.

Bragin A, Mody I, Wilson CL, Engel J Jr (2002) Local Generation of Fast Ripples in Epileptic Brain. *J Neurosci*, 22: 2012–2021.

Bragin A, Wilson CL, Almajano J, Mody I, Engel J (2004) High-frequency oscillations after status epilepticus: epileptogenesis and seizure genesis. *Epilepsia,* 45:1017–1023.

Bray PF (1972) A unifying concept of idiopathic epilepsy. *Monogr Hum Genet*, 6: 193.

Brooks-Kayal AR, Shumate MD, Jin H, Rikhter TY, Coulter DA (1998) Selective changes in single cell $GABA_A$ receptor subunit expression and function in temporal lobe epilepsy. *Nat Med*, 4: 1166–1172.

Brückner C and Heinemann U (2000) Effects of standard anticonvulsant drugs on different patterns of epileptiform discharges induced by 4-aminopyridine in combined entorhinal cortex-hippocampal slices. *Brain Res*, 859: 15–20.

Buzsaki G (2009) Rhythms of the Brain (Oxford University Press).

Buzsáki G, Horváth Z, Urioste R, Hetke J, Wise K (1992) High-Frequency Network Oscillation in the Hippocampus. *Science*, 256: 1025–1027.

Buzsáki G, Penttonen M, Bragin A, Nádasdy Z, Chrobak JJ (1995) Possible physiological role of the perforant path-CA1 projection. *Hippocampus*, 5: 141–146.

Canteras NS and Swanson LW (1992) Projections of the ventral subiculum to the amygdala, septum, and hypothalamus: a PHAL anterograde tract-tracing study in the rat. *J Comp Neurol,* 324: 180–194.

Chen LL, Feng HF, Mao XX, Ye Q, Zeng LH (2013) One hour of pilocarpine-induced status epilepticus is sufficient to develop chronic epilepsy in mice, and is associated with mossy fiber sprouting but not neuronal death. *Neurosci Bull*, 29(3):295-302

Cobb SR, Buhl EH, Halasy K, Paulsen O, Somogyi P (1995) Synchronization of neuronal activity in hippocampus by individual GABAergic interneurons. *Nature*, 378: 75–78.

Cohen I, Navaro V, Clemenceau S, Baulac M, Miles R (2002) On the origin of interictal activity in human temporal lobe in vitro. *Science,* 298: 1418-1421.

Compagnone NA and Mellon SH (2000) Neurosteroids: Biosynthesis and function of these novel neuromodulators. *Front Neuroendocrinol*, 21: 1–56.

Cossart R, Dinocourt C, Hirsch JC, Merchan-Perez A, De Felipe J, Ben-Ari Y, Esclapez M, Bernard C (2001) Dendritic but not somatic GABAergic inhibition is decreased in experimental epilepsy. *Nat Neurosci*, 4: 52–62.

Członkowska AI, Krząścik P, Sienkiewicz-Jarosz H, Siemiątkowski M, Szyndler J, Bidziński A, Płaźnik A (2000) The effects of neurosteroids on picrotoxin-, bicuculline- and NMDA-induced seizures, and a hypnotic effect of ethanol. *Pharmacol Biochem Behav*, 67: 345–353.

D'Arcangelo G, Panuccio G, Tancredi V, Avoli M (2005) Repetitive low-frequency stimulation reduces epileptiform synchronization in limbic neuronal networks. *Neurobiol Dis*, 19: 119–128.

D'Antuono M, Benini R, Biagini G, D'Arcangelo G, Barbarosie M, Tancredi V, Avoli M (2002) Limbic Network Interactions Leading to Hyperexcitability in a Model of Temporal Lobe Epilepsy. *J Neurophysiol*, 87: 634–639.

D'Antuono M, Louvel J, Köhling R, Mattia D, Bernasconi A, Olivier A, Turak B, Devaux A, Pumain R, Avoli M (2004) $GABA_A$ receptor-dependent synchronization leads to ictogenesis in the human dysplastic cortex. *Brain J Neurol*, 127: 1626–1640.

De Guzman P, D'Antuono M, Avoli M (2004) Initiation of electrographic seizures by neuronal networks in entorhinal and perirhinal cortices in vitro. *Neuroscience,* 123: 875–886.

De Lanerolle NC, Lee TS, Spencer DD (2010) Astrocytes and epilepsy. *Neurotherapeutics*, 7: 424–438.

DeLorenzo RJ, Hauser WA, Towne AR, Boggs JG, Pellock JM, Penberthy L, Garnett L, Fortner CA, Ko D (1996) A prospective, population-based epidemiologic study of status epilepticus in Richmond, Virginia. *Neurology*, 46: 1029–1035.

Demir R, Haberly LB, Jackson MB (2001) Epileptiform discharges with in-vivo-like features in slices of rat piriform cortex with longitudinal association fibers. *J Neurophysiol*, 86: 2445–2460.

Demont-Guignard S, Benquet P, Gerber U, Biraben A, Martin B, Wendling F (2012) Distinct

hyperexcitability mechanisms underlie fast ripples and epileptic spikes. *Ann Neurol,* 71:342–352.

Devinsky O, Vezzani A, Najjar S, De Lanerolle NC, Rogawski MA (2013) Glia and epilepsy: excitability and inflammation. *Trends Neurosci,* 36: 174–184.

Dinocourt C, Petanjek Z, Freund TF, Ben-Ari Y, Esclapez M (2003) Loss of interneurons innervating pyramidal cell dendrites and axon initial segments in the CA1 region of the hippocampus following pilocarpine-induced seizures. *J Comp Neurol*, 459: 407–425.

Djukic B, Casper KB, Philpot BD, Chin LS, McCarthy KD (2007) Conditional Knock-Out of Kir4.1 Leads to Glial Membrane Depolarization, Inhibition of Potassium and Glutamate Uptake, and Enhanced Short-Term Synaptic Potentiation. *J Neurosci*, 27: 11354–11365.

Draguhn A, Traub RD, Schmitz D, Jefferys JGR (1998) Electrical coupling underlies high-frequency oscillations in the hippocampus in vitro. *Nature*, 394: 189–192.

Du F, Whetsell WO Jr, Abou-Khalil B, Blumenkopf B, Lothman EW, Schwarcz R (1993) Preferenctial neuronal loss in layer III of the entorhinal cortex in patients with temporal lobe epilepsy. *Epilepsy Res*, 16(3):223-33.

During MJ and Spencer DD (1993) Extracellular hippocampal glutamate and spontaneous seizure in the conscious human brain. *The Lancet,* 341: 1607–1610.

Dzhala VI and Staley KJ (2004) Mechanisms of fast ripples in the hippocampus. *J Neurosci,* 24:8896–8906.

Dzhala VI and Staley KJ (2003) Transition from interictal to ictal activity in limbic networks in vitro. *J Neurosci*, 23: 7873-7380.

Edwards HE, Mo V, Burnham WM, MacLusky NJ (2001) Gonadectomy unmasks an inhibitory effect of progesterone on amygdala kindling in male rats. *Brain Res,* 889: 260–263.

Engel J Jr (2001) Mesial Temporal Lobe Epilepsy: What Have We Learned? *The Neuroscientist,* 7: 340–352.

Engel J Jr (1996) Introduction to temporal lobe epilepsy. *Epilepsy Res,* 26: 141–150.

Engel J Jr and Ackermann RF (1980) Interictal EEG spikes correlate with decreased, rather than increased, epileptogenicity in amygdaloid kindled rats. *Brain Res,* 190: 543–548.

Engel J Jr, Bandler R, Griffith NC, Caldecott-Hazard S (1991). Neurobiological evidence for epilepsy-induced interictal disturbances. *Adv Neurol,* 55: 97–111.

Engel J Jr, Bragin A, Staba R, Mody I (2009) High-frequency oscillations: what is normal and what is not? *Epilepsia*, 50:598–604.

Engel J Jr, Lopes da Silva F (2012) High-frequency oscillations — Where we are and where we need to go? *Prog Neurobiol.* 98: 316–318.

Farrant M and Nusser Z (2005) Variations on an inhibitory theme: phasic and tonic activation of $GABA_A$ receptors. *Nat Rev Neurosci,* 6:215–229.

Ferando I, Mody I (2012) $GABA_A$ receptor modulation by neurosteroids in models of temporal lobe epilepsies. *Epilepsia*, 53:89–101.

Finch DM, Babb TL (1981) Demonstration of caudally directed hippocampal efferents in the rat by intracellular injection of horseradish peroxidase. *Brain Res,* 214: 405–410

Fisher RS, van Emde Boas W, Blume W, Elger C, Genton P, Lee P, Engel J Jr (2005) Epileptic seizures and epilepsy: definitions proposed by the International League Against Epilepsy (ILAE) and the International Bureau for Epilepsy (IBE). *Epilepsia,* 46: 470–472.

French JA, Williamson PD, Thadani VM, Darcey TM, Mattson RH, Spencer SS, Spencer DD (1993) Characteristics of medial temporal lobe epilepsy: I. Results of history and physical examination. *Ann Neurol*, 34: 774–780.

Friedman A, Kaufer D, Heinemann U (2009) Blood-brain barrier breakdown-inducing astrocytic transformation: Novel targets for the prevention of epilepsy. *Epilepsy Res,* 85: 142–149.

Fritschy JM, Kiener T, Bouilleret V, Loup F (1999) GABAergic neurons and GABAA-receptors in temporal lobe epilepsy. *Neurochem Int,* 34: 435–445.

Fujita S, Toyoda I, Thamattoor AK, Buckmaster PS (2014) Preictal Activity of Subicular, CA1, and Dentate Gyrus Principal Neurons in the Dorsal Hippocampus before Spontaneous Seizures in a Rat Model of Temporal Lobe Epilepsy. *J Neurosci*, 34: 16671–16687.

Fukuda A, Czurkó A, Hida H, Muramatsu K, Lénárd L, Nishino H (1995) Appearance of deteriorated neurons on regionally different time tables in rat brain thin slices maintained in physiological condition. *Neurosci Lett*, 184: 13–16.

Galvan M, Grafe P, Bruggencate G (1982) Convulsant actions of 4- aminopyridine on the guinea-pig olfactory cortex slice. *Brain Res,* 241:75–86.

Gangisetty O and Reddy DS (2010) Neurosteroid withdrawal regulates $GABA_A$ receptor α4-subunit expression and seizure susceptibility by activation of progesterone receptor-independent early growth response factor-3 pathway. *Neuroscience*, 170: 865–880.

Gavrilovici C, D'Alfonso S, Dann M, Poulter MO (2006) Kindling-induced alterations in GABAA receptor-mediated inhibition and neurosteroid activity in the rat piriform cortex. *Eur J Neurosci*, 24: 1373–1384.

Glykys J and Mody I (2007) Activation of $GABA_A$ Receptors: Views from Outside the Synaptic Cleft. *Neuron,* 56: 763–770.

Goldring S, Edwards I, Harding GW, Bernardo KL (1992) Results of anterior temporal lobectomy that spares the amygdala in patients with complex partial seizures. *J Neurosurg*, 77: 185–193.

Grasse DW, Karunakaran S, Moxon KA (2013) Neuronal synchrony and the transition to spontaneous seizures. *Exp Neurol*, 248: 72–84.

Gregory RP, Oates T, Merry RTG (1993) Electroencephalogram epileptiform abnormalities in candidates for aircrew training. *Electroencephalogr Clin Neurophysiol*, 86: 75–77.

Haberly LB (1998) Olfactory cortex. In: The synaptic organization of the brain (4th Ed.) New York, NY, US: Oxford University Press. pp. 377–416.

Haberly LB (2001) Parallel-distributed processing in olfactory cortex: new insights from morphological and physiological analysis of neuronal circuitry. *Chem Senses,* 26:551–576.

Hagiwara A, Pal SK, Sato TF, Wienisch M, Murthy VN (2012) Optophysiological analysis of associational circuits in the olfactory cortex. *Front Neural Circuits,* 6:18.

Halassa MM, Fellin T, Haydon PG (2007) The tripartite synapse: roles for gliotransmission in health and disease. *Trends Mol Med*, 13: 54–63.

Halonen T, Tortorella A, Zrebeet H, Gale K (1994) Posterior piriform and perirhinal cortex relay seizures evoked from the area tempestas: role of excitatory and inhibitory amino acid receptors. *Brain Res,* 652: 145–148.

Hayashi K, Kubo K, Kitazawa A, Nakajima K (2015) Cellular dynamics of neuronal migration in the hippocampus. *Neurogenesis,* 9: 135.

Heinemann U, Konnerth A, Pumain R, Wadman WJ (1986) Extracellular calcium and potassium concentration changes in chronic epileptic brain tissue. *Adv Neurol*, 44: 641–661.

Henshall DC (2007) Apoptosis signalling pathways in seizure-induced neuronal death and epilepsy. *Biochem Soc Trans*, 35: 421–423.

Henshall DC, Clark RS, Adelson PD, Chen M, Watkins SC, Simon RP (2000). Alterations in bcl-2 and caspase gene family protein expression in human temporal lobe epilepsy. *Neurology*, 55: 250–257.

Herrington R, Lévesque M, Avoli M (2014) Neurosteroids modulate epileptiform activity and associated high-frequency oscillations in the piriform cortex. *Neuroscience*, 256: 467–477.

Herrington R, Lévesque M, Avoli M (2015) Neurosteroids differentially modulate fast and slow interictal discharges in the hippocampal CA3 area. *Eur J Neurosci*, 41(3):379-89.

Herzog AG (2002) Altered reproductive endocrine regulation in men with epilepsy: implications for reproductive function and seizures. *Ann Neurol*, 51: 539–542.

Herzog AG, Seibel MM, Schomer DL, Vaitukaitis JL, Geschwind N (1986) Reproductive endocrine disorders in men with partial seizures of temporal lobe origin. *Arch Neurol,* 43: 347–350.

Hjorth-Simonsen A (1972) Projection of the lateral part of the entorhinal area to the hippocampus and fascia dentata. *J Comp Neurol*, 146: 219–232.

Hosie AM, Wilkins ME, da Silva HM, and Smart TG (2006). Endogenous neurosteroids regulate $GABA_A$ receptors through two discrete transmembrane sites. *Nature*, 444: 486–489.

Huberfeld G, Clemenceau S, Cohen I, Pallud J, Wittner L, Navarro V, Baulac M, Miles R (2008) [Epileptiform activities generated in vitro by human temporal lobe tissue] *Neurochirurgie,* 54(3):148-58.

Huberfeld G, Menendez de la Prida L, Pallud J, Cohen I, Le Van Quyen M, Adam C, Clemenceau S, Baulac M, Miles R (2011) Glutamamtergic pre-ictal discharges emerge at the transition to seizure in human epilepsy. *Nat Neurosci,* 14(5): 627-634.

Ibarz JM, Foffani G, Cid E, Inostroza M, Menendez de la Prida L (2010) Emergent dynamics of fast ripples in the epileptic hippocampus. *J Neurosci,* 30:16249–16261.

Illig KR (2005) Projections from orbitofrontal cortex to anterior piriform cortex in the rat suggest a role in olfactory information processing. *J Comp Neurol*, 488: 224–231.

Inaba Y and Avoli M (2006) Volume-conducted epileptiform events between adjacent necortical slices in an interface tissue chamber. *J Neurosci Methods,* 151: 287-290.

Insausti R (1993) Comparative anatomy of the entorhinal cortex and hippocampus in mammals. *Hippocampus*, 3: 19–26.

Insausti R, Amaral DG, Cowan WM (1987) The entorhinal cortex of the monkey: II. Cortical afferents. *J Comp Neurol*, 264: 356–395.

Irwin RP, Lin SZ, Rogawski MA, Purdy RH, Paul SM (1994) Steroid potentiation and inhibition of N-methyl-D-aspartate receptor- mediated intracellular Ca^{2+} responses: Structure-activity studies. *J Pharmacol Exp Ther*, 271: 677–682.

Jabbari B, Russo MB, Russo ML (2000) Electroencephalogram of asymptomatic adult subjects. *Clin Neurophysiol*, 111: 102–105.

Jacobs J, LeVan P, Chander R, Hall J, Dubeau F, Gotman J (2008) Interictal high-frequency oscillations (80–500 Hz) are an indicator of seizure onset areas independent of spikes in the human epileptic brain. *Epilepsia*, 49: 1893–1907.

Jacobs J, LeVan P, Châtillon CÉ, Olivier A, Dubeau F, Gotman J (2009) High frequency oscillations in intracranial EEGs mark epileptogenicity rather than lesion type. *Brain*, 132: 1022–1037.

Jacobs J, Zijlmans M, Zelmann R, Chatillon CÉ, Hall J, Olivier A, Dubeau F, Gotman J (2010) High-frequency electroencephalographic oscillations correlate with outcome of epilepsy surgery. *Ann Neurol,* 67: 209–220.

Jefferys JG, Menendez de la Prida L, Wendling F, Bragin A, Avoli M, Timofeev I, Lopes da Silva FH (2012) Mechanisms of physiological and epileptic HFO generation. *Prog Neurobiol,* 98:250–264.

Jefferys JG (1995) Nonsynaptic modulation of neuronal activity in the brain: electric currents and extracellular ions. *Physiol Rev*, 75: 689–723.

Jefferys JG Haas HL (1982) Synchronized bursting of CA1 hippocampal pyramidal cells in the absence of synaptic transmission. *Nature*, 300: 448–450.

Jefferys JG, Jiruska P, de Curtis M, Avoli M (2012) Limbic Network Synchronization and Temporal Lobe Epilepsy. In: Noebels JL, Avoli M, Rogawski MA, et al., editors. Jasper's Basic Mechanisms of the Epilepsies [Internet]. 4th edition. Bethesda (MD): National Center for Biotechnology Information (US).

Jensen MS, Yaari Y (1997) Role of intrinsic burst firing, potassium accumulation, and electrical coupling in the elevated potassium model of hippocampal epilepsy. *J Neurophysiol*, 77: 1224–1233.

Jirsa VK, Stacey WC, Quilichini PP, Ivanov AI, Bernard C (2014) On the nature of seizure dynamics. *Brain J Neurol*, 137: 2210–2230.

Jiruska P, Csicsvari J, Powell AD, Fox JE, Chang WC, Vreugdenhil M, Li X, Palus M, Bujan AF, Dearden RW, Jefferys JG (2010) High-frequency network activity, global increase in neuronal activity, and synchrony expansion precede epileptic seizures in vitro. *J Neurosci*, 30:5690–5701.

Jiruska P, de Curtis M, Jefferys JG, Schevon CA, Schiff SJ, Schindler K (2013) Synchronization and desynchronization in epilepsy: controversies and hypotheses. *J Physiol*, 591: 787–797.

Jung-Testas I, Hu ZY, Baulieu EE, Robel P (1989) Neurosteroids: biosynthesis of pregnenolone and progesterone in primary cultures of rat glial cells. *Endocrinology*, 125: 2083–2091.

Kaminski RM, Marini H, Kim WJ, Rogawski MA (2005) Anticonvulsant Activity of Androsterone and Etiocholanolone. *Epilepsia*, 46: 819–827.

Kapur J and MacDonald RL (1996) Pharmacological properties of gamma-aminobutyric acidA receptors from acutely dissociated rat dentate granulecells. *Mol Pharmacol*, 50: 458–466.

Killian NJ, Jutras MJ, Buffalo EA (2012) A map of visual space in the primate entorhinal cortex. *Nature*, 491: 761–764.

Kim GH, Lee HW, Park H, Lee SK, Lee SA, Kim YI, Song HK, Shin DJ, Hong SB (2010) Seizure exacerbation and hormonal cycles in women with epilepsy. *Epilepsy Res,* 90: 214–220.

Kiss J, Buzsaki G, Morrow JS, Glantz SB, Leranth C (1996) Entorhinal cortical innervation of parvalbumin-containing neurons (basket and chandelier cells) in the rat ammon's horn. *Hippocampus*, 6: 239–246.

Kivi A, Lehmann TN, Kovács R, Eilers A, Jauch R, Meencke HJ, Von Deimling A, Heinemann U, Gabriel S (2000) Effects of barium on stimulus-induced rises of $[K^+]_o$ in human epileptic non-sclerotic and sclerotic hippocampal area CA1. *Eur J Neurosci*, 12: 2039–2048.

Knopp A, Frahm C, Fidzinski P, Witte OW, Behr J (2008) Loss of GABAergic neurons in the subiculum and its functional implications in temporal lobe epilepsy. *Brain J Neurol,* 131: 1516–1527.

Köhling R, Höhling JM, Straub H, Kuhlmann D, Kuhnt U, Tuxhorn I, Ebner A, Wolf P, Pannek HW, Gorji A, Speckmann EJ (2000) Optical monitoring of neuronal activity during spontaneous sharp waves in chronically epileptic human neocortical tissue. *J Neurophysiol,* 84(4): 2161-5.

Köhling R, Vreugdenhil M, Bracci E, Jefferys JG (2000) Ictal epileptiform activity is facilitated by hippocampal GABAA receptor-mediated oscillations. *J Neurosci*, 20: 6820–6829.

Kringelbach ML and Rolls ET (2004) The functional neuroanatomy of the human orbitofrontal cortex: evidence from neuroimaging and neuropsychology. *Prog Neurobiol*, 72: 341–372.

Kulik A, Nishimaru H, Ballanyi K (2000) Role of bicarbonate and chloride in GABA- and glycine-induced depolarization and $[Ca^{2+}]_i$ rise in fetal rat motoneurons i*n situ*. *J Neurosci*, 20: 7905–7913.

Kuzniecky RI and Jackson GD (2005) Magnetic Resonance in Epilepsy: Neuroimaging Techniques (Academic Press).

Kwan P and Brodie MJ (2001) Neuropsychological effects of epilepsy and antiepileptic drugs. *The Lancet*, 357: 216–222.

Lambert JJ, Belelli D, Peden DR, Vardy AW, Peters JA (2003) Neurosteroid modulation of $GABA_A$ receptors. *Prog Neurobiol*, 71: 67–80.

Lamsa K, Kaila K (1997) Ionic mechanisms of spontaneous GABAergic events in rat hippocampal slices exposed to 4- aminopyridine. *J Neurophysiol,* 78:2582–2591.

Laufs H, Richardson MP, Salek-Haddadi A, Vollmar C, Duncan JS, Gale K, Lemieux L, Löscher W, Koepp MJ (2011) Converging PET and fMRI evidence for a common area involved in human focal epilepsies. *Neurology*, 77: 904–910.

Lawrence C, Martin BS, Sun C, Williamson J, Kapur J (2010) Endogenous neurosteroid synthesis modulates seizure frequency. *Ann Neurol*, 67: 689–693.

Laxer K, Blum D, Abou-Khalil BW, Morrell MJ, Lee DA, Data JL, Monaghan EP (2000) Assessment of ganaxolone's anticonvulsant activity using a randomized, double-blind, presurgical trial design. Ganaxolone presurgical study group. *Epilepsia*, 41: 1187–1194.

Leach JP and Abassi H (2013) Modern management of epilepsy. *Clin Med*, 13: 84–86.

Leroy C, Poisbeau P, Keller AF, Nehlig A (2004) Pharmacological plasticity of GABA(A) receptors at dentate gyrus synapses in a rat model of temporal lobe epilepsy. *J Physiol*, 557: 473–487.

Lévesque M, Bortel A, Gotman J, Avoli M (2011) High-frequency (80–500 Hz) oscillations and epileptogenesis in temporal lobe epilepsy. *Neurobiol Dis*, 42: 231–241.

Lévesque M, Salami P, Behr C, Avoli M (2013) Temporal lobe systemic epileptiform activity following systemic administration of 4-aminopyridine in rats. *Epilepsia*, 54(4): 596-604.

Lévesque M, Salami P, Gotman J, Avoli M (2012) Two seizure-onset types reveal specific patterns of high-frequency oscillations in a model of temporal lobe epilepsy. *J Neurosci,* 32: 13264-13272

Lillis KP, Kramer MA, Mertz J, Staley KJ, White JA (2012) Pyramidal cells accumulate chloride at seizure onset. *Neurobiol Dis*, 47: 358–366.

Liot G, Bossy B, Lubitz S, Kushnareva Y, Sejbuk N, Bossy-Wetzel E (2009) Complex II inhibition by 3-NP causes mitochondrial fragmentation and neuronal cell death via an NMDA- and ROS-dependent pathway. *Cell Death Differ*, 16: 899–909.

Lopantsev V, Avoli M (1998a) Participation of $GABA_A$-mediated inhibition in ictal-like discharges in the rat entorhinal cortex. *J Neurophysiol*, 79: 352-360.

Lopantsev V, Avoli M (1998b) Laminar organization of epileptiform discharges in the rat entorhinal cortex in vitro. *J Physiol*, 509: 785-79.

Lopes da Silva FH, Witter MP, Boeijinga PH, Lohman AH (1990) Anatomic organization and physiology of the limbic cortex. *Physiol Rev*, 70: 453–511.

Loscher W, Ebert U (1996) The role of the piriform cortex in kindling. *Prog Neurobiol,* 50:427–481.

Loup F, Wieser HG, Yonekawa Y, Aguzzi A, Fritschy JM (2000) Selective alterations in $GABA_A$ receptor subtypes in human temporal lobe epilepsy. *J Neurosci*, 20: 5401–5419.

Lowenstein DH, Bleck T, Macdonald RL (1999) It's time to revise the definition of status epilepticus. *Epilepsia*, 40: 120–122.

Lu L, Leutgeb JK, Tsao A, Henriksen EJ, Leutgeb S, Barnes CA, Witter MP, Moser MB, Moser EI (2013) Impaired hippocampal rate coding after lesions of the lateral entorhinal cortex. *Nat Neurosci*, 16: 1085–1093.

Luna VM, Pettit DL (2010) Asymmetric rostro-caudal inhibition in the primary olfactory cortex. *Nat Neurosci,* 13:533–535.

Luskin MB, Price JL (1983) The topographic organization of associational fibers of the olfactory system in the rat, including centrifugal fibers to the olfactory bulb. *J Comp Neurol,* 216:264–291.

Maglóczky Z, Wittner L, Borhegyi Z, Halász P, Vajda J, Czirják S, Freund TF (2000) Changes in the distribution and connectivity of interneurons in the epileptic human dentate gyrus. *Neuroscience,* 96: 7–25.

Majewska MD (1992) Neurosteroids: endogenous bimodal modulators of the $GABA_A$ receptor. Mechanism of action and physiological significance. *Prog Neurobiol*, 38: 379–395.

Mann EO and Mody I (2008) The multifaceted role of inhibition in epilepsy: seizure-genesis through excessive GABAergic inhibition in autosomal dominant nocturnal frontal lobe epilepsy. *Curr Opin Neurol*, 21: 155–160.

Mantegazza M, Curia G, Biagini G, Ragsdale DS, Avoli M (2010) Voltage-gated sodium channels as therapeutic targets in epilepsy and other neurological disorders. *Lancet Neurol*, 9: 413–424.

Marco P, Sola RG, Pulido P, Alijarde MT, Sánchez A, Ramón y Cajal S, DeFelipe J (1996) Inhibitory neurons in the human epileptogenic temporal neocortex. *Brain*, 119: 1327–1347.

Massey CA, Sowers LP, Dlouhy BJ, Richerson GB (2014) Mechanisms of sudden unexpected death in epilepsy: the pathway to prevention. *Nat Rev Neurol*, 10: 271–282.

Matsumoto H and Marsan CA (1964) Cortical cellular phenomena in experimental epilepsy: Interictal manifestations. *Exp Neurol*, 9: 286–304.

McEwen BS (1991) Non-genomic and genomic effects of steroids on neural activity. *Trends Pharmacol Sci*, 12: 141–147.

McNamara JO (1994) Cellular and molecular basis of epilepsy. *J Neurosci*, 14: 3413–3425.

Mellon SH and Griffin LD (2002) Neurosteroids: biochemistry and clinical significance. *Trends Endocrinol Metab,* 13:35–43.

Mellon SH, Griffin LD, Compagnone NA (2001) Biosynthesis and action of neurosteroids. *Brain Res Rev*, 37: 3–12.

Michelson HB and Wong RK (1994) Synchronization of inhibitory neurones in the guinea-pig hippocampus in vitro. *J Physiol,* 477:35–45.

Michelson HB and Wong RK (1991) Excitatory synaptic responses mediated by $GABA_A$ receptors in the hippocampus. *Science*, 253: 1420–1423.

Mienville JM and Vicini S (1989) Pregnenolone sulfate antagonizes $GABA_A$ receptor-mediated currents via a reduction of channel opening frequency. *Brain Res*, 489: 190–194.

Mihalek RM, Banerjee PK, Korpi ER, Quinlan JJ, Firestone LL, Mi ZP, Lagenaur C, Tretter V, Sieghart W, Anagnostaras SG, Sage JR, Fanselow MS, Guidotti A, Spigelman I, Li Z, DeLorey TM, Olsen RW, Homanics GE (1999). Attenuated sensitivity to neuroactive steroids in γ-aminobutyrate type A receptor delta subunit knockout mice. *Proc Natl Acad Sci*, 96: 12905–12910.

Miles R and Wong RK (1987) Inhibitory control of local excitatory circuits in the guinea-pig hippocampus. *J Physiol*, 388: 611–629.

Miles R and Wong RK (1983) Single neurones can initiate synchronized population discharge in the hippocampus. *Nature*, 306: 371–373.

Miles R, Blaesse P, Huberfeld G, Wittner L, Kaila K (2012) Chloride homeostasis and GABA signaling in temporal lobe epilepsy. In Jasper's Basic Mechanisms of the Epilepsies, JL Noebels, M Avoli, MA Rogawski, RW Olsen, AV Delgado-Escueta, eds. (Bethesda (MD): National Center for Biotechnology Information (US).

Mormann F, Kreuz T, Andrzejak RG, David P, Lehnertz K, Elger CE (2003) Epileptic seizures are preceded by a decrease in synchronization. *Epilepsy Res,* 53: 173–185.

Murthy VN (2012) Optophysiological analysis of associational circuits in the olfactory cortex. *Front Neural Circuits*, 6: 18.

Naber PA, Lopes da Silva FH, Witter MP (2001) Reciprocal connections between the entorhinal cortex and the subiculum are in register with the projections from CA1 to the subiculum, *Hippocampus*, 11(2): 99-104.

Nagao T, Alonso A, Avoli M (1996) Epileptiform activity induced by pilocarpine in the rat hippocampal-entorhinal slice preparation. *Neuroscience*, 72: 399–408.

Nigri A, Ferraro S, D'Incerti L, Critchley HD, Bruzzone MG, Minati L (2013) Connectivity of the amygdala, piriform, and orbitofrontal cortex during olfactory stimulation: a functional MRI study. *NeuroReport*, 24: 171–175.

O'Mara SM, Commins S, Anderson M, Gigg J (2001) The subiculum: a review of form, physiology and function. *Prog Neurobiol*, 64: 129–155.

Ogren JA, Bragin A, Wilson CL, Hoftman GD, Lin JJ, Dutton RA, Fields TA, Toga AW, Thompson PM, Engel J Jr, Staba RJ (2009) Three-dimensional hippocampal atrophy maps distinguish two common temporal lobe seizure-onset patterns. *Epilepsia*, 50: 1361–1370.

Ogren JA, Wilson CL, Bragin A, Lin JJ, Salamon N, Dutton RA, Luders E, Fields TA, Fried I, Toga AW, Thompson PM, Engel J Jr, Staba RJ. (2009). Three-dimensional surface maps link local atrophy and fast ripples in human epileptic hippocampus. *Ann Neurol*, 66: 783–791.

Olney, J.W., Collins, R.C., and Sloviter, R.S. (1986). Excitotoxic mechanisms of epileptic brain damage. Adv. Neurol. 44, 857–877.

Olton DS and Paras BC (1979) Spatial memory and hippocampal function. *Neuropsychologia*, 17: 669–682.

Ono T and Galanopoulou AS (2012) Epilepsy and Epileptic Syndrome. *Adv Exp Med Biol,* 724: 99-113.

Panuccio G, Sanchez G, Lévesque M, Salami P, de Curtis M, Avoli M (2012) On the ictogenic properties of the piriform cortex in vitro. *Epilepsia*, 53: 459–468.

Panuccio G, Curia G, Colosimo A, Cruccu G, Avoli M (2009) Epileptiform synchronization in the cingulate cortex. *Epilepsia,* 50: 521–536.

Pare D, de Curtis M, Llinas R (1992) Role of the hippocampal-entorhinal loop in temporal lobe epilepsy: extra- and intracellular study in the isolated guinea pig brain in vitro. *J Neurosci*, 12: 1867–1881.

Park-Chung M, Malayev A, Purdy RH, Gibbs TT, Farb DH (1999) Sulfated and unsulfated steroids modulate γ-aminobutyric acid (A) receptor function through distinct sites. *Brain Res*, 830: 72–87.

Parpura V, Basarsky TA, Liu F, Jeftinija K, Jeftinija S, Haydon PG (1994) Glutamate-mediated astrocyte–neuron signalling. *Nature*, 369: 744–747.

Patil AA (2007) Generalized Seizure Disorders. In xPharm: The Comprehensive Pharmacology Reference, S.J. Enna, and D.B. Bylund, eds. (New York: Elsevier), pp 1–4.

Payne JA, Rivera C, Voipio J, Kaila K (2003) Cation–chloride co-transporters in neuronal communication, development and trauma. *Trends Neurosci*, 26: 199–206.

Peng Z, Huang CS, Stell BM, Mody I, Houser CR (2004) Altered Expression of the δ Subunit of the $GABA_A$ Receptor in a Mouse Model of Temporal Lobe Epilepsy. *J Neurosci*, 24: 8629–8639.

Perreault P and Avoli M (1991) Physiology and pharmacology of epileptiform activity induced by 4-aminopyridine in rat hippocampal slices. *J Neurophysiol*, 65: 771–785.

Perreault P and Avoli M (1992) 4-aminopyridine-induced epileptiform activity and a GABA-mediated long- lasting depolarization in the rat hippocampus. *J Neurosci*, 12: 104–115.

Perucca P, Dubeau F, Gotman J (2014) Intracranial electroencephalographic seizure-onset patterns: effect of underlying pathology. *Brain,* 137: 183-196.

Piredda S and Gale K (1985) A crucial epileptogenic site in the deep prepiriform cortex. *Nature*, 317: 623–625.

Pitkänen A (2010). Therapeutic approaches to epileptogenesis— hope on the horizon. *Epilepsia*, 51(Suppl 3): 2–17.

Pitkänen A and Sutula TP (2002) Is epilepsy a progressive disorder? Prospects for new therapeutic approaches in temporal-lobe epilepsy. *Lancet Neurol*, 1: 173–181.

Prince DA (1978) Neurophysiology of Epilepsy. *Annu Rev Neurosci*, 1: 395–415.

Pugnaghi M, Monti G, Biagini G, Meletti S (2013) Temporal lobe epilepsy exacerbation during pharmacological inhibition of endogenous neurosteroid synthesis. Case Rep, bcr2012008204–bcr2012008204.

Queiroz CM and Mello LE (2007) Synaptic plasticity of the CA3 commissural projection in epileptic rats: an in vivo electrophysiological study. *Eur J Neurosci*, 25: 3071–3079.

Rajasekaran K, Joshi S, Sun C, Mtchedlishvilli Z, Kapur J (2010) Receptors with low affinity for neurosteroids and GABA contribute to tonic inhibition of granule cells in epileptic animals. *Neurobiol Dis*, 40: 490–501.

Ratté S and Lacaille J (2006) Selective degeneration and synaptic reorganization of hippocampal interneurons in a chronic model of temporal lobe epilepsy. *Adv Neurol*, 97: 69–76.

Reddy DS (2003) Is there a physiological role for the neurosteroid THDOC in stress-sensitive conditions? *Trends Pharmacol Sci*, 24: 103–106.

Reddy DS (2004a) Pharmacology of catamenial epilepsy. *Methods Find Exp Clin Pharmacol*, 26: 547–561.

Reddy DS (2004b) Pharmacology of Endogenous Neuroactive Steroids. *Crit Rev Neurobiol*, 15: 197–234.

Reddy DS (2010) Neurosteroids: endogenous role in the human brain and therapeutic potentials. *Prog Brain Res,* 186:113–137.

Reddy DS (2011) Role of anticonvulsant and antiepileptogenic neurosteroids in the pathophysiology and treatment of epilepsy. *Front Neuroendocr Sci,* 2:38.

Reddy DS and Rogawski MA (2012) Neurosteroids— Endogenous Regulators of Seizure Susceptibility and Role in the Treatment of Epilepsy. In Jasper's Basic Mechanisms of the Epilepsies, JL Noebels, M Avoli, MA Rogawski, RW Olsen, AV Delgado-Escueta, eds. (Bethesda (MD): National Center for Biotechnology Information (US)) pp 984–997.

Robel P and Baulieu EE (1994) Neurosteroids: Biosynthesis and function. *Trends Endocrinol Metab*, 5: 1–8.

Royet JP, Plailly J, Delon-Martin C, Kareken DA, Segebarth C (2003) fMRI of emotional responses to odors: influence of hedonic valence and judgment, handedness, and gender. *NeuroImage*, 20: 713–728.

Rupprecht R, Hauser CAE, Trapp T, Holsboer F (1996) Neurosteroids: Molecular mechanisms of action and psychopharmacological significance. *J Steroid Biochem Mol Biol,* 56:163–168.

Rutecki PA, Grossman RG, Armstrong D, Irish-Loewen S (1989) Electrophysiological connections between the hippocampus and entorhinal cortex in patients with complex partial seizures. *J*

Neurosurg, 70: 667–675.

Sah N, Sikdar SK (2013) Transition in subicular burst firing neurons from epileptiform activity to suppressed state by feed forward inhibition. *Eur J Neurosci*, 38(4): 2542-56.

Salami P, Lévesque M, Gotman J, Avoli M (2012) A comparison between automated detection methods of high-frequency oscillations (80– 500 Hz) during seizures. *J Neurosci Meth*, 211: 265–271.

Salazar P, Tapia R, Rogawski MA (2003) Effects of neurosteroids on epileptiform activity induced by picrotoxin and 4-aminopyridine in the rat hippocampal slice. *Epilepsy Res,* 55:71–82.

Scharfman HE (2003) Insight into Molecular Mechanisms of Catamenial Epilepsy. *Epilepsy Curr,* 3: 86–88.

Schindler K, Leung H, Elger CE, Lehnertz K (2007) Assessing seizure dynamics by analysing the correlation structure of multichannel intracranial EEG. *Brain*, 130: 65–77.

Schmidt D and Schachter SC (2014) Drug treatment of epilepsy in adults. *BMJ*, 348: g254.

Scoville WB and Milner B (1957) Loss of recent memory after bilateral hippocampal lesions. *J Neurol Neurosurg Psychiatry*, 20: 11–21.

Seifert G and Steinhäuser C (2013) Neuron-astrocyte signaling and epilepsy. *Exp Neurol,* 244: 4–10.

Selye H (1941) Anesthetic Effect of Steroid Hormones. *Exp Biol Med*, 46: 116–121.

Shao LR, Dudek FE (2011) Repetitive perforant-path stimulation induces epileptiform bursts in minislices of dentate gyrus from rats with kainite-induced epilepsy. *J Neurophysiol,* 105(2): 522-527.

Sharp PE and Green C (1994) Spatial correlates of firing patterns of single cells in the subiculum of the freely moving rat. *J Neurosci*, 14: 2339–2356.

Sherwin I (1984) Ictal-interictal unit firing pattern differences in penicillin-induced primary and secondary epileptogenic foci. *Exp Neurol*, 84: 463–477.

Shiri Z, Herrington R, Lévesque M, Avoli M (2015) Neurosteroidal modulation of *in vitro* epileptiform activity is enhanced in pilocarpine-treated epileptic rats. *Neurobiol Dis,* 78: 24-34.

Shiri Z, Manseau F, Lévesque M, Williams S, Avoli M (2015) Interneuron activity leads to initiation of low-voltage fast-onset seizures. *Ann Neurol*, 77: 541–546.

Shorvon SD (2011) The etiologic classification of epilepsy. *Epilepsia*, 52: 1052–1057.

Sivilotti L and Nistri A (1991) GABA receptor mechanisms in the central nervous system. *Prog Neurobiol*, 36: 35–92.

Sloviter RS (1983) "Epileptic" brain damage in rats induced by sustained electrical stimulation of the perforant path. I. Acute electrophysiological and light microscopic studies. *Brain Res Bull*, 10: 675–697.

Sloviter RS, Dichter MA, Rachinsky TL, Dean E, Goodman JH, Sollas AL, Martin DL (1996) Basal expression and induction of glutamate decarboxylase and GABA in excitatory granule cells of the rat and monkey hippocampal dentate gyrus. *J Comp Neurol*, 373: 593–618.

Sousa A and Ticku MK (1997) Interactions of the neurosteroid dehydroepiandrosterone sulfate with the GABA(A) receptor complex reveals that it may act via the picrotoxin site. *J Pharmacol Exp Ther*, 282: 827–833.

Spencer SS (2002) When should temporal lobe epilepsy be treated surgically? *Lancet Neurol,* 1: 375–382.

Spencer SS, Spencer DD (1994) Entorhinal–hippocampal interactions in medial temporal lobe epilepsy. *Epilepsia*, 35: 721–727.

Staba RJ, Wilson CL, Bragin A, Fried I, Engel J Jr (2002) Quantitative analysis of high-frequency oscillations (80-500 Hz) recorded in human epileptic hippocampus and entorhinal cortex. *J Neurophysiol*, 88: 1743–1752.

Stafstrom CE (2005) The role of the subiculum in epilepsy and epileptogenesis. *Epilepsy Curr*, 5: 121–129.

Stanton PK, Jones RS, Mody I, Heinemann U (1987) Epileptiform activity induced by lowering extracellular [Mg^{2+}] in combined hippocampal-entorhinal cortex slices: Modulation by receptors for norepinephrine and N-methyl-d-aspartate. *Epilepsy Res,* 1: 53–62.

Stell BM, Brickley SG, Tang CY, Farran M, Mody I (2003) Neuroactive steroids reduce neuronal excitability by selectively enhancing tonic inhibition mediated by d subunit-containing $GABA_A$ receptors. *Proc Natl Acad Sci*, 100:14439–14444.

Steward O (1976) Topographic organization of the projections from the entorhinal area to the hippocampal formation of the rat. *J Comp Neurol*, 167: 285–314.

Steward O, Scoville SA (1976) Cells of origin of entorhinal cortical afferents to the hippocampus and fascia dentate of the rat. *J Comp Neurol*, 169(3):347-70.

Storm JF (1987) Action potential repolarization and a fast after-hyperpolarization in rat hippocampal pyramidal cells. *J Physiol*, 385: 733–759.

Stringer JL and Lothman EW (1992) Reverberatory seizure discharges in hippocampal–parahippocampal circuits. *Exp Neurol*, 116: 198–203.

Sudbury JR and Avoli M (2007) Epileptiform synchronization in the rat insular and perirhinal cortices in vitro. *Eur J Neurosci*, 26: 3571–3582.

Surges R, Sarvari M, Steffens M, Els T (2006) Characterization of rebound depolarization in hippocampal neurons. *Biochem Biophys Res Commun*, 348: 1343–1349.

Suzuki N and Bekkers JM (2011) Two layers of synaptic processing by principal neurons in piriform cortex. *J Neurosci,* 31:2156–2166.

Swartzwelder H, Anderson W, Wilson W (1988) Mechanism of electrographic seizure generation in

the hippocampal slice in Mg^{2+}-free medium: the role of $GABA_A$ inhibition. *Epilepsy Res,* 2: 239–245.

Taubøll E, Sveberg L, Svalheim S (2015) Interactions between hormones and epilepsy. *Seizure*, 28: 3–11.

Teskey GC and Farrell JS (2015) Epilepsy. In International Encyclopedia of the Social & Behavioral Sciences (Second Edition), JD Wright, ed. (Oxford: Elsevier), pp 852–855.

Toyoda I, Bower MR, Leyva F, Buckmaster PS (2013) Early activation of ventral hippocampus and subiculum during spontaneous seizures in a rat model of temporal lobe epilepsy. *J Neurosci*, 33: 11100-11115.

Toyoda I, Fujita S, Thamattoor AK, Buckmaster PS (2015) Unit activity of hippocampal interneuron's before spontaneous seizures in an animal model of temporal lobe epilepsy. *J Neurosci,* 35(16): 6600-6618.

Traub RD, Borck C, Colling SB, Jefferys JG (1996) On the structure of ictal events in vitro. *Epilepsia,* 37: 879-891.

Traub RD, Miles R, Jefferys JG (1993) Synaptic and intrinsic conductances shape picrotoxin-induced synchronized after-discharges in the guinea-pig hippocampal slice. *J Physiol*, 461: 525–547.

Traub RD, Whittington MA, Buhl EH, LeBeau FE, Bibbig A, Boyd S, Cross H, Baldeweg T (2001) A possible role for gap junctions in generation of very fast EEG oscillations preceding the onset of, and perhaps initiating, seizures. *Epilepsia*, 42: 153–170.

Traub RD and Wong RK (1982) Cellular mechanism of neuronal synchronization in epilepsy. *Science*, 216: 745–747.

Traynelis SF and Dingledine R (1988) Potassium-induced spontaneous electrographic seizures in the rat hippocampal slice. *J Neurophysiol*, 59: 259–276.

Truccolo W, Donoghue JA, Hochberg LR, Eskandar EN, Madsen JR, Anderson WS, Brown EN, Halgren E, Cash SS (2011) Single-neuron dynamics in human focal epilepsy. *Nat Neurosci*, 14: 635–641.

Uusisaari M, Smirnov S, Voipio J, Kaila K (2002) Spontaneous epileptiform activity mediated by GABA(A) receptors and gap junctions in the rat hippocampal slice following long-term exposure to GABA(B) antagonists. *Neuropharmacology*, 43: 563–572.

Van Groen T and Lopes da Silva FH (1986) Organization of the reciprocal connections between the subiculum and the entorhinal cortex in the cat: II. An electrophysiological study. *J Comp Neurol*, 251: 111–120.

Varela F, Lachaux JP, Rodriguez E, Martinerie J (2001) The brainweb: Phase synchronization and large-scale integration. *Nat Rev Neurosci*, 2: 229–239.

Vaughan DN and Jackson GD (2014) The piriform cortex and human focal epilepsy. *Epilepsy*, 5: 259.

Velasco AL, Wilson CL, Babb TL, Engel J (2000) Functional and anatomic correlates of two frequently observed temporal lobe seizure-onset patterns. *Neural Plast,* 7: 49–63

Verkhratsky A and Steinhäuser C (2000) Ion channels in glial cells. *Brain Res Brain Res Rev*, 32: 380–412.

Vezzani A, French J, Bartfai T, Baram TZ (2011) The role of inflammation in epilepsy. *Nat Rev Neurol*, 7: 31–40.

Viitanen T, Ruusuvuori E, Kaila K, Voipio J (2010) The K^+–Cl^- cotransporter KCC2 promotes GABAergic excitation in the mature rat hippocampus. *J Physiol*, 588: 1527–1540.

Vismer MS, Forcelli PA, Skopin MD, Gale K, Koubeissi MZ (2015) The piriform, perirhinal, and entorhinal cortex in seizure generation. *Front Neural Circuits*, 9: 27.

Vivar C and Van Praag H (2013) Functional circuits of new neurons in the dentate gyrus. *Front Neural Circuits*, 7: 15.

Voskuyl RA and Albus H (1985) Spontaneous epileptiform discharges in hippocampal slices induced by 4-aminopyridine. *Brain Res*, 342: 54–66.

Wang Y and Qin ZH (2010) Molecular and cellular mechanisms of excitotoxic neuronal death. *Apoptosis*, 15(11): 1382–1402.

Wendling F, Bartolomei F, Mina F, Huneau C, Benquet P (2012) Interictal spikes, fast ripples and seizures in partial epilepsies – combining multi-level computational models with experimental data. *Eur J Neurosci,* 36:2164–2177.

Wendling F, Bartolomei F, Bellanger JJ, Chauvel P (2002) Epileptic fast activity can be explained by a model of impaired GABAergic dendritic inhibition. *Eur J Neurosci*, 15: 1499–1508.

Wiebe S (2000) Epidemiology of Temporal Lobe Epilepsy. *Can J Neurol Sci,* Suppl 1: S6-10.

Wilson CL, Khan SU, Engel J, Isokawa M, Babb TL, Behnke EJ (1998) Paired pulse suppression and facilitation in human epileptogenic hippocampal formation. *Epilepsy Res*, 31: 211–230.

Winston JS, Gottfried JA, Kilner JM, Dolan RJ (2005) Integrated Neural Representations of Odor Intensity and Affective Valence in Human Amygdala. *J Neurosci*, 25: 8903–8907.

Wirrell EC (2010) Prognostic significance of interictal epileptiform discharges in newly diagnosed seizure disorders. *J Clin Neurophysiol*, 27: 239–248.

Witter MP, and Groenewegen HJ (1984) Laminar origin and septotemporal distribution of entorhinal and perirhinal projections to the hippocampus in the cat. *J Comp Neurol*, 224: 371–385.

Witter MP, Groenewegen HJ (1990) The subiculum: cytoarchitectonically a simple structure, but hodologically complex. *Prog Brain Res,* 83(4):47-58.

Witter MP, Groenewegen HJ, Lopes da Silva FH & Lohman AH (1989) Functional organization of the extrinsic and intrinsic circuitry of the parahippocampal region. *Prog Neurobiol,* 33: 161–253.

Witter MP, Ostendorf RH & Groenewegen HJ (1990). Heterogeneity in the dorsal subiculum of the rat. distinct neuronal zones project to different cortical and subcortical targets. *Eur J Neurosci,* 2: 718–725.

Witter MP (2007) The perforant path: projections from the entorhinal cortex to the dentate gyrus. *Prog Brain Res*, 163: 43–61.

Witter MP, Van Hoesen GW, Amaral DG (1989) Topographical organization of the entorhinal projection to the dentate gyrus of the monkey. *J Neurosci*, 9: 216–228.

Wittner L, Maglóczky Z, Borhegyi Z, Halász P, Tóth S, Eross L, Szabó Z, Freund TF (2001) Preservation of perisomatic inhibitory input of granule cells in the epileptic human dentate gyrus. *Neuroscience*, 108: 587–600.

Wohlfarth KM, Bianchi MT, Macdonald RL (2002) Enhanced neurosteroid potentiation of ternary GABA(A) receptors containing the delta subunit. *J Neurosci,* 22:1541–1549.

Wong RK and Prince DA (1981) Afterpotential generation in hippocampal pyramidal cells. *J Neurophysiol*, 45: 86–97.

Wozny C, Knopp A, Lehmann TN, Heinemann U, Behr J (2005) The subiculum: a potential site of ictogenesis in human temporal lobe epilepsy. *Epilepsia*, 46(Suppl 5): 17–21.

Wu JY, Sankar R, Lerner JT, Matsumoto JH, Vinters HV, Mathern GW (2010) Removing interictal fast ripples on electrocorticography linked with seizure freedom in children. *Neurology*, 75: 1686–1694.

Wu FS, Gibbs TT, Farb DH (1991) Pregnenolone sulfate: a positive allosteric modulator at the N-methyl-D-aspartate receptor. *Mol Pharmacol*, 40: 333–336.

Wyeth MS, Zhang N, Mody I, Houser CR (2010) Selective reduction of cholecystokinin-positive basket cell innervation in a model of temporal lobe epilepsy. *J Neurosci*, 30: 8993–9006.

Yaari Y, Konnerth A, Heinemann U (1983) Spontaneous epileptiform activity of CA1 hippocampal neurons in low extracellular calcium solutions. *Exp Brain Res*, 51: 153–156.

Ylinen A, Bragin A, Nadasdy Z, Jando G, Szabo I, Sik A, et al (1995) Sharp wave-associated high-frequency oscillation (200 Hz) in the intact hippocampus: network and intracellular mechanisms. *J Neurosci*, 15:30–46.

Zhang ZJ, Koifman J, Shin DS, Ye H, Florez CM, Zhang L, Valiante TA, Carlen PL (2012) Transition to seizure: ictal discharge is preceded by exhausted presynaptic GABA release in the hippocampal CA3 region. *J Neurosci*, 32: 2499–2512.

Zhu WJ and Vicini S (1997) Neurosteroid Prolongs GABAA Channel Deactivation by Altering Kinetics of Desensitized States. *J Neurosci*, 17: 4022–4031.

Ziburkus J, Cressman JR, Barreto E, Schiff SJ (2006) Interneuron and pyramidal cell interplay during in vitro seizure-like events. *J Neurophysiol*, 95: 3948–3954.

Zijlmans M, Jacobs J, Zelmann R, Dubeau F, Gotman J (2009) High- frequency oscillations mirror disease activity in patients with epilepsy. *Neurology*, 72:979–986.

Zijlmans M, Jacobs J, Kahn YU, Zelmann R, Dubeau F, Gotman J (2011) Ictal and interictal high frequency oscillations in patients with focal epilepsy. *Clin Neurophysiol*, 122: 664–671.